University of Alberta

Harmonic Impact of Modern Residential Loads on Distribution Power System and Mitigation Solutions

by

Hui Wang

A thesis submitted to the Faculty of Graduate Studies and Research
in partial fulfillment of the requirements for the degree of

Master of Science

in

Power Engineering and Power Electronics

Electrical and Computer Engineering

©Hui Wang
Fall 2011
Edmonton, Alberta

Abstract

The mass penetration of both energy-efficient and consumer electronics into residential houses is introducing a totally new harmonic situation in today's distribution systems and complicating the mitigation solutions.

In order to study the collective effect of today's distributed harmonic sources, this thesis developed an harmonic load model for residential service transformers and a detailed multi-grounded system model to conduct a system-wide harmonic study. The simulation results are consistent with the field measurements. The evolution of the resultant impacts over the next several years, as affected by the market trends of home appliances, is also determined.

Mitigation studies were done from two perspectives. One is the system modifications. Various sensitivity studies were performed and analyzed to clarify which factors are important in terms of harmonic mitigation. Another mitigation study involved a zero sequence filter, whose fundamental theory was studied and effectiveness was tested and verified in simulations.

Acknowledgements

I would like to show my appreciation to all who helped me to complete this thesis. The expert guidance and advice from my supervisor, Dr. Wilsun Xu, made its completion possible. I also give special thanks to Diogo Salles Correa, Pooya Bagheri and Chen Jiang for their constructive feedback in our technical discussions. I thank my fellow students in the power Disturbance and Signaling Research Lab for providing a supportive and friendly environment. I especially thank Hooman Erfania, who was always keen to share his knowledge and experience.

I thank my mother and grandmother for supporting me even when going through the extremely tough financial problems. I am deeply obliged with my father, although he passed away five years ago and knows nothing about this story. The conviction and spirit for challenges he built in me made everything in these five years possible.

Finally, I thank the committee members of this examination for the valuable comments that helped in improving the quality of this thesis: Dr. Wilsun Xu, Dr. Yunwei Li and Dr. Amit Kumar.

Contents

List of Tables

List of Figures

Chapter 1

Introduction

The term *harmonics,* which describes the distortion of a waveform, is one of the most popular terms in the area of electrical power systems quality. When electronic power converters first became commonplace in the late 1970s, many utility engineers became quite concerned about the ability of a power system to accommodate harmonic distortion. Many negative predictions were made about the fate of power systems if these devices were permitted to exist [1].

However, over the years until the start of the 21st century, it turned out harmonic problems were not actually very numerous on utility systems. Only a small percentage of the utility distribution feeders in North America had harmonics problems severe enough to require attention [2]. The reason for the overstated worry at the first place is quite obvious, by then, major harmonic sources (such as big factory and commercial building) were always known to utility. This deterministic harmonic condition allowed engineers to easily isolate those harmonic sources from the distribution system. Thus, harmonic mitigation initially faced few technical barriers, until that time.

However, after the beginning of the 21st century, the dramatic proliferation of non-linear residential loads prompted new concerns about harmonic distortion, and the old pessimistic concern seemed to be coming back [3]. One of the main

differences between the earlier harmonic source and the current ones is that the latter are smaller and being more distributed than the former large lumped harmonic sources.

This trend is leading to a totally different modern harmonic problem, which is becoming urgent. The harmonic voltage and current distortion levels are exceeding today's allowable distortion limits and already causing severe problems. In this introductory chapter, the harmonic situation in today's distribution system will be described, and an overview of harmonics-related issues will be presented. A brief survey of harmonic-assessment methods and mitigations will also be provided. Today's challenges are then introduced and discussed.

Finally, this chapter presents this thesis's research objectives and outline.

1.1.   Harmonic Situation in Today's Distribution Systems

The study of harmonics in distribution systems was traditionally focused on the analysis of networks with dominant harmonic sources at known locations. These source are usually associated with large individual industrial loads [3] [6].

However, today's distribution systems are facing a totally new harmonic challenge: the widespread use of electronics-based home appliances. Figure 1.1 shows the harmonic current spectrum of different brands' CFLs. The horizontal solid line is the harmonic compatibility level defined for lighting equipment by

IEC 61000-3-2 [29]. This standard assesses and sets the limit for equipment drawing input current $\leq$ 16A per phase. Figure 1.1 shows that the home appliances in North America do not actually comply with IEC 61000-3-2, and that their emitting harmonic current is usually much higher than this standard's limits.
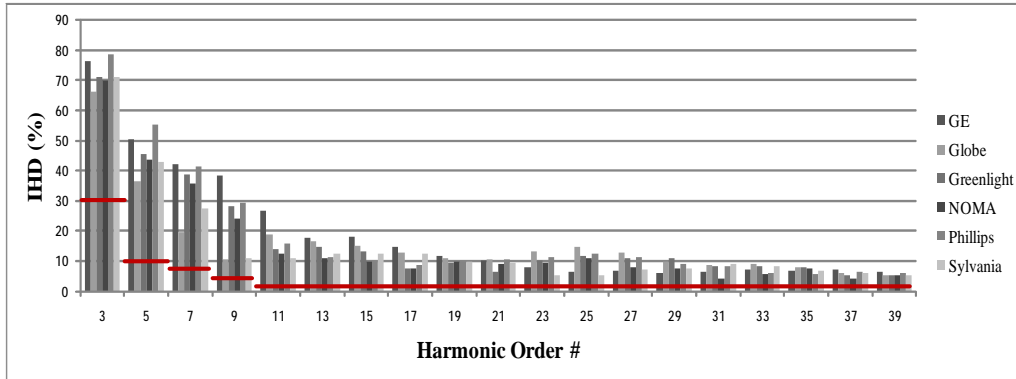
Figure 1.1 Harmonic spectrum of different brands' CFLs

Because of their energy-saving ability, the use of electronics-based home appliances is increasing more swiftly than ever before. According to [30], in the last ten years, 25% traditional incandescent lamps have been replaced by compact fluorescent lamps (CFLs), and more than 40% more are expected to be upgraded to CFLs in the next decade. As this relative amount increases, the impact of the current harmonics from the collective load of mass-installed CFLs may become noticeable [31] [32]. Therefore, harmonic problem in today's distribution systems is becoming worse.

Figure 1.2 shows the typical spectrum of a 3MW service transformer measured in 2008, in Edmonton, AB. The horizontal solid line is the harmonic limits defined

in IEEE std. 519-1992 for an industrial load with the same power[1] as that in the investigated neighborhood. Therefore, the injected harmonic current from today's residential neighborhoods already exceeded the standard for an industrial load. This finding clearly indicates that aggregated residential loads must be treated seriously in terms of harmonic injection, in the same way that industrial loads have been treated.
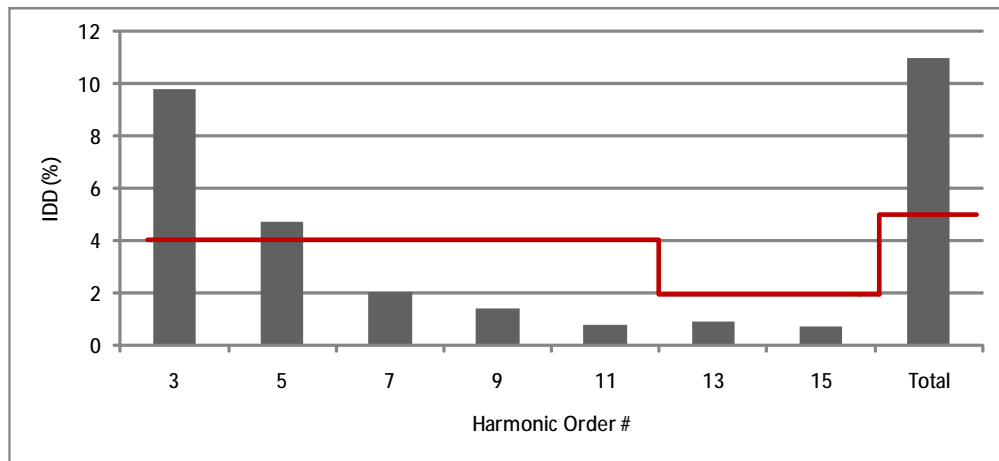
Figure 1.2 Typical spectrum of a service transformer

The following harmonic-related problems have been found in today's distribution systems:

- Stress on cables: harmonics cause voltage and current stress on power cables and lead to dielectric failure [4].

---

[1] When $I_{SC}/I_L<20$, where I_{SC} is the maximum short-circuit current at PCC, I_L is the maximum demand load current at PCC.

- Shortening of capacitor life: power factor correction capacitors provide low shunt impedance for high-order harmonics. Harmonic currents flowing through capacitor banks can increase the dielectric loss and thermal stress. When this stress is excessive, the capacitor can be overloaded, and damage may occur [6].

- Amplification due to resonance: amplification of harmonic levels resulting from series and parallel resonances can occur as capacitors are added to the power system. If voltage amplification occurs, magnified harmonic currents will also exist in the resonant circuit [7].

- Premature ageing: the insulation of electrical plant components can age prematurely [8].

- Losses and pulsating torque on electrical machines: in rotating machines, losses increase due to harmonics, and overheating may happen as a result [9]. Pulsating torques can be produced, resulting in a higher audible noise [7].

- Transformer overheating: in transformers, the primary effect is the additional heat generated by the losses caused by the harmonic content of the load current. Delta-connected windings can be overloaded by the circulation of zero-sequence harmonic currents [10]-[12].

- Telephone interference: harmonic effects have also been observed to degrade communication system performance due to interference caused by power system harmonics with the communication system frequency [7].

- Malfunction of electronic loads: power electronic loads sensitive to AC supply voltage characteristics, such as zero crossing, can malfunction [12], [28].

- Metering errors: metering and instrumentation can be affected by harmonic components [4], [12].

1.2.   Methods for Harmonic Assessment and New Challenges

Harmonic power system analysis basically requires the same type of information as that required for the analysis of the system under steady-state conditions. The exception to this requirement is the harmonic current source, which must be studied through appropriate models to represent non-linear harmonic characteristics and interaction with the primary system. A precise representation of the power system elements will be necessary if an accurate prediction of the harmonic response is required. Figure 1.3 shows the component blocks of harmonic assessment. As it shows, models for harmonic sources and models for network components are the two key issues for harmonic assessment.
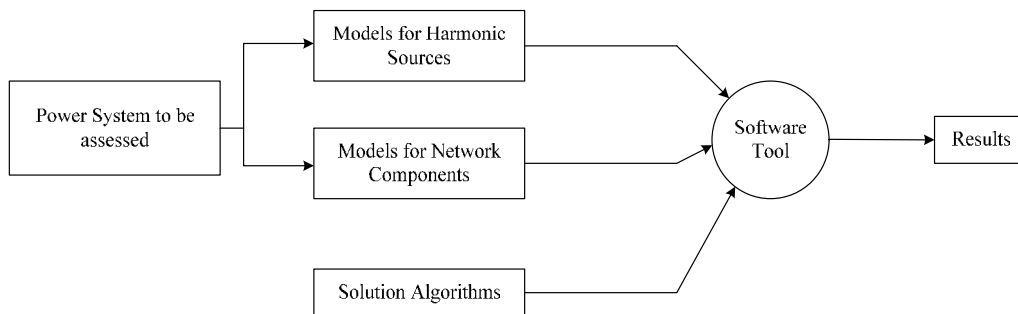
Figure 1.3 Harmonic assessment procedure diagram

1.2.1   Models for Harmonic Sources

In general, harmonic sources are a type of load in power systems. Examples are variable frequency drives (VFDs) and industry facilities. Previously, these big harmonic-generating loads in a distribution system were known to utilities and their specifications were also available. Therefore, reference [13]-[17] proposed an accurate harmonic model for a specific non-linear load in either the time domain or the frequency domain. This kind of model is precise, but complicated and requires the detailed information of each specific load, but such information cannot be obtained for systems. The increased use of modern home appliances (non-linear loads) makes it impossible to include a detail and precise model for each home appliance in a system.

Reference [18]-[22] realized this problem and started to use the concept of the "aggregate harmonic load." This kind of model no longer considers each appliance at the bottom. Measurements at the PCC (Point of Common Coupling) are required to build up the model. The idea is to use various statistics tools to fit the measurement data in order to obtain a stochastic harmonic model. Due to the load type change and different operation conditions under each PCC, a representative stochastic harmonic model requires a large number of measurement samples at each PCC. Every time a new model is needed, measurements are also needed. On the other hand, a stochastic model considers each harmonic condition as a component of a total random event, which hides the nature of the harmonic mechanism behind it. This situation limits the understanding of how harmonics

build up in today's distribution systems. Therefore, a more generic and physically meaningful harmonic load model is needed for today's distribution system harmonic analysis.

1.2.2   Models for Distribution Network

As stated above, many of the harmonic problems encountered in a distribution system in North America are related to the system's special network configuration, such as neutral potential voltage rise and telephone interference.

Figure 1.4 shows the layout of a typical multi-grounded distribution system in North America. This kind of distribution system is generally grounded at various locations across the system. According to the National Electric Safety Code [23], the neutral conductor needs to be grounded at least four times per mile to qualify as a multi-grounded system. Grounding refers to the intentional connection of a system component to the earth by means of a conductor. The objectives of grounding are to ensure the proper operation of a system and the safety of the line workers, public and animals. However, grounding can affect the power system performance and power quality. The multi-grounded nature of a [24]-[26] distribution system often complicates its performance analysis as well.

On the other hand, the single-phase service transformer with two windings at the secondary side is the typical transformer adopted in North America (as shown in Figure 1.4). The grounding of the service transformer and the house grounding at

the secondary side further complicate the configuration of the distribution network.
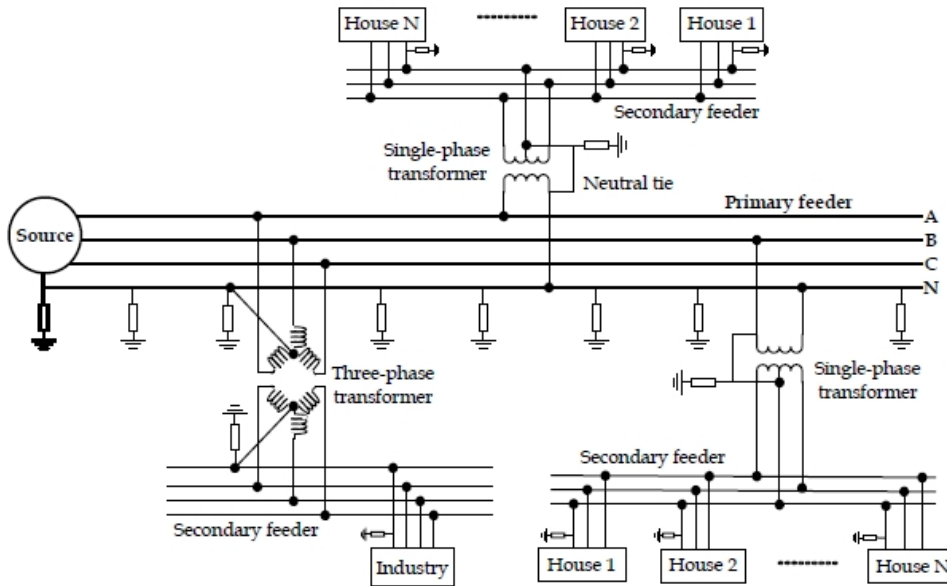
Figure 1.4 Layout of multi-grounded distribution system

The multi-grounded distribution system, as stated above, has complications and causes problems. Multi-grounding complicates the system design, especially in terms of satisfying the power quality and safety requirements. Both theoretical and technical challenges are associated with the performance analysis. The symmetrical-components-based techniques used previously cannot be applied to the analysis of the multi-phase systems with a multi-grounded neutral because these techniques do not recognize the mutual coupling effects and the neutral network. In the presence of a neutral conductor, these models combine its impedance with the impedances of the phase conductors and treat the grounding resistances as zero, i.e., as a solidly grounded neutral. Therefore, multi-phase

(including neutral grounded system) harmonic analysis is needed for today's distribution system harmonic analysis.

1.3.   Methods for Harmonic Mitigation and New Challenges

Two methods of harmonic mitigation have been tried: system modifications and the use of filtering devices.

System modification has been considered as a potential method for controlling harmonic distortion. In section 1.2.2, the complications of distribution configuration were described. The multi-grounded system introduced many system variables that may affect the power quality problems. Few studies have been done to investigate this issue. When the harmonic sources are all through a system, this problem becomes even more complicated and challenging.

The other common previous method for harmonic mitigation is the use of passive filtering techniques applied to the PCC of big harmonic loads [27]. Therefore, the effectiveness of the installed filter was easily checked and evaluated. This work was based on the fact that harmonic loads were known to utilities. This situation totally changed due to the wide-spread use of nonlinear home appliances. It is impossible to install a filter for each service transformer, and even for each house. Determining where to install the filter to maximize its effectiveness becomes a major challenge.

Excessive neutral harmonic currents resulting in telephone noise, conductor and transformer heating, voltage distortion, are becoming the most important issue to be considered in power distribution systems. How to mitigate zero sequence harmonics is drawing increasing attention, and has become another challenge for harmonic control in today's distribution systems.

1.4.   Thesis Objectives

The scope of this thesis is the study of the harmonic impact of residential non-linear sources on a distribution power system. As stated above, the mass penetration of energy-efficient consumer electronic devices is resulting in significant distortions to the voltage and current waveforms in power distribution systems. This new emerging situation is of great concern to the utility industry. Some key questions are:

- Is the current distribution system capable of accepting more nonlinear loads?

- What could be the consequences of excessive harmonic loads?

- How can the situation be managed?

In this context and considering the new challenges mentioned in section 1.4, the overall objective of this thesis is to provide technical information, study results and solution options to develop a proactive strategy for dealing with today's

distribution systems and problems caused by the modern nonlinear residential loads.

1.5.   Organization of the Thesis

A fundamental step towards answering the questions in section 1.4 is to develop a tool that can assess and predict harmonic distortion levels for the current and future power distribution systems. Chapter 2 proposes a simplified service transformer model based on the bottom-up house model developed in one of the projects done in the PDS-LAB, University of Alberta. This aggregated harmonic model at the transformer level can fully represent the injected harmonic features of today's service transformers in North America, due to this model's accurate measurement data for modern home appliances used in the bottom level of the bottom-up house model. The key difference between this model and the statistical model in reference is that the new model is more physically meaningful, and provides more information for understanding how the harmonics build up in today's distribution systems.

As stated in section 1.2.2, modern power distribution systems in North America are adopting multi-grounded neutral configurations. The presence of the neutral conductor and its grounding arrangement make it difficult to understand and characterize the system's harmonic behavior. Examples are telephone interference and stray voltage problems when the system experiences excessive harmonics in

normal operating conditions. Chapter 2 also describes the detail of how to model a MGN distribution system.

At the distribution level, this thesis will try to answer the following questions:

1) What are the potential power quality impacts of mass distributed nonlinear loads on power distribution systems? The example impacts include voltage distortion, zero sequence harmonics, neutral voltage/current rise, harmonic-caused stray voltages, telephone inference, and increased losses. The following is a more detailed list:

  - harmonic voltage and current distortion levels in the system, in both positive and zero sequences;

  - telephone interference in the form of IT factors;

  - neutral current/voltage rise and associated stray voltage potentials;

  - impact of harmonics on line losses; and

  - overloading of feeder and substation capacitors (fuse blow).

2) How serious will the impacts become when more and more energy-efficient appliances and consumer electronics are used in the residential loads? What are the technical and economic implications for utilities?

3) If the consequences are serious, what are the strategies and options available for utilities to manage the problem? The strategies may include rate mechanisms for cost-recovering and the establishments of connection standards and limits.

Chapter 3 performs a base case study on an ideal case and an actual case network, as well as load evolution. All the simulation studies are focused on trying to answer the above questions and on improving our understanding of today's distribution systems' harmonic characteristics. The simulation results are further compared with field measurements.

As stated in section 1.3, traditional harmonic mitigation is no longer efficient and capable of handling today's excessive harmonic problems in residential distribution systems. The locations of harmonic sources are unknown, they are scattered everywhere through the system. All these problems make harmonic mitigation strategies complicated for utilities.

In Alberta, Canada, more than three utility companies have been experiencing the excessive harmonic problems (telephone interference is the usual symptom) in residential distribution systems. Various mitigation methods have been conducted to try to solve these problems, including balancing the loads among three phases, fixing the broken neutral, and installing more grounds. However, no theory supports these mitigation methods, so the utilities have no guidelines to follow.

No clear research study so far has reported either if those methods are really workable, or to what extent they might work. The first part of Chapter 4 performs various sensitivity simulations to test these methods' feasibility, and more analysis follows to explain each phenomenon.

Neutral harmonic currents as stated in section 1.3 are becoming the most important consideration in power distribution systems. Chapter 4 proposes a zero sequence filter to deal with excessive zero sequence harmonic currents. Its effectiveness is carefully studied.

The main conclusions from this thesis and suggestions for future studies and improvements are presented in Chapter 5.

Chapter 2

Modeling and Simulation of Distribution System

The mass penetration of both energy efficient and consumer electronic devices into residential homes are resulting in significant distortions to the voltage and current waveforms in power distribution systems. To investigate the collective harmonic impacts of the distributed home appliances on today's distribution system, an accurate and reliable system-wide model is needed. This includes harmonic load model and primary distribution system model. These two modeling is discussed in the first section of this chapter. Then the second section gives the detail of the simulation procedure.

2.1. Distributed Harmonic Source Modeling

In order to evaluate the impact of distributed nonlinear residential loads on primary power distribution systems, a harmonic model at service transformer level is needed. Take advantage of the so-called bottom-up harmonic model for residential house developed by PDS-LAB in University of Alberta, the same strategy has been applied to get the service transformer harmonic model. The key idea is to somehow combine multi-house harmonic models into one aggregated harmonic model.

Figure 2.1 shows the pyramid like structure, with various home appliances on the bottom, house next, and then service transformer on the top. The service transformer harmonic model is built up in the similar way of building up a pyramid.
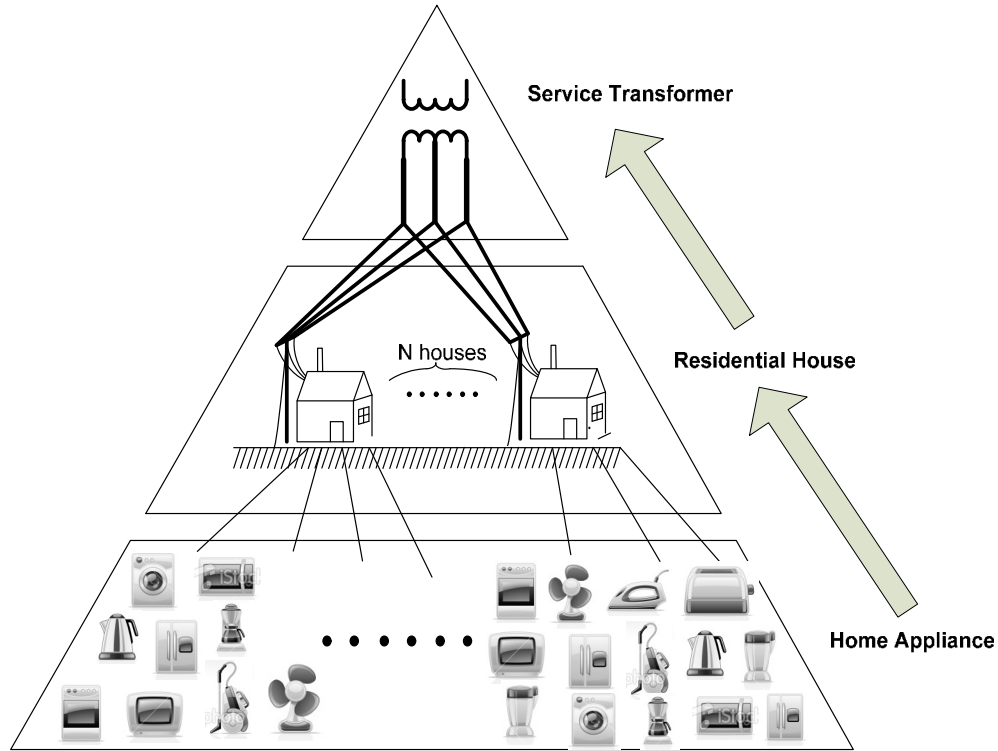
Figure 2.1 Pyramid structure of bottom-up service transformer harmonic model

In view of the available data from other research institutions about the penetration level of the main home appliances in the future (Appendix A), the trend information is also involved in the home appliance harmonic model, which, in turn, is integrated into our service transformer harmonic model. This is very useful and essential because the utility could be fully prepared before something

really bad happen if they are aware of how the harmonic voltage/current levels in

the network will change in the next 5 or 10 years.

2.1.2.1. Multi-House harmonic Load Model

To build up the harmonic model at service transformer level, multi-house

harmonic load model is needed as the bottom "bricks". Appendix A gives the

detailed information about how a bottom-up single-house harmonic model is built

up. With this bottom-up single-house harmonic model, the multi-house harmonic

load model is developed in this section.

The model structure of bottom-up single-house harmonic model is shown in

Figure 2.2. It consists of two Norton equivalent circuit model under each phase,

and one linear impedance between two phases[2].
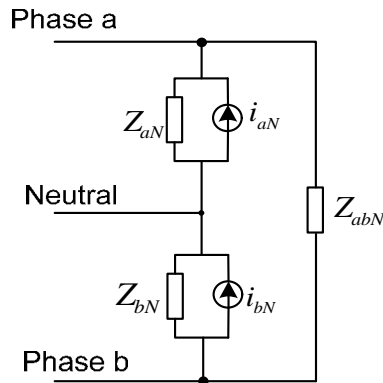
Figure 2.2 Bottom-up house harmonic model

---

[2] Each house has loads connected to phase a, phase b and between phase a & b. Appliances connected between phase a & b are practically linear, that is why it is assumed there is no harmonic current source.

It is noted that a bottom-up single-house harmonic model is a time series model, which means each parameter in Figure 2.2 is a function of time over a day.

As show in Figure 2.3, residential houses are supplied through single-phase distribution (service) transformers connecting the primary to the secondary system and are modeled by the standard North American single-phase transformer [34]. The standard secondary load service is a 120/240 V three-wire service. Each distribution transformer normally supplies ten to twenty customers. Due to this relationship, the bottom-up house harmonic model (as shown in Figure 2.2) may have the potential to combine to a transformer model.
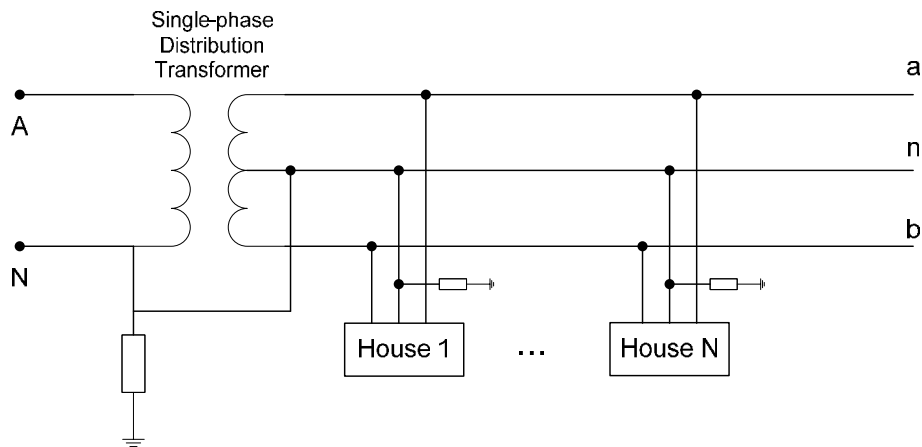
Figure 2.3 Typical service transformer connected to N houses

The basic structure of the multi-house harmonic model is combining each house harmonic model, shown in Figure 2.3, in parallel to create the transformer equivalent circuit in Figure 2.4.
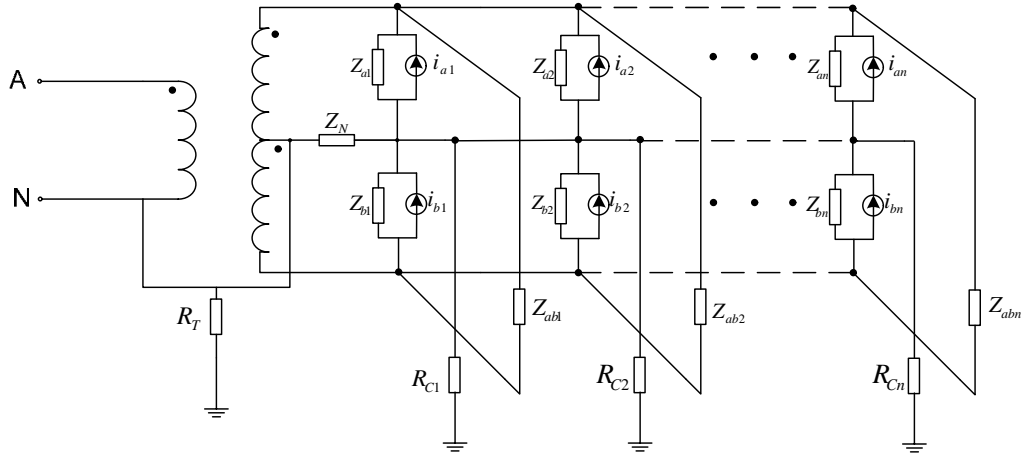
Figure 2.4 Multi-house equivalent model

The steps for the bottom-up multi-house modeling are as follows:

1. 10-20 house harmonic models are randomly generated as components of the transformer model by bottom-up signle-house harmonic model.

2. Connect the house models into the circuit shown in Figure 2.4. The connected house linear impedances are paralleled as a new linear impedance Z_{trans} and the nonlinear current sources are added up together generating a new current source $I_{NL\text{-}trans}$.

The final output of the simulation is the total multi-house current for phase a $i_{aN}(h)$ and for phase b $i_{bN}(h)$ in both fundamental and harmonic, and linear impedance connected to phase a Z_{aN}, to phase b Z_{bN} and between phase and phase b Z_{abN}, as shown in Figure 2.5.
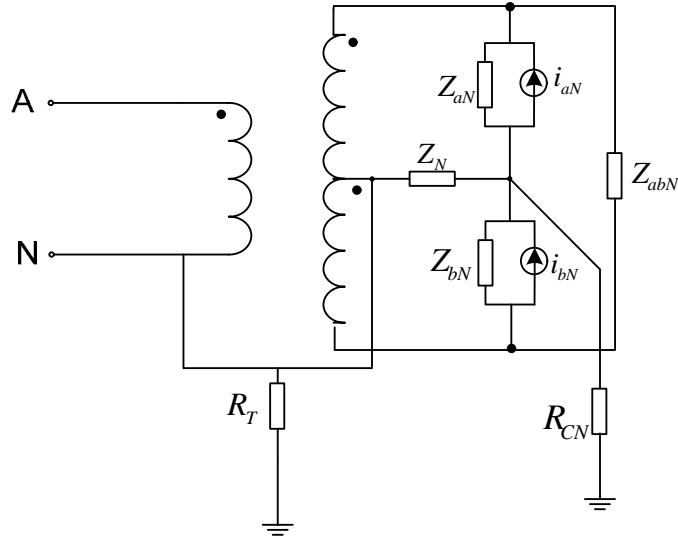
Figure 2.5 The residential distribution multi-house model

2.1.1. Modeling of Service Transformer

Now the bottom-up multi-house model is almost built up except the pyramid top, which is the service transformer harmonic model. In order to reduce the complexity of the harmonic power flow simulations a simplified model including both the service transformer and the houses connected is proposed. This simplification is very important when one needs to perform a system-wide harmonic simulation. A typical distribution feeder in North America comprises around 500 service transformers. To include all the details of the secondary side of each service transformer would make the whole model at system level very complicated, unreliable, and not necessary as well. In addition, computation time would be dramatically increased due to the detail model of secondary side, which is not under our concern.

2.1.3.1. Service Transformer Model Simplification Procedure

Figure 2.6 shows the circuit configuration of a typical service transformer [35]. The neutral line of primary side and secondary side are short circuited, and further grounded with a resistor R_T. Z_N is the secondary neutral line impedance. R_C is the house grounding impedance. Loads are connected between *+120V* line, *-120V* line and neutral. The harmonic model (i.e. Z_a, i_a and Z_b, i_b and Z_{ab}) can be acquired from the bottom-up harmonic source model, as discussed in last section. They are treated as known variables here. P, N and G on the left hand represent the common points connected to primary system's phase, neutral and ground respectively.
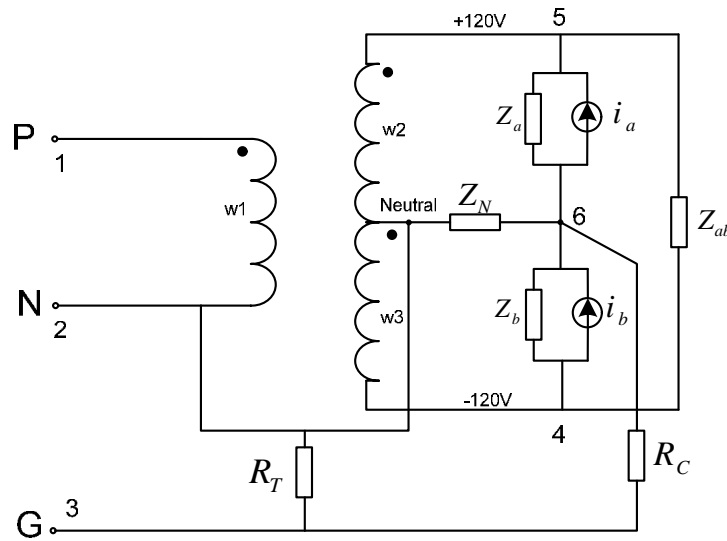
Figure 2.6 Service transformer connected to the harmonic house model

The three-winding service transformer can be mathematically represented by the following equation [36]:

$$V_w^{pu} = Z_w^{pu} I_w^{pu}$$

Equation 2.1

Where V_w^{pu}, Z_w^{pu} and I_w^{pu} are per-unit values of the voltage, impedance and current of the winding w_1, w_2 and w_3, as shown by equations below [37]:

$$V_w^{pu} = \begin{bmatrix} V_{w1}^{pu} & V_{w2}^{pu} & V_{w3}^{pu} \end{bmatrix}$$

Equation 2.2

$$I_w^{pu} = \begin{bmatrix} I_{w1}^{pu} & I_{w2}^{pu} & I_{w3}^{pu} \end{bmatrix}^T$$

Equation 2.3

$$Z_w^{pu} = \begin{bmatrix} Z_p^{pu} + Z_m^{pu} & Z_m^{pu} & Z_m^{pu} \\ Z_m^{pu} & Z_s^{pu} + Z_m^{pu} & Z_m^{pu} \\ Z_m^{pu} & Z_m^{pu} & Z_s^{pu} + Z_m^{pu} \end{bmatrix}$$

Equation 2.4

Where Z_P^{pu} and Z_S^{pu} are the leakage impedance in per unit of the primary and secondary side of the transformer, respectively. Z_m^{pu} is the magnetizing impedance, which can be neglected since it is much larger compared to Z_P^{pu} and Z_S^{pu}.

The parameters Z_P^{pu} and Z_S^{pu} can be obtained from the nameplate impedance of the transformer $(R_T^{pu} + X_T^{pu})$ through the following equations [38]:

$$Z_P^{pu} = 0.5R_T^{pu} + j0.8X_T^{pu}$$

<div align="right">Equation 2.5</div>

$$Z_s^{pu} = R_T^{pu} + j0.4X_T^{pu}$$

<div align="right">Equation 2.6</div>

To transform these per unit values into physical ones, the following transformation needs to be used:

$$I_w^{pu} = U_I I_w$$

<div align="right">Equation 2.7</div>

$$V_w^{pu} = U_v V_w$$

<div align="right">Equation 2.8</div>

in which:

$$U_I = diag\left\{\frac{1}{I_{w1}}, \frac{1}{I_{w2}}, \frac{1}{I_{w3}}\right\}$$

<div align="right">Equation 2.9</div>

$$U_V = diag\left\{\frac{1}{V_{w1}}, \frac{1}{V_{w2}}, \frac{1}{V_{w3}}\right\}$$

<div align="right">Equation 2.10</div>

where I_{wk} and V_{wk} are the current and voltage base values of the kth winding. Therefore,

$$v_w = Z_w I_w$$

<div align="right">Equation 2.11</div>

$$Z_w = U_V^{-1} Z_w^{pu} U_I$$

Equation 2.12

The admittance matrix of three windings then would be as follows:

$$Y_w = Z_w^{-1}$$

Equation 2.13

Apart from the three branches of the transformer (three windings), there are six other branches, represented by R_T, R_C, Z_N, $Z_a I_a$, $Z_b I_b$ and Z_{ab}. Therefore, without considering the branch connections, the Y matrix of all branches is as follows [39]:

$$Y_B = \begin{bmatrix} Y_w & 0 \\ 0 & diag\left\{ \begin{bmatrix} \dfrac{1}{R_T} & \dfrac{1}{Z_N} & \dfrac{1}{Z_a} & \dfrac{1}{Z_b} & \dfrac{1}{Z_{ab}} & \dfrac{1}{R_C} \end{bmatrix} \right\} \end{bmatrix}_{9 \times 9}$$

Equation 2.14

To transform branch Equation 2.14 into nodal equation (there are totally 6 nodes, as marked in Figure 2.6), the incidence matrix is defined:

$$T_v = \begin{bmatrix} t_{ij} \end{bmatrix}_{9 \times 6}$$

Equation 2.15

Where the subscripts '9' and '6' refer to the number of nodes and branches, respectively. The values of t_{ij} are defined as follows,

t_{ij}

$$= \begin{cases} 1 & \text{if node j is connected to branch i and the branch current flows to j} \\ -1 & \text{if node j is connected to branch i and the branch current flows from j} \\ 0 & \text{otherwise} \end{cases}$$

<div align="right">Equation 2.16</div>

Therefore, for the transformer configuration shown in Figure 2.6:

$$T_V = \begin{bmatrix} -1 & 1 & 0 & 0 & 0 & 0 \\ 0 & 1 & 0 & 0 & -1 & 0 \\ 0 & -1 & 0 & 1 & 0 & 0 \\ 0 & 1 & -1 & 0 & 0 & 0 \\ 0 & 1 & 0 & 0 & 0 & -1 \\ 0 & 0 & 0 & 0 & 1 & -1 \\ 0 & 0 & 0 & -1 & 0 & 1 \\ 0 & 0 & 0 & -1 & 1 & 0 \\ 0 & 0 & -1 & 0 & 0 & 1 \end{bmatrix}$$

<div align="right">Equation 2.17</div>

Nodes voltage and current can be obtained by using the incident matrix, as follows:

$$V_B = T_V V_N$$

<div align="right">Equation 2.18</div>

$$I_N = T_V^T I_B$$

<div align="right">Equation 2.19</div>

where the subscript *B* refers to branch and the subscript *N* to node.

Finally, the admittance nodal matrix can be represented as follows:

$$Y_N = T_v^T Y_B T_v$$

Equation 2.20

In order to investigate the equivalent circuit seen from primary system (i.e. *P*, *N* and *G* ports), we need to eliminate the internal three notes (node 4, 5 and 6). The nodal equations are:

$$\begin{bmatrix} I_{PN} \\ I_{inter} \end{bmatrix} = \begin{bmatrix} Y_{11_{2\times2}} & Y_{12_{2\times3}} \\ Y_{21_{3\times2}} & Y_{22_{3\times3}} \end{bmatrix} \begin{bmatrix} V_{PN} \\ V_{inter} \end{bmatrix}$$

Equation 2.21

where, Y_{11}, Y_{12}, Y_{21} and Y_{22} are the sub-matrix of Y_N, $V_{PN} = [V_P \ V_N]^T$, $V_{nter} = [V_4 \ V_5 \ V_6]^T$, $I_{PN} = [I_P \ I_N]^T$, $I_{inter} = [I_4 \ I_5 \ I_6]^T$.

According to Figure 2.6, I_{inter} is known,

$$I_{inter} = \begin{bmatrix} -i_b \\ i_b \\ -i_a + i_b \end{bmatrix}$$

Equation 2.22

Eliminating V_{inter}, Equation 2.21 can be simplified to:

$$\left[Y_{11} - Y_{12}Y_{22}^{-1}Y_{21} \right] V_{PN} = I_{PN} - \left[Y_{12}Y_{22}^{-1} \right] I_{inter}$$

Equation 2.23

Equation 2.23 gives the matrix format of nodes P and N (G is the reference node, so it is not included in the matrix). A new equivalent Y matrix can be defined as:

$$Y_{eq} = Y_{11} - Y_{12}Y_{22}^{-1}Y_{21}$$

Equation 2.24

and the current source:

$$I_S = \left[Y_{12}Y_{22}^{-1} \right] I_{inter}$$

Equation 2.25

In order to separate harmonic current source i_a, i_b, the following expression can be obtained:

$$I_S = Y_{12}Y_{22}^{-1} \left(\begin{bmatrix} 0 \\ 1 \\ -1 \end{bmatrix} i_a + \begin{bmatrix} -1 \\ 0 \\ 1 \end{bmatrix} i_b \right) = a \cdot i_a + b \cdot i_b$$

Equation 2.26

From the mathematical development above, the equivalent circuit shown in Figure 2.7 is then proposed.
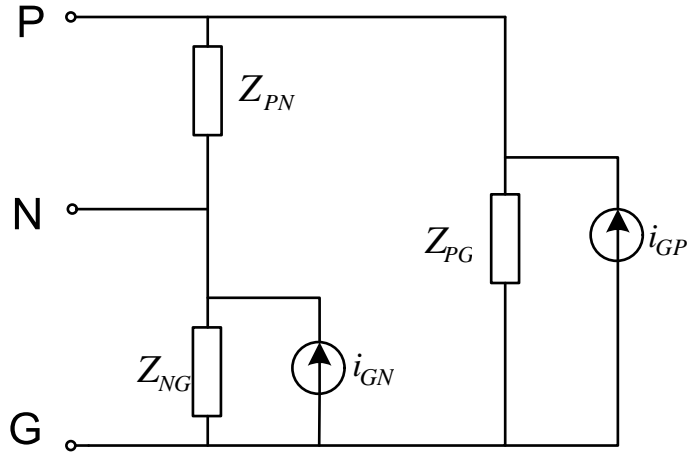
Figure 2.7 Simplified model of the distribution transformer

There are five parameters in this model, which are Z_{PN}, Z_{NG}, Z_{PG}, i_{GN} and i_{GP}. The nodal admittance matrix of the simplified model circuit is given by:

$$\begin{bmatrix} I_P + i_{GP} \\ I_N + i_{GN} \end{bmatrix} = Y_{SM} \begin{bmatrix} V_P \\ V_N \end{bmatrix} = \begin{bmatrix} \dfrac{1}{Z_{PN}} + \dfrac{1}{Z_{PG}} & -\dfrac{1}{Z_{PN}} \\ -\dfrac{1}{Z_{PN}} & \dfrac{1}{Z_{PN}} + \dfrac{1}{Z_{NG}} \end{bmatrix} \begin{bmatrix} V_P \\ V_N \end{bmatrix}$$

Equation 2.27

Comparing admittance matrix Y_{eq} in Equation 2.24 and Y_{SM} in Equation 2.27, we have:

$$Y_{SM}(1,1) = Y_{eq}(1,1)$$

Equation 2.28

$$Y_{SM}(2,2) = Y_{eq}(2,2)$$

Equation 2.29

$$Y_{SM}(1,2) = -Y_{eq}(1,2)$$

Equation 2.30

According to the Kirchhoff's circuit law at nodes in the simplified model:

$$i_{GP} = -\left(a(1)\cdot i_a + b(1)\cdot i_b\right)$$

Equation 2.31

$$i_{GN} = -\left(a(2)\cdot i_a + b(2)\cdot i_b\right)$$

Equation 2.32

Therefore, from the service transformer impedance $(R_T^{pu} + X_T^{pu})$ and from the data of the target harmonic source, the five parameters in the simplified model can be acquired from Equation 2.28 to Equation 2.32.

2.1.3.2. Simplified Model Validation

The service transformer simplified model developed in the above section is compared against the complete configuration in order to validate its accuracy. Both circuits are built on the toolbox *Simulink* from Matlab, as shown in Figure 2.8.

One case scenario is chosen for simulation. Table 2.1 shows the values of Z_a, Z_b, Z_{ab}, i_a, i_b for that scenario:
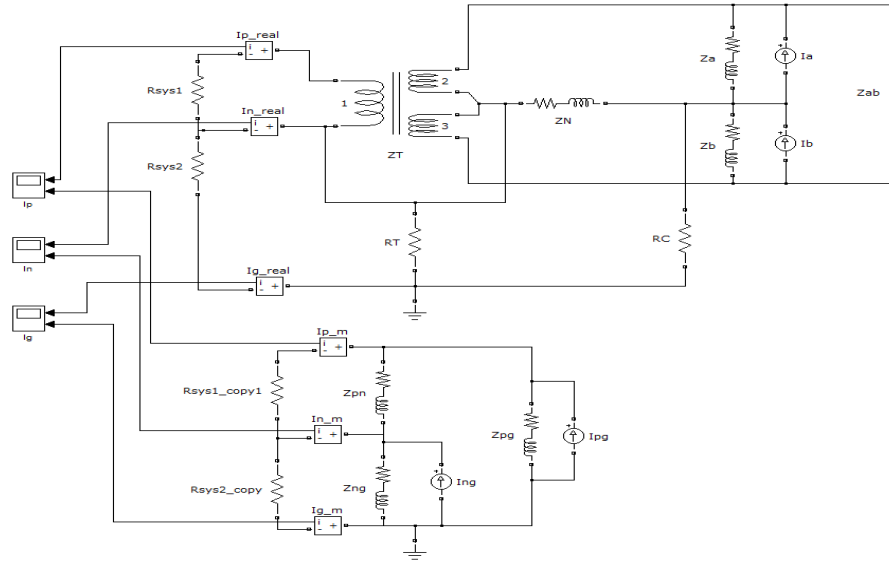
Figure 2.8 Complete and simplified service transformer models in Simulink

Table 2.1 Parameters for the validation scenario

Parameters	Values
Z_a	20.2417+0.0525i (ohm)
Z_b	26.9889+0.07i (ohm)
Z_{ab}	23.98+0.39i (ohm)
i_a	-2.8624 (A)
i_b	24.0308 (A)

Based on the mathematical development for the simplified transformer model, presented in above section, the corresponding parameters (i.e. Z_{PN}, Z_{PG}, Z_{NG}, i_{PG}, i_{NG}) in the simplified model can be found and are shown in Table 2.2:

Table 2.2 Parameters for the simplified model

Parameters	Values
Z_{PN}	6.0632e4+3.5123e3i (ohm)
Z_{NG}	3.7808+0.0202i (ohm)
Z_{PG}	6.2975e5-4.0495e5i (ohm)
i_{PG}	0.1763-0.0002i (A)
i_{NG}	-0.4695-0.1901i (A)

Figure 2.9 shows the validation results by comparing the currents I_p, I_n and I_g for both complete and simplified transformer models. The simulations show that the simplified circuit gives out the same output currents as the complete model. Furthermore, the impedance seen from port *P*, *N* and *G* show the same value for both circuits.
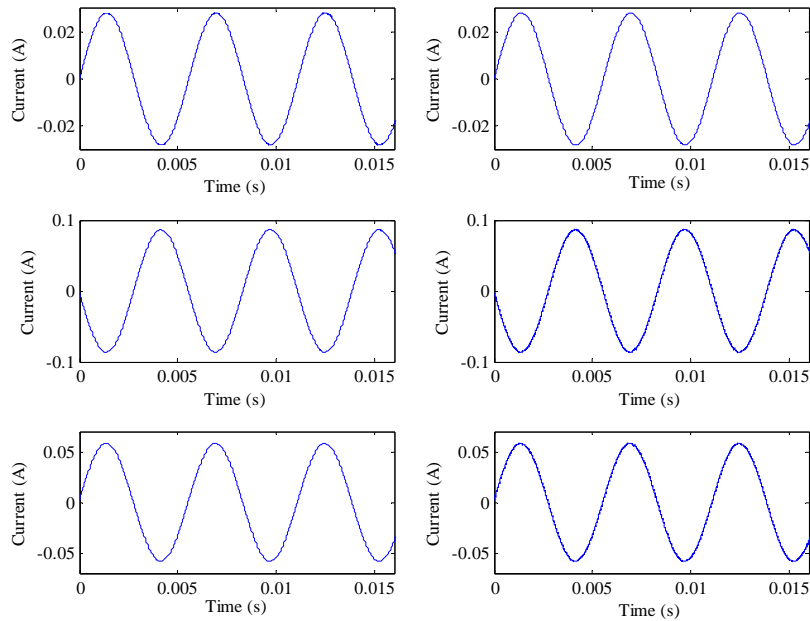
Figure 2.9 Validation results

2.1.2. Modeling of Distribution System

Now we have built up the whole service transformer harmonic model, to perform the system-wide simulation, we need to develop a distribution network model to analyze the impact of the distribution nonlinear loads on the primary distribution system.

The objective is to analyze the impact of the harmonic loads on the primary system. Telephone interference will be one of the issues needed to be carefully investigated. Therefore, a detailed multi-phase system model is required. In this context, the network configuration shown in Figure 2.10 is adopted for the primary system harmonic analysis. This model is called ideal case in this thesis.
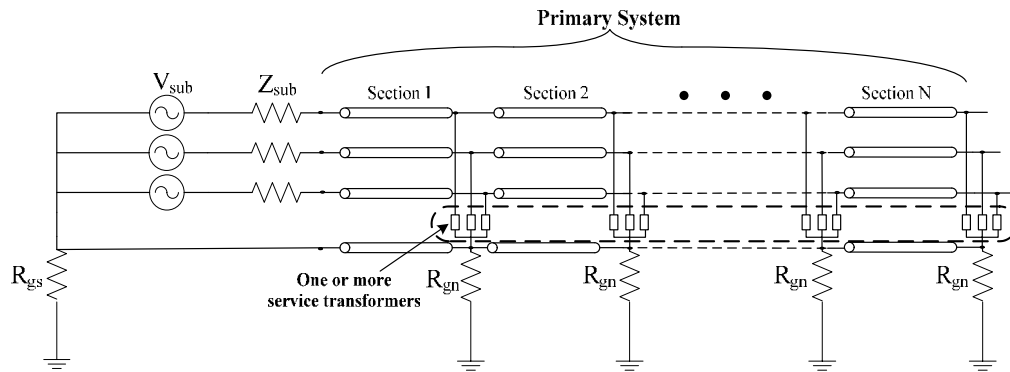
Figure 2.10 Distribution network model to study the impact of the harmonic loads on the primary system

In Figure 2.10, the portion of the network inside the dashed rectangle represents one or more service transformers connected to the secondary system composed of several residential homes, which is represented by the simplified model proposed in section 2.1.1.

As shown in Figure 2.10, the general configuration of the primary distribution system adopted for the simulations is a four-wire, multi-grounded system (three-phase conductors plus a multi-grounded neutral).

The loading of a distribution feeder is inherently unbalanced because of the large number of unequal single-phase loads that must be served. Because of the nature of the distribution system, conventional power-flow and short-circuit programs used for transmission system studies are not adequate. Multiphase harmonic power flow [40] is employed to simulate several case scenarios for this type of configuration in order to evaluate the impact of the distributed nonlinear loads connected to the secondary system.

The supply system (substation) is represented by a three-phase voltage (fundamental frequency) source star connected. R_{gs} is the grounding resistance of substation grid.

The primary feeder is connected to the three-phase voltage source through a three-phase (Y_g/Y_g) substation transformer. The grounded wye-wye connection is primarily used to supply single-phase and three-phase loads on four-wire multi-grounded systems [41]. The mathematical representation used for a three-phase substation transformer, connected between node k and m, is given by Equation 2.33 [41], where Z_{aa}, Z_{bb} and Z_{cc} are the self-impedances, and Z_{ab}, Z_{bc} and Z_{ac} are the mutual impedances:

$$\begin{bmatrix} V_{ag}^k \\ V_{bg}^k \\ V_{cg}^k \end{bmatrix} = \begin{bmatrix} V_{ag}^m \\ V_{bg}^m \\ V_{cg}^m \end{bmatrix} + \begin{bmatrix} Z_{aa} & Z_{ab} & Z_{ac} \\ Z_{ab} & Z_{bb} & Z_{bc} \\ Z_{ac} & Z_{bc} & Z_{cc} \end{bmatrix} \times \begin{bmatrix} I_a \\ I_b \\ I_c \end{bmatrix}$$

Equation 2.33

Normally, the neutral wire of the primary system in most power flow software is usually merged into the phase wires using Kron reduction technique ([41],[37]). Since the neutral wire is not explicitly represented, neutral wire currents and voltages remain unknown. For the study of the impact of distributed nonlinear sources, knowing the neutral wire currents and voltages is of special interest.
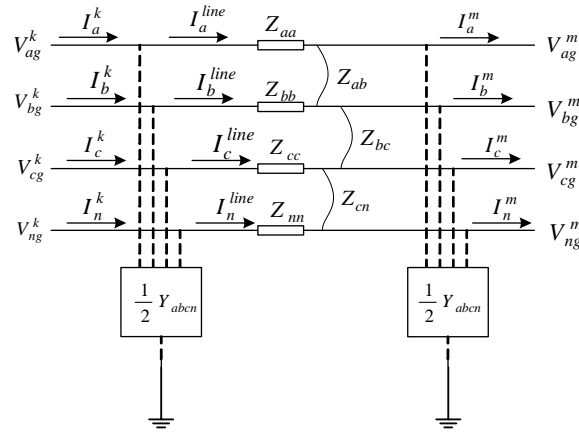
Figure 2.11 Four-wire grounded wye line segment with series and shunt component

As mentioned before, the primary feeder is represented by a four-wire multi-grounded distribution line. For the harmonic impact analysis, the line is represented by the lumped *PI* model [41], which includes both self and mutual impedances parameters. The PI model of a four-wire grounded wye distribution line is shown in Figure 2.11, including both series impedance and shunt admittance parameters. In order to facilitate the visualization of Figure 2.11, not all mutual impedances are represented, but they are taken into account as shown in equations below. Applying the Kirchhoff Current Law (KCL) in the node *k* of the line segment illustrated below, the following relationship can be found:

$$\begin{bmatrix} I_a^{line} \\ I_b^{line} \\ I_c^{line} \\ I_n^{line} \end{bmatrix} = \begin{bmatrix} I_a^{k} \\ I_b^{k} \\ I_c^{k} \\ I_n^{k} \end{bmatrix} - \frac{1}{2} \times \begin{bmatrix} Y_{aa} & Y_{ab} & Y_{ac} & Y_{an} \\ Y_{ba} & Y_{bb} & Y_{bc} & Y_{bn} \\ Y_{ca} & Y_{cb} & Y_{cc} & Y_{cn} \\ Y_{na} & Y_{nb} & Y_{nc} & Y_{nn} \end{bmatrix} \times \begin{bmatrix} V_{ag}^{k} \\ V_{bg}^{k} \\ V_{cg}^{k} \\ V_{ng}^{k} \end{bmatrix}$$

Equation 2.34

And by applying the Kirchhoff Voltage Law (KVL) between nodes *k* and *m*, we have:

$$\begin{bmatrix} V_{ag}^{k} \\ V_{bg}^{k} \\ V_{cg}^{k} \\ V_{ng}^{k} \end{bmatrix} = \begin{bmatrix} V_{ag}^{m} \\ V_{bg}^{m} \\ V_{cg}^{m} \\ V_{ng}^{m} \end{bmatrix} + \begin{bmatrix} Z_{aa} & Z_{ab} & Z_{ac} & Z_{an} \\ Z_{ba} & Z_{bb} & Z_{bc} & Z_{bn} \\ Z_{ca} & Z_{cb} & Z_{cc} & Z_{cn} \\ Z_{na} & Z_{nb} & Z_{nc} & Z_{nn} \end{bmatrix} \times \begin{bmatrix} I_a^{line} \\ I_b^{line} \\ I_c^{line} \\ I_n^{line} \end{bmatrix}$$

Equation 2.35

Furthermore, the neutral of the primary feeder is grounded at regular intervals with identical resistances (R_{gn}).

2.2. Simulation Technique

This section describes the steps necessary to perform the multiphase harmonic power flow (*MHLF*) simulations to study the impact of distributed nonlinear residential loads on the primary system. From the simulation results, it will be possible to analyze the impact of distributed nonlinear source on the following important issues:

- Harmonic voltage and current distortion levels in the system

- Telephone interference in the form of IT factors

- Neutral current/voltage rise

- Impact of harmonics on line losses;

- Overloading of substation capacitors

In order to perform the harmonic power flow simulations the following procedure is proposed:

Step 1: Determine the type of appliances per household

Step 2: From the load trend data, determine the number of appliances per household

Step 3: Generate the model for the linear and nonlinear appliances

Step 4: Determine each appliance daily usage pattern to build the harmonic single-houses model and connect the houses to the service transformers

Step 5:   Build simplified model for all service transformers, as explained on Section 2.1.3

Step 6:   For time snapshot T_1, connect the fundamental frequency component of the simplified transformer model to the primary system and run power flow

Step 7:   Shift the angle of each house harmonic current spectrum to match the fundamental frequency power flow results

Step 8:   Connect the shifted harmonic components of the simplified transformer models and run harmonic power flow. Save the results

Step 9:   Go back to Step 6, and repeat it for another time snapshot (T_2), until last snapshot

Step 10:   Go back to Step 2 for another load penetration level (load growth)

Figure 2.12 shows a flowchart illustrating these steps.

Load Trend	Secondary System Model	Fundamental and Harmonic Power Flow
Determine the appliance types per household	Model for linear and nonlinear appliances	At time T
Determine the penetration of each appliance per household	Appliance daily usage pattern	Connect the fundamental frequency component of the transformers simplified model to the primary system
	Build harmonic houses model and connect them to the service transformer	Shift the angle of harmonic current spectrum to match the fundamental load flow
	Build simplified model for all service transformers	Connect the shifted harmonic components of the simplified transformer models Run Harmonic Power Flow
		$T = T_{i+1}$

Figure 2.12 Simulation technique to study the impact of the harmonic loads on the primary system

2.3. Summary

In this Chapter, a service transformer harmonic model has been built up based on the bottom-up house model. The final model is a three-port Norton equivalent circuit model, as shown in Figure 2.7. All the parameters in this model are in format of time series, which also means they are the function of time over a day.

The multi-grounded distribution system was then introduced. Due to the neutral condition is the special interest in this thesis, it has been modeled in multi-phase harmonic load flow software (*MHLF*). Based on these two models, a system-wide harmonic simulation can then be performed. The procedure of this simulation has also been detailed described.

Chapter 3

Simulation Study Results

The objective of this chapter is to investigate the impact of the distributed nonlinear residential loads on the primary distribution system harmonic levels. This chapter provides a systematic analysis of different power quality indices used to quantify different harmonic distortion problems of primary distribution systems. The harmonic power flow simulations are performed considering the distribution network modeled on Chapter 2, which is referred to as an ideal feeder. Several case studies are analyzed in order to have a better understanding about how the increasing residential load penetration affects the harmonic levels of the distribution system. In this part, the simulation results are also compared with the field measurements conducted from 2008 to 2011, in Alberta, Canada.

An actual case model[3] was also built up, and various simulations were conducted. The results are compared with the ideal case to confirm its rationality.

3.1. Study Scenarios

This section gives an overview about the different case study scenarios to be conducted in this chapter. Each case study provides different types of information

---

[3] This real case is based on a typical distribution system in Edmonton, Canada

aiming to understand the current and the future impact of the nonlinear residential loads. The following study scenarios are evaluated:

- **Base Case**: First, a base case scenario with typical distribution system parameters and for a particular load penetration is appreciated in order to verify if the proposed modeling discussed on Chapter 2 convey adequate results.

- **Load Evolution**: From the load trend data presented in Appendix A, it investigated the impact of changing the penetration of different residential appliances on the system harmonic level. It must be noticed that the same distribution network from the base case is used and the number of customers remains the same as in the base case. Only the appliances penetration for each existing customer will change according to the load trend. The first load evolution scenario to be evaluated is the "Natural" Load Evolution Study, which considers the evolution (according to the respective load trend data) of all appliances. Then, the evolution of only one appliance type is evaluated in order to determine which appliances have more impact. Three scenarios are analyzed:

  - CFL Load Evolution Study

  - PC Load Evolution Study

  - TV Load Evolution Study

3.2. Indices of Interest

In this section, the indices of interest to quantify the impact of the distributed nonlinear residential loads on the primary distribution system are presented. In this thesis, only odd harmonics from 3rd to 15th order are considered.

The following indices are analyzed according to each issue [5]:

Harmonic voltage and current distortion levels in the distribution system:

- o Harmonic spectrum of dominant sequences harmonics. It is more likely to encounter 3rd zero sequence, 5th negative sequence, 7th positive sequence harmonics, etc.

- o Voltage Individual Harmonic Distortion (IHD_V)

$$IHD_V(\%) = \frac{V_h}{V_1} \times 100$$

<div align="right">Equation 3.1</div>

- o Voltage Total Harmonic Distortion (THD_V):

$$THD_V(\%) = \frac{\sqrt{\sum_{h=3}^{H} V_h^2}}{V_1} \times 100$$

<div align="right">Equation 3.2</div>

- o Individual Demand Distortion (IDD):

$$IDD(\%) = \frac{I_h}{I_L} \times 100$$

<div align="right">Equation 3.3</div>

Where, I_L is the maximum fundamental current during a day.

o   Total Demand Distortion (*TDD*):

$$TDD(\%) = \frac{\sqrt{\sum_{h=3}^{H} I_h^2}}{I_L} \times 100$$

Equation 3.4

Telephone interference in the form of IT factors:

o   Total IT product:

$$IT_{total} = \sqrt{\sum_{h=1}^{H} (w_h I_h^0)^2}$$

Equation 3.5

o   Contribution of each harmonic to the IT:

$$IT_h = w_h I_h^0$$

Equation 3.6

where w_h is the C-message weighting [42], used in the USA and Canada. I_h^0 is the zero sequence current at harmonic *h* (only odd harmonics), *H* is the maximum harmonic order (in this thesis, *H* = *15*).

Neutral conductor current/voltage rise on the primary system:

o   Neutral voltage and current harmonic spectrum

o   Neutral voltage RMS

Impact of harmonics on the primary system losses:

- o   Fundamental and harmonic power losses at phases, neutral and grounding circuits

Impact of harmonics on the substation capacitor loading limits

- o   Capacitor indices including: apparent power, RMS and peak voltage and RMS current.

The results will be condensed by using the associated cumulative distribution function (*cdf*). In the results of next subsections an index based on the cumulative distribution function will be used [4], as follows.

"*Time 95% cdf value*" is obtained by two steps:

- o   Average of the voltage/current profile between all sections (daily average profile).

- o   Build the cumulative distribution function (*cdf*) for 24 hours and obtain the 95% value.

Figure 3.1 below shows an example to determine the 95% value, considering the 3rd harmonic voltage profiles of three sections. From the 3rd harmonic voltage profile for 24 hours, one can find that the 3rd harmonic voltage is lower than 0.81 V, 95% of the time. This index will be useful to facilitate the visualization of the load growth and sensitivity studies results.
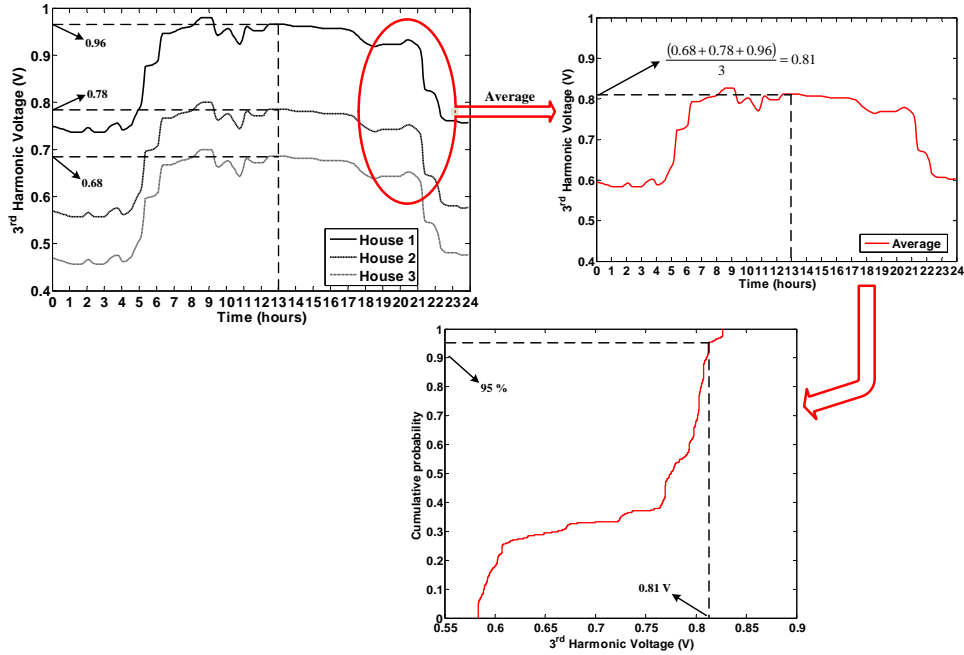
Figure 3.1 Procedure to determine "daily average profile" and the "*time 95% cdf value*"

3.3. Simulation Results

The following sections present the results for the base case and load growth.

3.3.1. Base Case

Figure 3.2 shows the distribution network employed to study the impact of the distributed nonlinear sources on the primary system for all above mentioned case studies. The modeling of this network was discussed in Chapter 2. This network is referred in this thesis as an ideal feeder; however a actual feeder is also analyzed in the next section. Table 3.1 presents the system parameters for the base case harmonic power flow simulations.
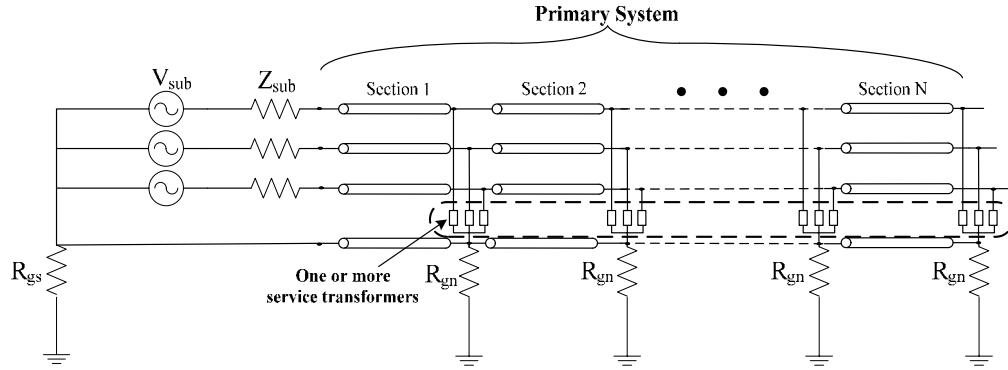
Figure 3.2 Distribution network model for primary system analysis

Table 3.1 Base case system parameters

Base Case System Parameters		Values
Primary System	Supply system voltage Substation MVA level Substation positive sequence impedance Substation zero sequence impedance Substation grounding (R_{gs}) MGN grounding resistance (R_{gn}) Grounding span of the MGN neutral (s) Feeder length Feeder conductor type	14400 V @ 60 Hz 242 MVA 0.688 + j2.470 ohms 0.065 + j2.814 ohms 0.15 ohms 15 ohms 75 m 15 km 4 - 336.4 ACSR
Services Transformer	Number of transformers per phase Voltage (V_H/V_L) rating KVA rating Impedance Resistance Grounding resistance (R_T)	12 per km 14400/120 V 37.5 kVA 2 % 1.293 % 12 ohms
Secondary System	Customer grounding resistance (R_C) Neutral impedance (Z_N) Number of houses (N)	1 ohm 0.55 + j0.365 ohm/km 10

Table 3.1 shows that this ideal feeder under analysis has 12 transformers at each kilometer and for each phase so that the total number of service transformers is 12 x 3 phases x 15 km = 540.

The simulations results are presented in the next subsections. As mentioned in the previous section, the "daily average profile" represents the average between the voltages/currents daily profile at different locations at the primary system. And the "*time 95% cdf value*" is determined from the cumulative distribution function over the daily average profile.

Before proceed to the results, Figure 3.3 provides the average level of load imbalance on the distribution system shown in Figure 3.2, considering the base case parameters. The negative and zero sequence load imbalance ratios are given by Equation 3.7 and Equation 3.8, respectively.
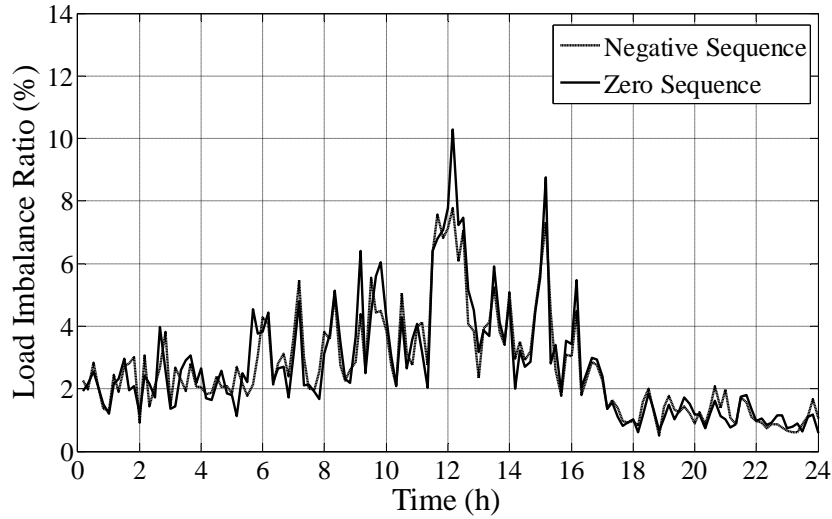
Figure 3.3 Average imbalance level on the distribution network

$$\text{Negative Seq. Load Imbalance Ratio} = \frac{I_{\text{negative sequence}}}{I_{\text{positive sequence}}}$$

<div align="right">Equation 3.7</div>

$$\text{Zero Seq. Load Imbalance Ratio} = \frac{I_{\text{zero sequence}}}{I_{\text{positive sequence}}}$$

<div align="right">Equation 3.8</div>

3.3.1.1. Harmonic voltage and current distortion levels in the system

First, the harmonic three phase voltages at every 1 km along the primary feeder are obtained for the three phases. Then, the sequence components are calculated and for each harmonic the dominant sequence is determined. Then, through the procedure to condense data illustrated in Figure 3.1, the daily average profile associated to the dominant sequence voltage of each harmonic is determined and shown in Figure 3.4(a). The daily average profile of the THD_V is shown as well. Finally, from Figure 3.4(a), the *time 95% cdf value* of the dominant sequence voltage individual harmonic distortion (IHD_V) and THD_V can be determined and are shown in Figure 3.4(b).

The daily average profile associated to the zero sequence voltage of each harmonic is shown in Figure 3.5 along with the *95% cdf value* associated to the zero sequence voltage IHD_V.

(a) Daily average profile

(b) Time 95% cdf value
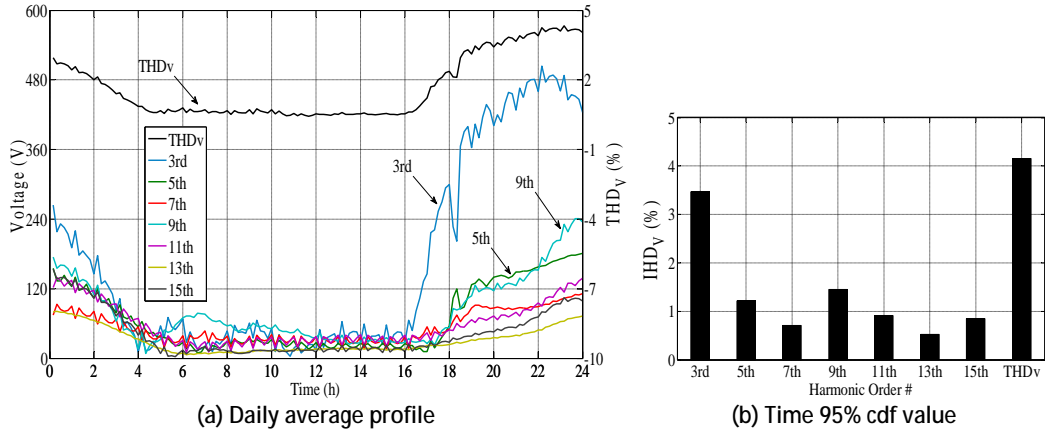
Figure 3.4 Average over the dominant sequence voltages at the primary system

(a) Daily average profile

(b) Time 95% cdf value
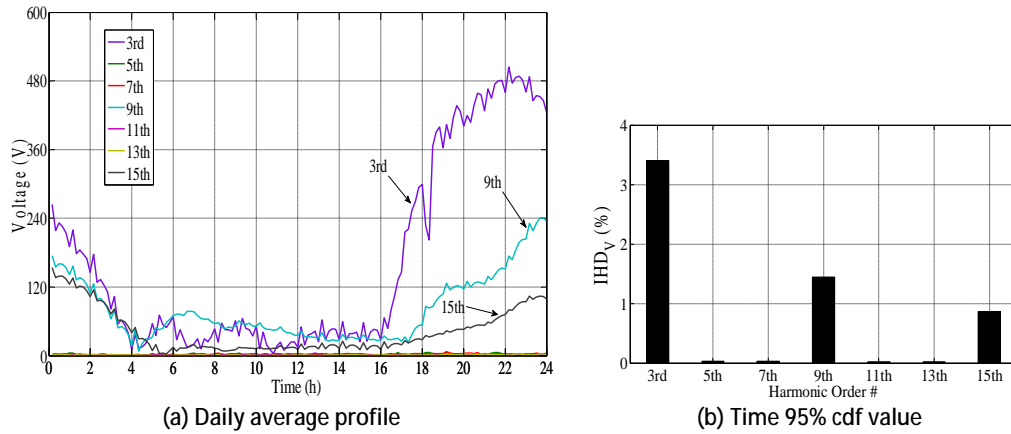
Figure 3.5 Average over the zero sequence voltages at the primary system

The main findings are as follows:

- It can be observed that the harmonic levels are more prominent during the period between 18:00 and 24:00, during which there is a high usage of nonlinear appliances. The results show that the nonlinear residential loads can often create considerable harmonic distortion on the system.

Likewise, the harmonic phase currents at each section of the primary feeder shown at Figure 3.2 and the respective sequence components are obtained. Then,

the daily average profile associated to the dominant sequence current of each harmonic is determined and shown in Figure 3.6(a). The daily average profile of the *TDD* is shown as well. Finally, from Figure 3.6(a), the *time 95% cdf value* of the individual demand distortion (*IDD*) and *TDD* can be determined and are shown in Figure 3.6(b).

The daily average profile associated to the zero sequence current of each harmonic is shown in Figure 3.7 along with the *95% cdf value* associated to the zero sequence voltage *IHD_V*.

(a) Daily average profile   (b) Time 95% cdf value
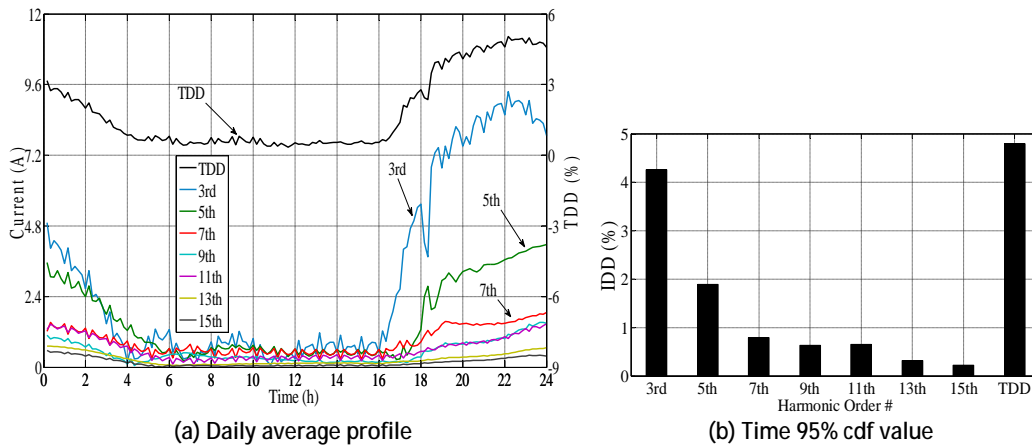
Figure 3.6 Average over the dominant sequence currents at the primary system

- Figure 3.4 to Figure 3.7 show that the 3rd harmonic is the most dominant component. Furthermore, from Figure 3.4, one can observe that the dominant (zero) sequence 9th harmonic voltage is higher than the dominant (negative) sequence 5th harmonic.

- Figure 3.7 shows that the zero sequence current is dominated by the triplen harmonics (3rd, 9th and 15th), which are related to the telephone interference, increased system losses, high neutral current (overload), etc.

- One can observe a good correlation between *THD_V* and *TDD* and the highest distortion is observed between 18:00 and 24:00 when the usage of nonlinear appliances becomes more intense, especially of PCs and CFLs.

(a) Daily average profile   (b) Time 95% cdf value
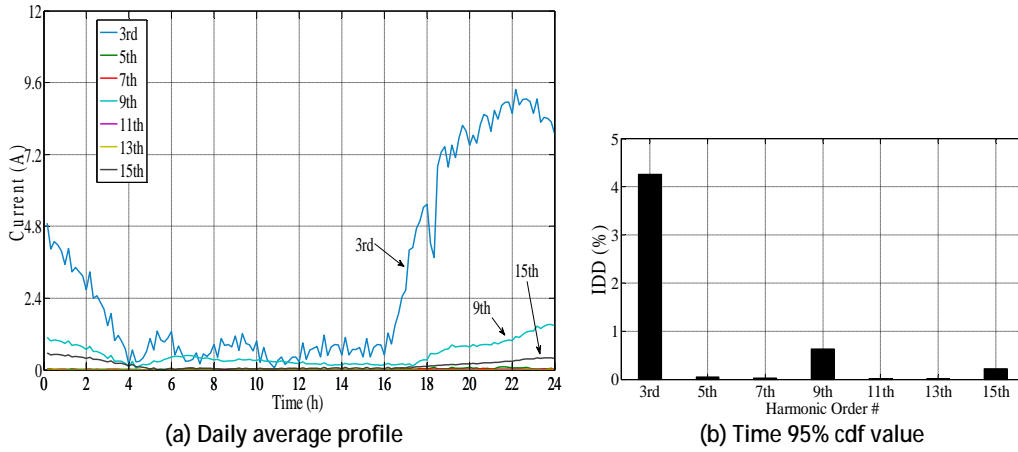
Figure 3.7 Average over the zero sequence currents at the primary system

3.3.1.2. Telephone interference in the form of IT factors

One of the consequences of increasing harmonic current levels is audible noise on telephones lines that run in parallel with distribution feeders. The impact on the telephone line is normally measured by calculating the IT factors given by Equation 3.5 and Equation 3.6. The results are shown in Figure 3.8.

- It is common for 540 Hz to be the dominant frequency in interference between telephone and electric power systems, even though third harmonic, 180 Hz, current has a higher magnitude, as shown by Figure 3.6(b). The design of the telephone system makes it more susceptible to inductively-coupled interference at 540 Hz than at 180 Hz.

- It can be seen from Figure 3.8 that the 9th and 15th harmonics are the main contributors of the total *IT product*.

(a) Daily average profile   (b) Time 95% cdf value
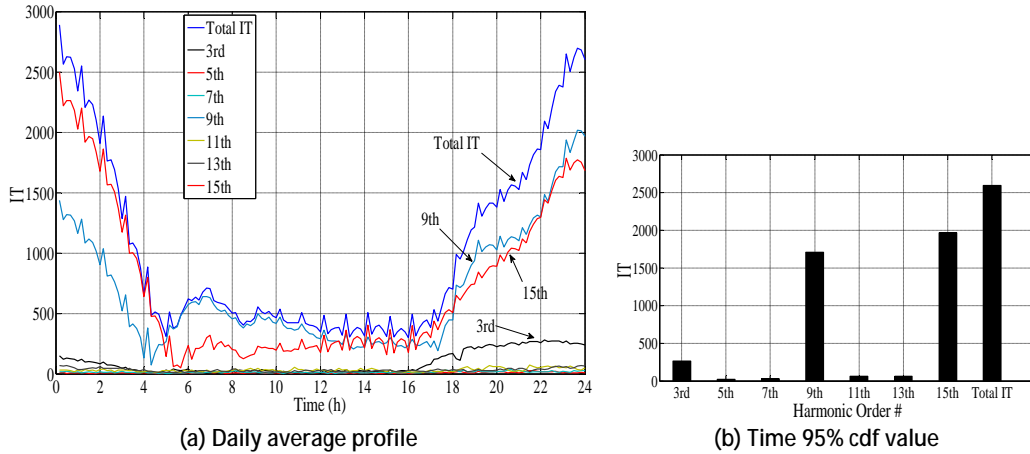
Figure 3.8 Average individual and total IT levels at the primary system

This section also investigates the impact of the nonlinear residential loads on the voltage induced at the end of a telephone line of 75 m parallel to the primary feeder, as shown in Figure 3.9. Typical parameters are used to model the telephone line. The results are shown in Figure 3.10.
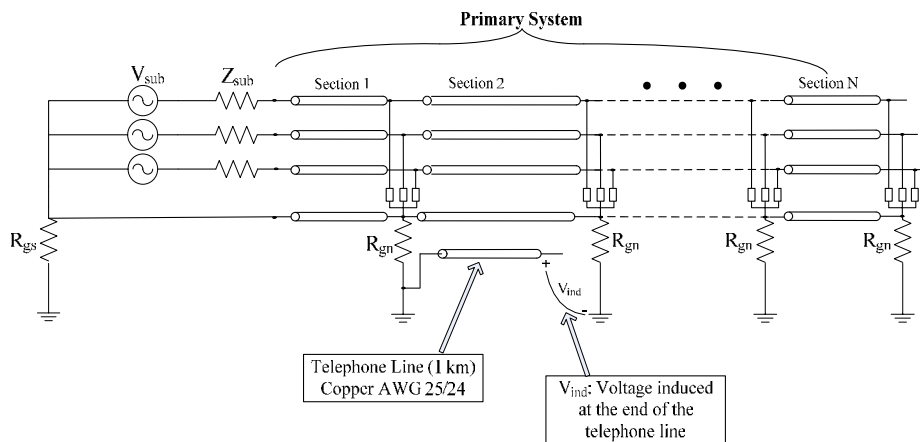
Figure 3.9 Schematic representation of the telephone line in parallel to the primary system

(a) Daily profile   (b) Time 95% cdf value
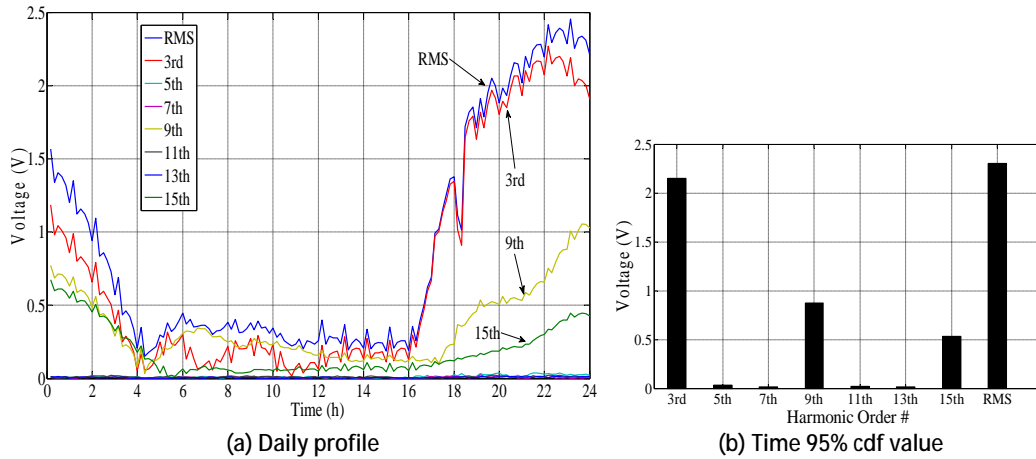
Figure 3.10 Voltage induced at the end of a telephone line

- The voltage induced is roughly proportional to the difference of zero sequence and the neutral current. As both parameters are dominated by the triplen harmonics, the spectrum of the telephone line induced voltage is mainly composed by the 3rd, 9th and 15th, as can be seen on Figure 3.10.

3.3.1.3. Neutral conductor current/voltage rise

This section analyzes the impact of the nonlinear residential loads on the average neutral current and voltage levels at the primary distribution system. The main findings are as follows:

- The harmonic components of the neutral voltage have levels and daily trend and do not follow the fundamental component trend.

- However, Figure 3.12 shows that the neutral current is dominated by the triplen (3rd, 9th and 15th) harmonics since these harmonics which add in series in the neutral line, which contributes for increasing neutral losses.

Because neutral lines are not fused or protected by circuit breakers, overheating of neutral conductors in a three-phase line can be a significant safety hazard.

- The triplen harmonics can be mitigated through LC tuned filters and phase shifting (zig-zag) transformers.
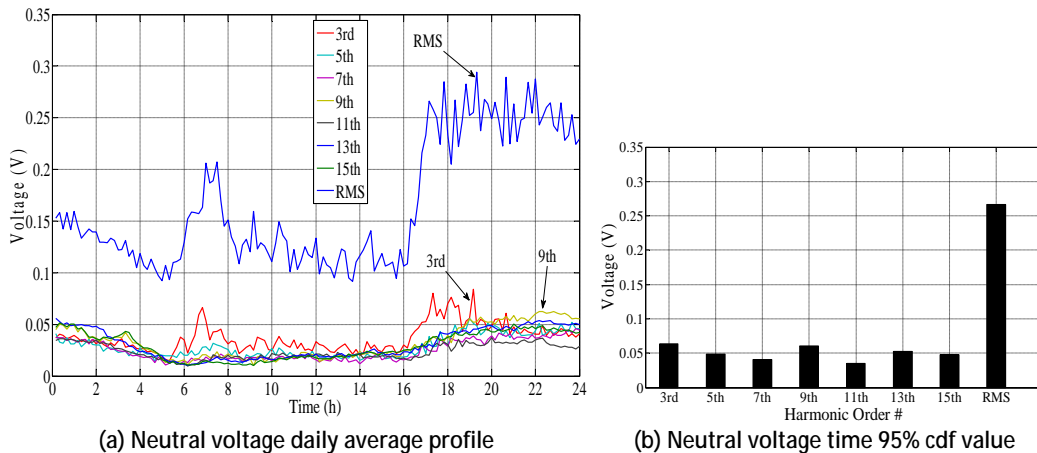
(a) Neutral voltage daily average profile   (b) Neutral voltage time 95% cdf value

Figure 3.11 Average neutral voltage level at the primary system
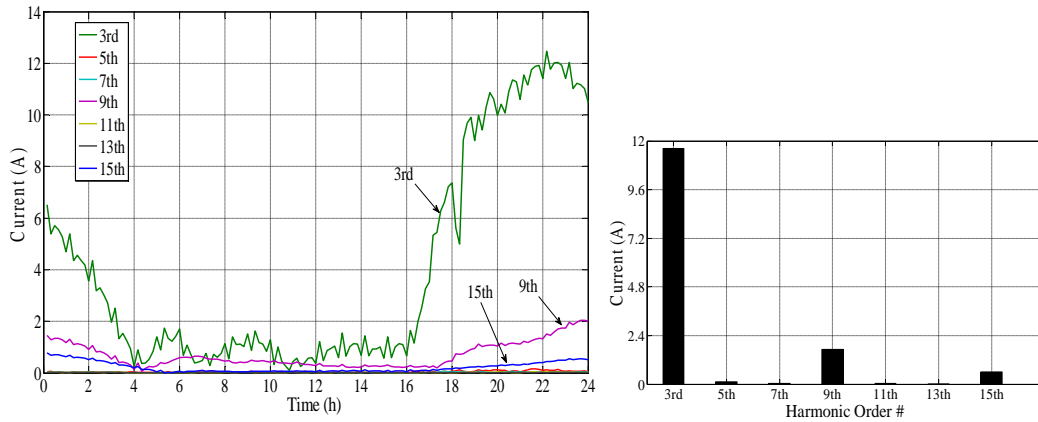
(a) Daily average profile   (b) Time 95% cdf value

Figure 3.12 Average neutral current level at the primary system

3.3.1.4. Impact of harmonics on the primary system losses

The nonlinear residential loads have an impact on the phase and neutral circuits total fundamental and harmonic losses. These parameters are illustrated on Figure 3.13.

- Figure 3.13 show that the harmonic losses are higher than the fundamental losses in the neutral circuit. This is expected because the neutral and zero sequence currents are dominated by the 3rd, 9th and 15th.

- The base case results shows that the fundamental and harmonic losses on the primary system remained at a low level so that it is not concern compared to the other indices previously analyzed.

- On the load growth studies, it will be evaluated the impact of increasing usage of nonlinear residential loads on the power losses. The use of energy efficient appliances may lead to the decrease of the fundamental current on the phase circuit and, consequently, fundamental power losses reduction. However, the harmonic levels will increase, which, in turn, leads to higher zero sequence current and higher neutral losses as well.
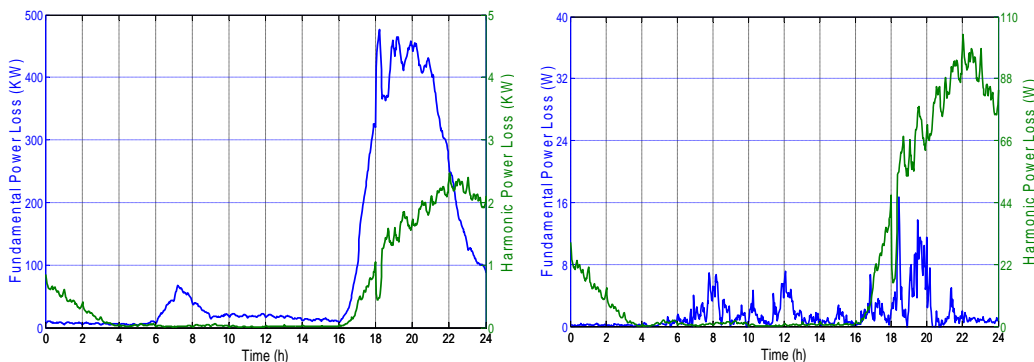
(a) Phases conductors power loss   (b) Neutral conductor power loss

Time 95% cdf Power Losses			
Circuit	Fundamental	Harmonic	Total
Phases	439.50 kW	2.19 kW	441.69 kW
Neutral	5.74 W	90.99 W	96.73 W
Total	439.52 kW	2.39 kW	441.91 kW

Figure 3.13 Daily profile active power losses at the primary system

3.3.2. Load Evolution

The objective of this section is to investigate the impact of changing the penetration of different residential appliances on the primary system harmonic level. It must be noticed that the distribution network from the base case is used. Moreover, the number of customers remains the same as in the base case, only the appliances penetration for each existing customer will change.

The first scenario to be evaluated is:

- "Natural" Load Evolution Study: The penetration of all appliances is changed for each year accordingly to the respective trend data presented in Appendix A.

- Then, the evolution of only one appliance type is evaluated in order to determine which appliances have more impact. Three scenarios are analyzed:

   o **CFL Load Evolution Study**: For each year, the penetration of incandescent and the CFL lamps are changed according to their

respective trend data. The penetration of the other appliances is not changed and remains the same as the first (base) year.

o **PC Load Evolution Study**: The penetration of laptops and desktop PCs is changed according to their respective trend data. The penetration of the other appliances is not changed and remains the same as the first (base) year.

o **TV Load Evolution Study**: The penetration of CRT TVs and LCD TVs is changed according to their respective trend data. The penetration of the other appliances is not changed and remains the same as the first (base) year.

3.3.2.1. Load Evolution Study Results

In this subsection, the appliance trend data from the bottom-up model is used for the harmonic power flow simulations in order to determine the primary system harmonic levels in the coming years. The objective is to give an estimation of the harmonic levels for several issues, like neutral voltage rise and telephone interference, in the coming years.

In order to facilitate the interpretation and comparison of the results, all the indices are represented by its associated *95% cdf value*, as it has been done in the previous section for the base case study.

For each power quality index, two different charts are provided:

- One refers to the PQ index absolute level for the next five years. This chart gives an idea of the trend behavior.

- The second chart provides the average annual growth rate for each PQ index. This chart provides an estimation of how much each PQ index will grow in the following years. This can be useful to see how long it will take to exceed some limit imposed by standards and utilities, like the voltage THD for example.

Harmonic voltage and current distortion levels in the primary system

As it was done for the base case, the harmonic three phase voltages at every 1 km along the primary feeder and the respective sequence components are obtained. Then, from the daily average profile, the *time 95% cdf value* of the dominant and zero sequence voltage magnitudes, individual harmonic distortion (IHD_V) and THD_V can be determined. This is repeated for the following years by changing the appliances penetration for each existing customer house according to the trend data.

Figure 3.14 (a) shows the *95% cdf value* of the harmonic dominant sequence voltages in the next 5 years. From the data provided in Figure 3.14(a) and Figure 3.14(b), it is possible to calculate the average annual growth rate associated to the phase voltage index, which is shown in Figure 3.14(c). For example, one can observe that the 5th harmonic dominant sequence voltage will increase an average

of 15% from one year to another. The results associated to the zero sequence voltage are shown in Figure 3.15.

Along with the results regarding "natural" load evolution, the results associated to individual appliances evolution are shown in order to verify which appliances contribute the most for the harmonic levels increase in the coming years.

(a) "Natural" load evolution: Time 95% cdf value (fundamental divided by 100)

(b) "Natural" load evolution: Time 95% cdf value

(c) Annual growth rate
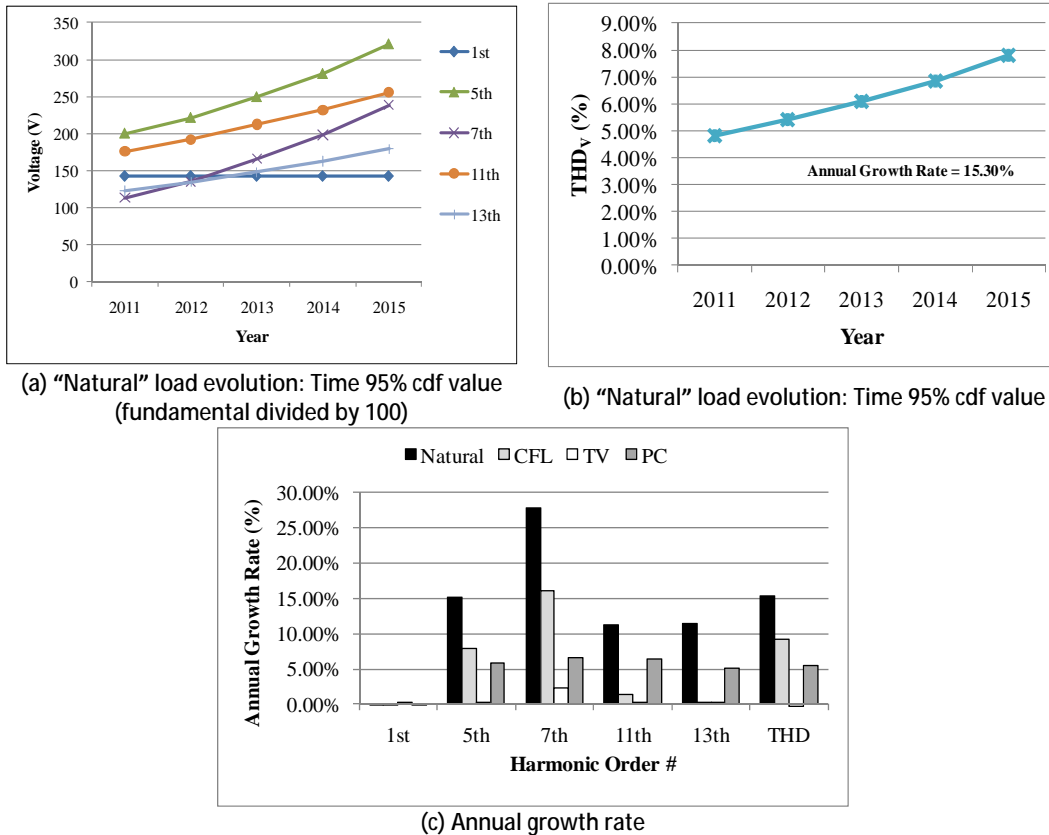
Figure 3.14 Average dominant sequence voltage at the primary system
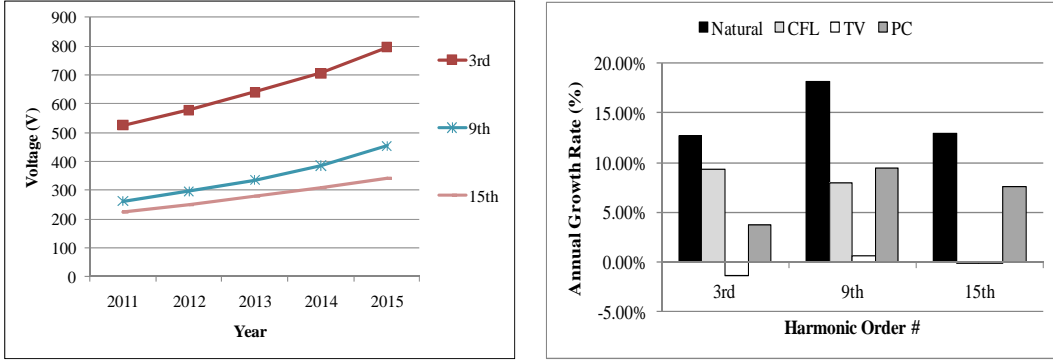
(a) "Natural" load evolution: Time 95% cdf value   (b) Annual growth rate

Figure 3.15 Average zero sequence voltage at the primary system

Similarly, Figure 3.16 and Figure 3.17 shows the *95% cdf values* associated to the dominant and zero sequences of the average current along the primary feeder in the next 5 years and the associated average annual growth rate.
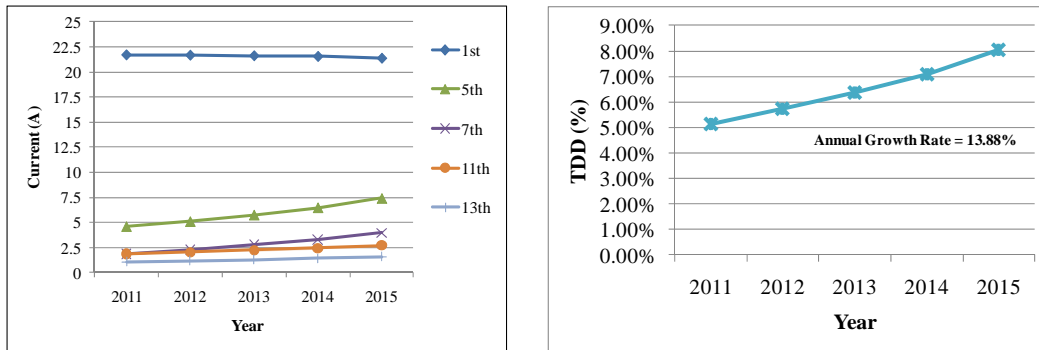
(a) "Natural" load evolution: Time 95% cdf value (fundamental divided by 10)
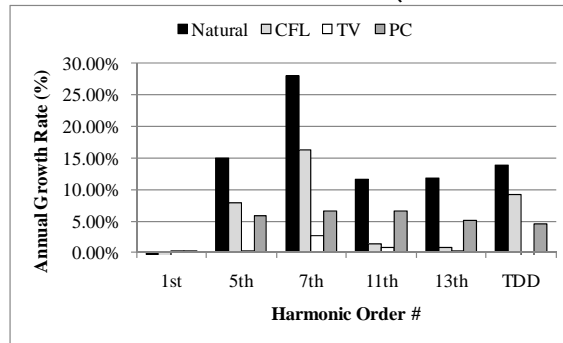
(b) Annual growth rate

Figure 3.16 Average dominant sequence current at the primary system

(a) "Natural" load evolution: Time 95% cdf value   (b) Annual growth rate
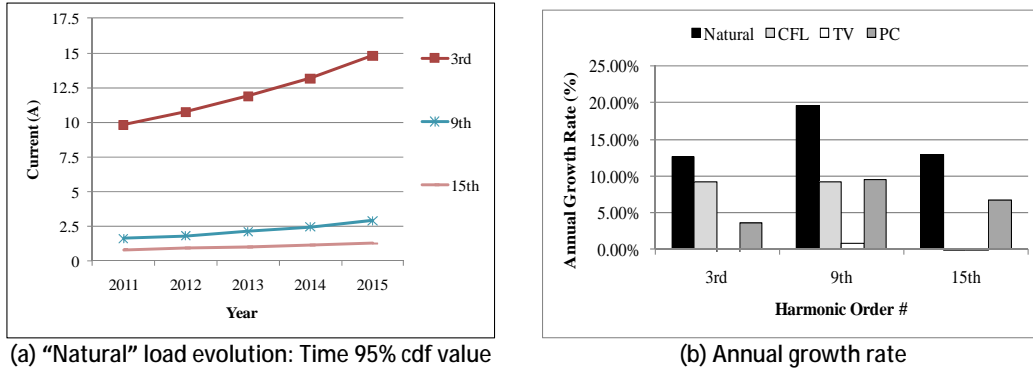
Figure 3.17 Average zero sequence current at the primary system

Telephone interference in the form of IT factors

From the phase currents obtained at each 1 km along the primary feeder, the IT levels can be calculated as it was done for the base case previously analyzed. The calculation is repeated for the next years and the average annual growth rate associated at the IT levels can be determined and is shown in Figure 3.18. The harmonic voltage induced at the telephone line can also be determined for the next years and it is illustrated in Figure 3.19.

One can observe a significant increase on the individual IT levels associated to the triplen harmonics, which are the major contributors for the telephone interference. Moreover, the CFLs are the main contributor for the 3rd harmonic IT level and the PCs devices are the main contributors for the increase of the 9th and 15th harmonic IT levels. As expected, these results show that different appliances impact differently at each harmonic component.
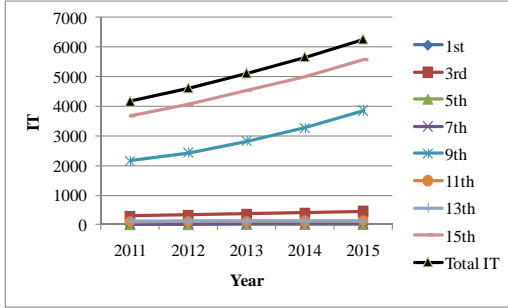
(a) "Natural" load evolution: Time 95% cdf value
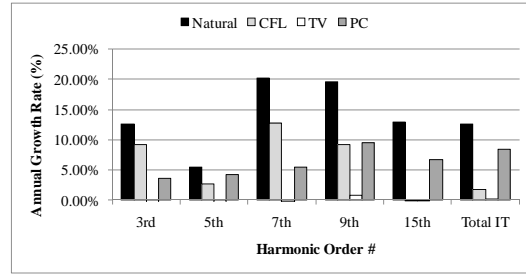
(b) Annual growth rate

Figure 3.18 Average individual and total IT levels at the primary system
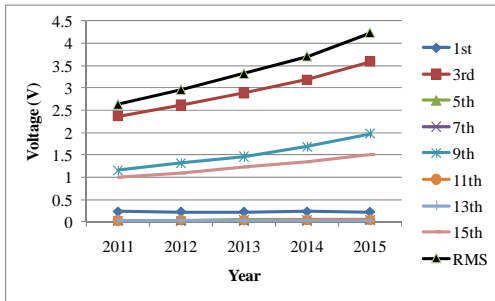
(a) "Natural" load evolution: Time 95% cdf value
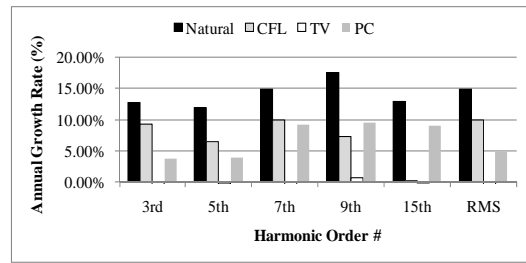
(b) Annual growth rate

Figure 3.19 Telephone line induced harmonic and RMS voltage

Neutral conductor current/voltage rise

The results below show the annual growth rate of the average harmonic current and voltage observed at the neutral circuit the primary system. Similarly to previous results, first, the daily neutral current and the neutral to ground voltage at each 1 km is obtained from the harmonic power flow simulations. Then, the daily average profiles of the neutral current and voltage are determined and the respective *95% time cdf value* can be calculated. This calculation is repeated for the next years and the results are shown at Figure 3.20(a) and Figure 3.21(a) for the neutral to ground and neutral current, respectively. From these results, the

average annual growth rate can be computed for each harmonic component and is illustrated in Figure 3.20(b) and Figure 3.21(b). The main findings are as follows:

- The main contributors for the neutral voltage and current growth in the coming years are the CFLs and PCs appliances.

- Figure 3.21(b) shows a noticeable increase of the 9th harmonic component of the neutral current on the coming years, which is in accordance to the individual 9th harmonic IT level annual growth shown in Figure 3.18. It is well known that these indices are the major contributors to telephone interference.
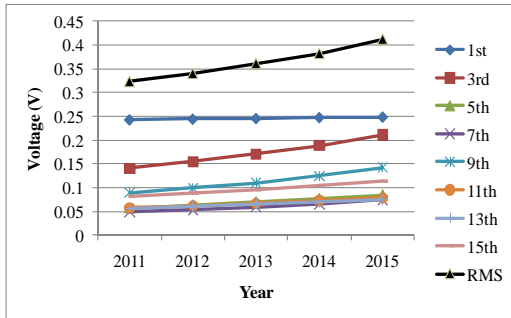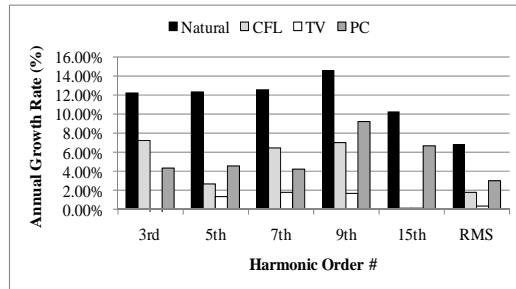
(a) "Natural" load evolution: Time 95% cdf value   (b) Annual growth rate

Figure 3.20 Average neutral voltage levels at the primary system
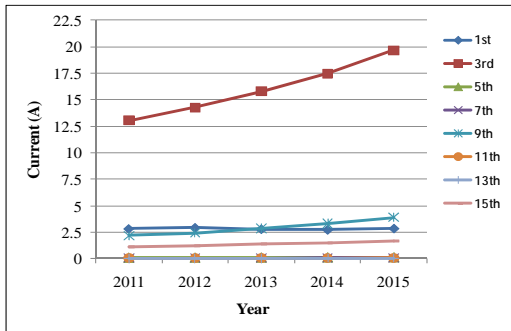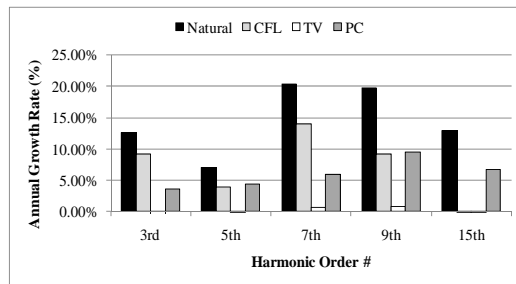
(a) "Natural" load evolution: Time 95% cdf value   (b) Annual growth rate

Figure 3.21 Average neutral current levels at the primary system

Impact of harmonics on the primary system losses

Figure 3.22 and Figure 3.23 show the total fundamental and harmonic power losses, respectively, on the phases and neutral circuits of the primary system on the next five years and correspondent average annual growth rate. The results correspond to the *95% cdf value* directly over the total daily active power losses of both the three-phase circuit and neutral circuit of the primary system.

The main findings are as follows:

- Figure 3.22(a) shows a small decrease on the fundamental power losses, which is caused by the use for of more energy efficient appliances, such as CFLs.

- One can also observe from Figure 3.23 that the CFLs and the PC are the largest contributors for the "natural load evolution" harmonic losses annual growth rate.

- Previous results have shown an increase of the dominant sequence of all harmonic components of the average current on the primary system. However, the increase on the zero sequence harmonic components (triplen harmonics) that has some noticeable impact on the system harmonic losses, as it can be seen from the behaviour of the neutral harmonic losses on the coming years shown in Figure 3.23(b).

- Figure 3.23(a) shows a relatively large increase on the harmonic power losses in the coming years due to the use of more nonlinear appliances. However, this does not represent a concern because the base case harmonic power losses levels are still very low for both phase and neutral circuits as shown in the previous section

"Natural" Load Evolution
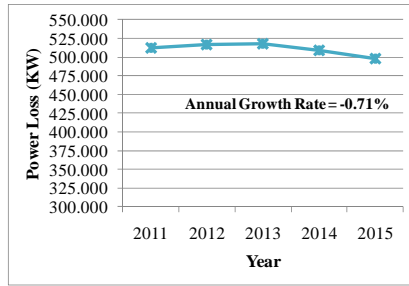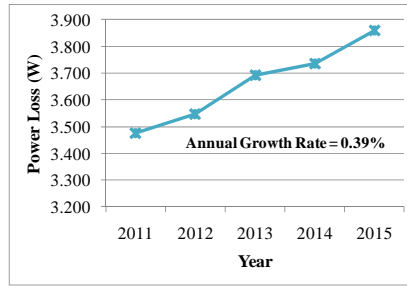
(a) Phases conductors power loss

(b) Neutral conductors power loss
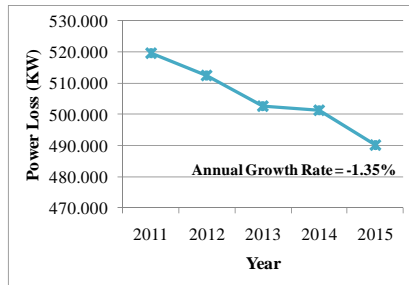
CFL Load Evolution

(a) Phases conductors power loss
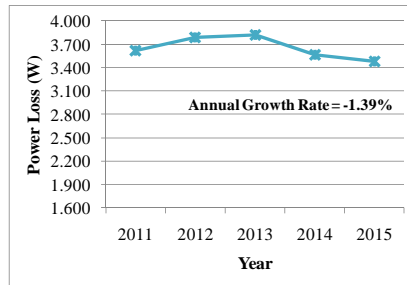
(b) Neutral conductors power loss
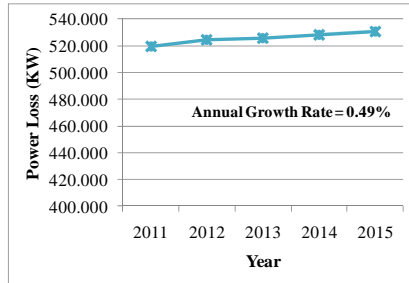
TV Load Evolution

(a) Phases conductors power loss
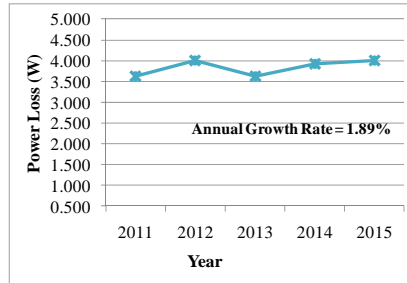
(b) Neutral conductors power loss
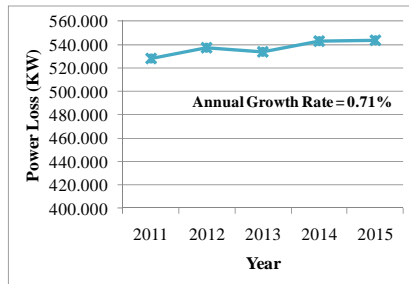
PC Load Evolution

(a) Phases conductors power loss
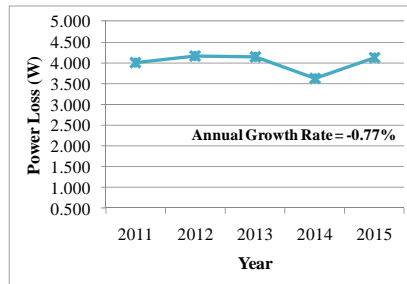
(b) Neutral conductors power loss

Figure 3.22 Total fundamental power losses at the primary system

"Natural" Load Evolution
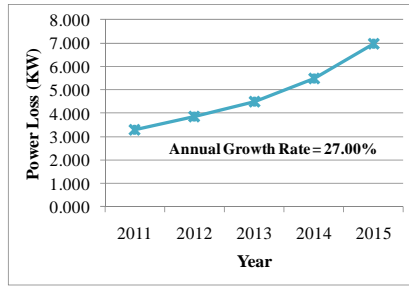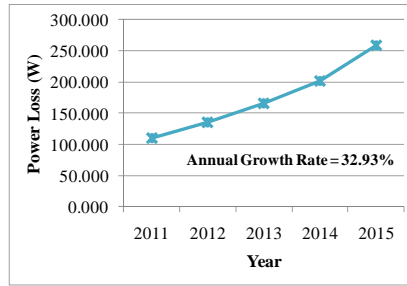
(a) Phases conductors power loss   (b) Neutral conductors power loss
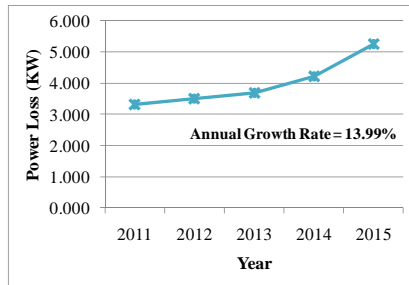
CFL Load Evolution

(a) Phases conductors power loss   (b) Neutral conductors power loss
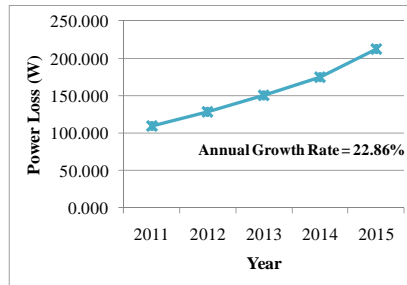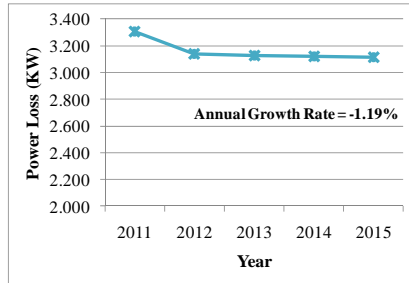
TV Load Evolution

(a) Phases conductors power loss   (b) Neutral conductors power loss
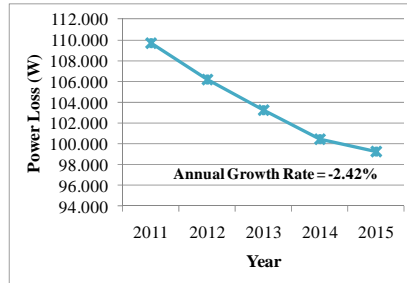
PC Load Evolution
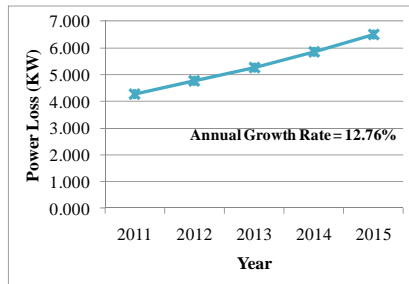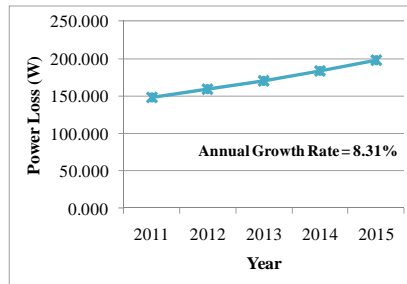
(a) Phases conductors power loss   (b) Neutral conductors power loss

Figure 3.23 Harmonic power losses at the primary system

Impact of load growth on the substation capacitor loading

In this subsection, the impact of the load growth on the loading of a substation shunt capacitor is evaluated. It must be noticed that for all previous results, there is no shunt capacitor connected at the substation. First, a typical substation capacitor with a capacity less than *3 Mvar* is considered and a value of *2.3 Mvar* is chosen defined by the estimated system resonance frequency (h_{res}), which can be calculated as follows:

System positive sequence impedance (Table 3.1): $Z_1 = 0.688 + j2.470\ ohms$

$$MVA_{sys} = 3 \times \frac{V^2}{Z_1} = 3 \times \frac{14400^2}{0.688 + j2.470} = 65 - j233\ \text{MVA}$$

$$h_{res} = \sqrt{\frac{M\,\text{var}_{sys}}{MVA_{cap}}} = \sqrt{\frac{233}{2.3}} = 10.07$$

So the estimated resonance frequency is 10.07^{th} harmonic, which is far enough away from 9th and 11th. Moreover, a frequency scan analysis also shows no resonance below 20th harmonic. So, *2.3 Mvar* capacitor bank at the substation is a non-resonance case.

The next step consists of verifying how the increasing penetration of nonlinear appliances impacts on the capacitor (harmonic) loading conditions using the following indices:

Table 3.2 Capacitor loading limits (related to its rating)

Index	Explanation	Limit
kvar	Apparent power of the capacitor (kvar = $I_{rms} \times V_{rms}$)	135%
V_{rms}	RMS voltage of the capacitor	110%
V_{peak}	Peak voltage of the capacitor	120%
I_{rms}	RMS current of the capacitor	180%

The results regarding the harmonic levels of the voltage and current at the capacitor are shown at Figure 3.24. It is observed that although there is an increase on the harmonic levels in the coming years, those do not affect the indices outlined in Table 3.2, as illustrated by Figure 3.25. Therefore, the observed load growth in the coming years does not represent a concern regarding the substation shunt capacitor loading levels.

(a) Harmonic current spectrum at the substation capacitor

(b) Harmonic voltage spectrum at the substation capacitor
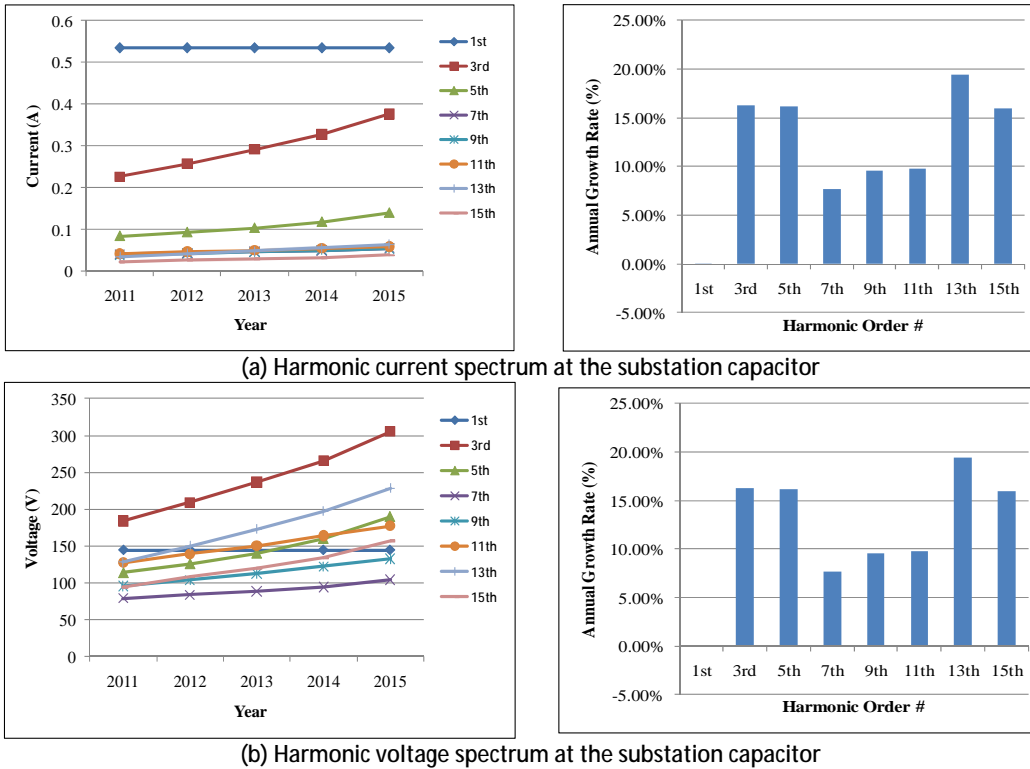
Figure 3.24 Harmonic voltage and current levels at the substation capacitor

(a) V$_{rms}$ (a) I$_{rms}$

(c) Apparent power   (d) V$_{peak}$
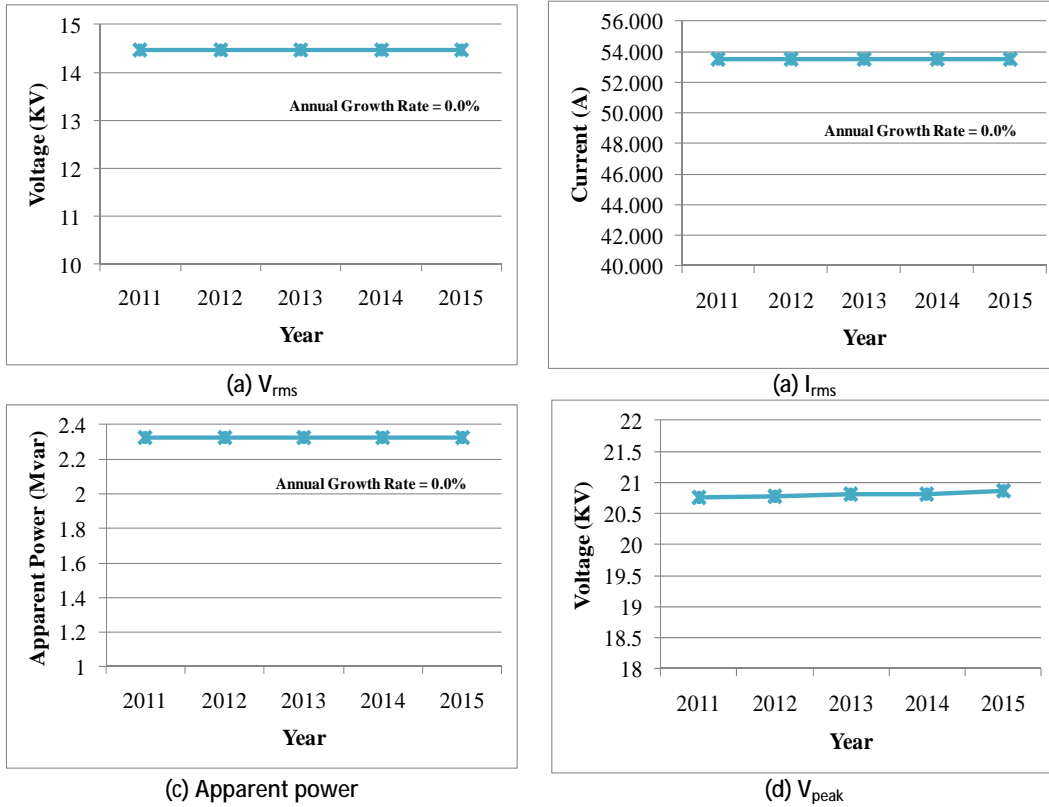
Figure 3.25 Capacitor loading indices

Impact of load growth on harmonic current penetration into the transmission system

The amount of harmonic current injected into the supply transmission system has also been studied. This harmonic current is defined as that at the sending end of the study feeder. Figure 3.26 shows the growth characteristics of the various harmonics entering into the transmission system. The results reveal that the 7th and 9th harmonics have a relatively higher growth rate. The typical growth rate is about 15% for different harmonics. This growth rate is very similar to that reported in the last section. That section shows the growth characteristics of average harmonic currents inside the feeder.
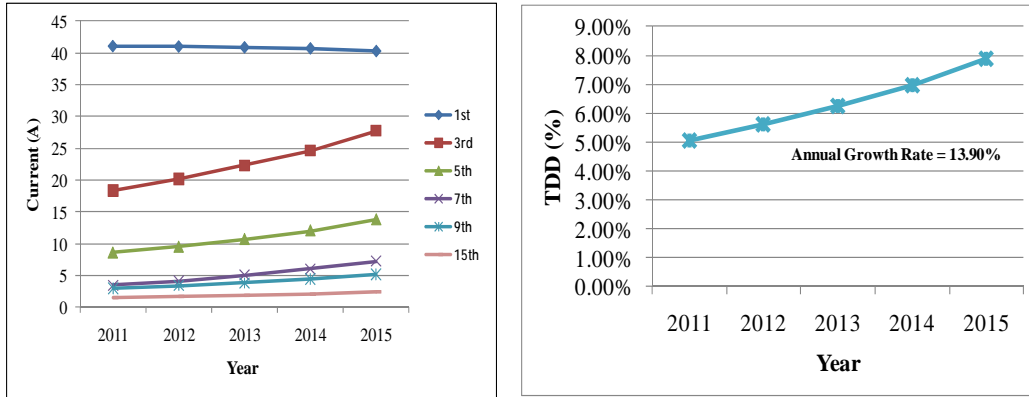
(a) Natural load evolution (fundamental divided by 10)
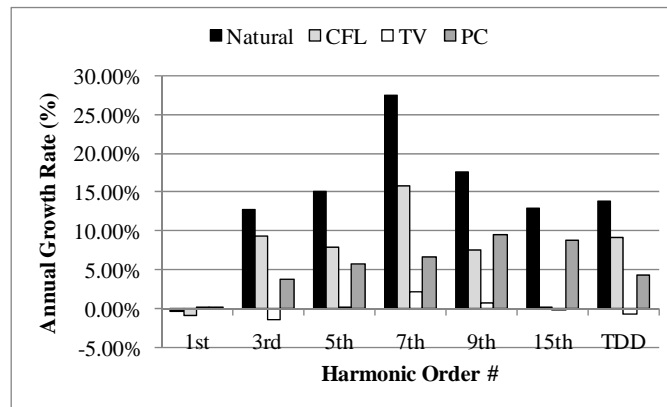
(b) Annual growth rate

Figure 3.26 Growth characteristics of the harmonics entering into transmission system

3.3.2.2. Main findings for primary system load growth study

Figure 3.27 shows a summary of the load evolution results for the main indices. The value between parenthesis and the one without above each bar refer to index level at the year 2011 and the average annual growth rate, respectively.
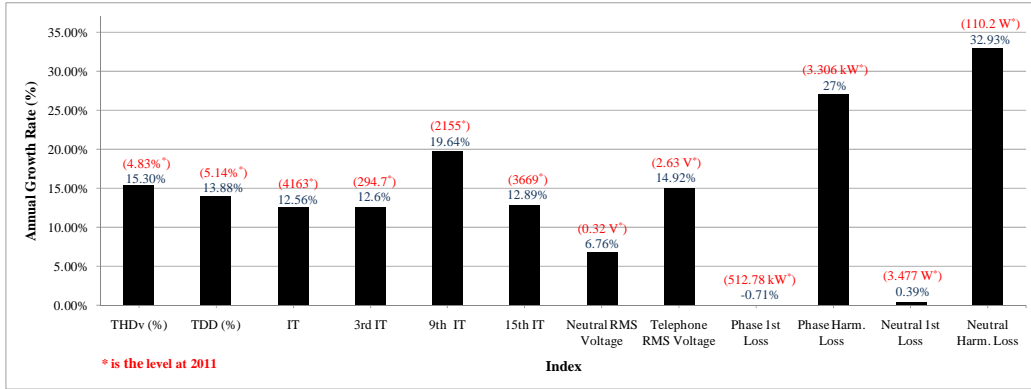
Figure 3.27 Average annual growth for main power quality indices

- 7th and 9th harmonics are the ones that have the highest annual growth rate mainly because of the penetration of CFLS and PCs.

- Voltage *THD* has an annual growth rate of 15% and the current *TDD* of 14%. The increase is mainly caused by CFLs and PCs.

- Neutral voltage/current rise:

    o *RMS* voltage has an annual growth rate of 6.8% mainly caused by the CFLS and PC penetration

- Telephone Interference:

    o *Total IT* presented an annual growth rate of 13% mainly caused by CFL and PC load growth.

    o CFL mainly caused the increase on 9th harmonic and PC on the 15th harmonic.

    o The same pattern is observed for telephone line induced voltage

- Power Loss:

o There is a decrease of less than 1% on the phases fundamental power losses due to the use of more energy efficient appliances.

o However, the phases harmonic power losses increase at an annual growth rate of 27%. However, this does not represent a concern because the harmonic power losses are still very low.

o CFLs and PCs are the appliances that most contribute to phases, neutral and grounding harmonic losses increase.

3.4. Actual Distribution System Analysis

In the previous sections, several case studies were analyzed in order to understand how the nonlinear residential loads impact on the harmonic levels of the primary system. This analysis was conducted over an ideal distribution power system. One additional and important step is to verify if these results are representative of a actual distribution system. Therefore, the objective of this section is to perform multiphase harmonic power flow simulations over a actual distribution feeder supplied by a 240/25 kV substation located at the city of Edmonton and managed by EPCOR Utilities Inc.

The study over the actual feeder is similar to the base case study conducted at Section 3.3 for the ideal feeder. The objective is to show if there is similarity of the distribution of the harmonic level on both the ideal and actual feeder. The location of analysis is the substation of both feeders. Furthermore, as it will be shown in the following sections, the actual feeder is composed of underground

cables so that it is investigated how the system harmonic levels behave when cables are presented and when only overhead lines are presented.

3.4.1. Actual System Modeling

This subsection presents an overview about the characteristics of the actual feeder that will be used for the harmonic power flow simulations. This feeder (labeled *'21SU'*) is supplied by the 240/25 kV Summerside substation located at the city of Edmonton and managed by the distribution company Epcor. Figure 3.28 show the configuration diagram of the *21SU* distribution feeder, in which one can observe the main trunk, three-phase, two-phase and single phase lateral branches. In this thesis, the branches that do not belong to the main trunk will be referred to as lateral branches. In Figure 3.28, the main trunk is represented by red color and the lateral branches are represented by the black color.

Table 3.3 provides the data associated to the main parameters of the actual feeder shown in Figure 3.28. Practically, all lateral branches are underground cables since they are located in the residential areas. The main trunk has also some sections of underground cables and the associated length is shown in table below.

In the following sections, it is investigated the harmonic levels for two scenarios:
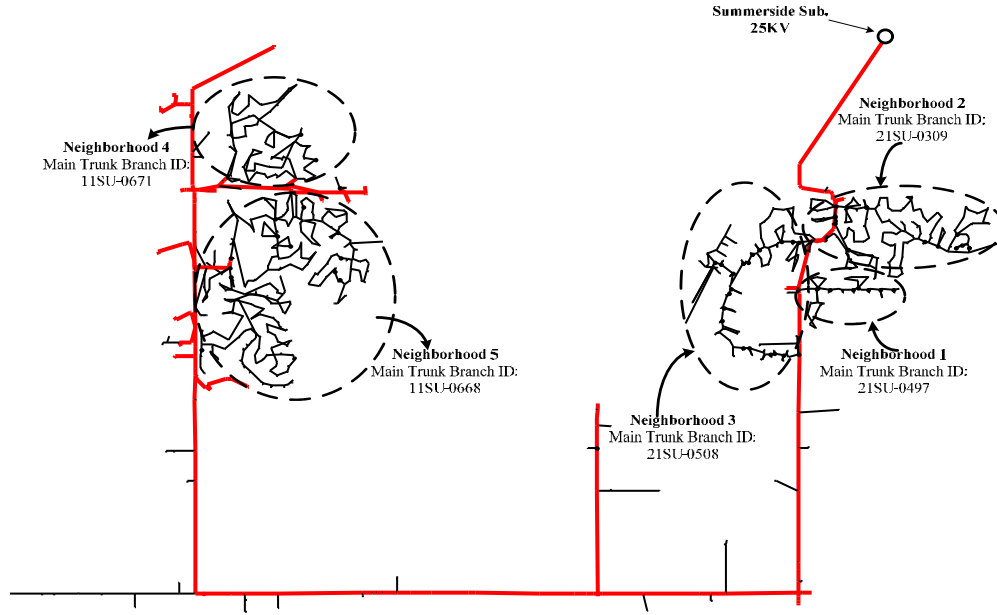
Figure 3.28 Actual distribution feeder schematic drawing

Table 3.3 Actual distribution feeder (*21SU*) main characteristics

Actual Feeder Parameters		Values
Primary System	Main trunk overhead line length	12.00 km
	Main trunk underground cable length	10.85 km
	Total length of three-phase lateral branches	8.02 km
	Total length of two-phase lateral branches	4.81 km
	Total length of single-phase lateral branches	54.89 km
	Substation voltage level	$25kV_{rms}$ (LL)
	Substation short-circuit level	305 MVA
	Substation equivalent impedance (including substation transformer)	$Z_+ = 0.035 + j2.05\ \Omega$ $Z_0 = 0.053 + j2.161\ \Omega$
Secondary System	Number of service transformers	536
	Total active power load	8.79 MW

- Original distribution feeder

- The underground cables of the main trunk of original feeder are replaced by overhead lines

The objective is to verify what the impact of the main trunk underground cables on the level of each harmonic component is. It is well known that the underground cables have greater shunt capacitances, which might lead to harmonic resonance.

In order to perform the harmonic power flow simulations over the actual feeder the following modifications/inclusions are made:

- The data provided by EPCOR do not contain information about the multi-grounded neutral circuit (MGN) grounding circuit, more specifically, about the grounding span and resistance. Therefore, it is adopted a grounding resistance of 15 ohms and a grounding span of 100 meters. The substation grounding resistance is 0.15 ohms.

- Both the main trunk and branches of *21SU* consist of various types of overhead and underground conductors. In order to facilitate the analysis, one type of overhead line and one type of underground cable are adopted for the harmonic power flow simulations. The criteria used to choose the types is based on those with the longest length in the system.

  o The overhead line was modeled as a three-phase, four-wire line segment model and with a conductor type 336.4 ACSR [41].

  o The underground cable was modeled as a three-phase, six-wire line segment model [41]. The cable type adopted for the simulations is the 500Al XLPE 25kV DBUR. Underground cable conductors

present a much higher shunt capacitance if compared to overhead lines.

- There is only information about the fundamental active power load connected at each service transformer of the 21SU feeder. In order to include the harmonic characteristics of the residential loads, the houses connected to each service transformer is modeled by the bottom up approach as it was done for the ideal feeder. It is assumed that the active power associated with each house is approximately 1kW. Hence, number of houses connected per each transformer is obtained by dividing active power load of that service transformer by 1kW.

- In order to reduce the complexity and the time duration of the simulations over the actual feeder, the concept of aggregated load model is applied to represent residential neighborhoods connected to the feeder main trunk.

The following subsection gives more details about the aggregated residential load model.

3.4.1.1. Aggregated Load Modeling

Figure 3.28 shows several residential areas composed by single and two-phase branches (and a few three-phase branches that do not belong to the main trunk) and service transformers supplying several houses. From a detailed analysis of that network it was possible to identify five residential areas, each one supplied by one main trunk branch, as can be seen in Figure 3.28. Each dashed circle

encompasses a group of branches and service transformers connected to one branch of the main trunk. Each group is denominated "Neighborhood". If a Neighborhood was connected to two or more branches of the main trunk, this would characterized a loop, which is not desirable since the protective devices might lose coordination among each other. For example, all the branches and service transformers inside the "Neighborhood 4" are supplied by the main trunk branch "*11 SU - 0671*".

Since, in this initial study, we are more interested in analyzing the harmonic levels on the main trunk feeder, it is proposed to build an aggregated load model for each "Neighborhood". This is like the extra top on the pyramid in Figure 2.1. Similarly, this procedure significantly reduces the complexity and the time duration of the multiphase harmonic power flow simulations since the aggregated load model of each neighborhood is represented by a 4x4 matrix (three phases and neutral). The steps to build the aggregated model are summarized below:

1. Identify the neighborhoods, which consists of locating the branches (and the service transformers) connected to one main trunk branch. It must be highlighted that there is no "Neighborhoods" connected to more than one main trunk branch since this would characterize a loop in the system.

2. Then, each service transformer with the respective bottom-up service transformer models are represented by the simplified model (discussed on Chapter 2), as it was done for the ideal feeder on Section 3.3.

3. Build the admittance matrix for each neighborhood including the lateral branches, service transformer and the main trunk branch feeding the respective neighborhood.

4. Since, in this initial analysis, we are not interested about the harmonic levels inside each node of the neighborhood, the admittance matrix built in Step 3 can be reduced to a 4x4 matrix, which refers to the sending end node of the main trunk branch connecting the respective neighborhood. All of the harmonic current sources introduces by the service transformers simplified models are also aggregated and reduced to four current sources each one connected to one of the phases. Therefore, the complexity of the simulations is reduced since each neighborhood is represented by a 4x4 matrix (three phases and neutral) and one 4x1 vector (associated with aggregated harmonic current sources).

5. Finally, the substation supply source, the main trunk admittance matrix, the neighborhoods aggregated 4x4 admittance matrices, the grounding circuit are represented in a multiphase harmonic power flow program in the same way it was explained for the ideal feeder on Chapter 3.

The following sections present key results regarding two scenarios:

- **Ideal and Actual Feeder Comparison**: The harmonic components of voltage and current injected at the substation of both ideal and actual feeder are compared in order to verify if there is some similarity at least regarding the distribution of the harmonic components. As the ideal feeder

is only composed by overhead lines, the underground cables of the main

trunk of the actual feeder are replaced by overhead lines.

- **Impact of Underground Cables**: The objective is to compare the

  harmonic levels of the current calculated at the substation of the actual

  feeder for two cases; original feeder and modified feeder, in which the

  main trunk cables are replaced by overhead lines.

3.4.2. Ideal and Actual Feeder Comparison: Base Case

The objective of this section is to determine if the results regarding the ideal

feeder presented on Section 3.3 are adequate. Therefore, some key results related

to the ideal feeder are compared to the actual feeder shown in Figure 3.28. First,

the base case study is analyzed and, then, the "natural" load evolution case study

is evaluated in the next subsection. The only modification over the actual feeder is

that the underground cables of the main trunk are replaced by overhead lines. It

must be noticed the lateral branches (i.e., the branches that do not belong to the

main trunk) remain unchanged even if those that are cables. Because of these

changes, the actual feeder will be referred to as "Modified Actual Feeder" in the

following results.

Since, the topology of the ideal and actual feeders are significantly different, the

location of analysis is at the substation of both feeders. As it was done before,

first the phase voltage to neutral (or current) at the substation location are

obtained, for a 24 hours period (to take into account different appliance usage), from the harmonic power simulations. Then the 95% cumulative distribution function (*cdf*) of this 24 hours period is determined and used for the comparison.

Figure 3.29 shows the daily active and reactive power calculated at the substation location of both ideal and modified actual feeder (i.e., only overhead lines). One can observe a good correlation between Figure 3.29(a) and Figure 3.29(b), which is expected because the loads for both case are modeled through the bottom-up approach and the topology of the networks does not impact significantly in the results. This suggests that the results presented on Section 3.3 associated to the ideal feeder can be used with confidence. This is also corroborated by the results associated to other indices as shown below.
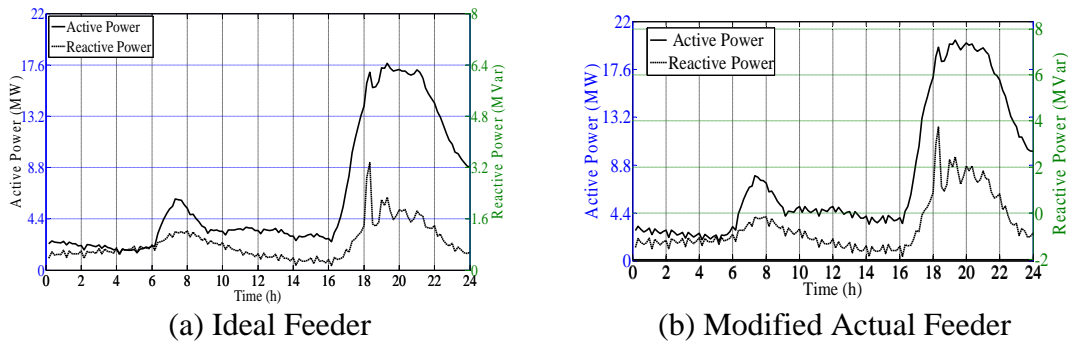
(a) Ideal Feeder   (b) Modified Actual Feeder
Figure 3.29 Daily active and reactive power at the substation

Figure 3.30 shows the 95% cdf dominant sequence harmonic current calculated at the substation of both ideal and modified actual feeder. One can observe a good correlation between the results, which reveals that the ideal feeder can produce representative results.
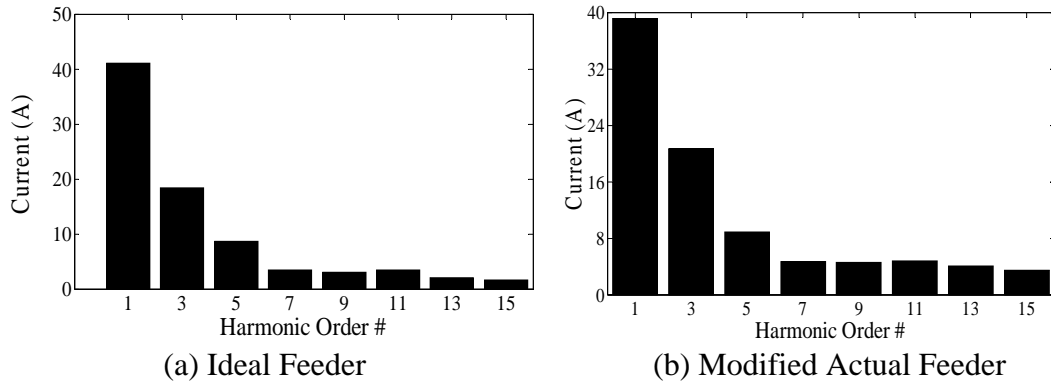
(a) Ideal Feeder   (b) Modified Actual Feeder

Figure 3.30 95% cdf value of the dominant sequence harmonic current at the substation (fundamental divided by 10)

Figure 3.31 illustrates the average zero sequence harmonic current calculated at the substation. One can observe that the fundamental current associated to the modified actual feeder is higher than the one associated to the ideal feeder revealing that the actual feeder loads are more unbalanced. Furthermore, there is a good correlation between harmonic components.

It can also be observed that the fundamental component of the zero sequence current for the modified actual feeder is higher if compared to the ideal feeder revealing a more unbalanced system, which is expected because in the ideal feeder the loads are evenly distributed.
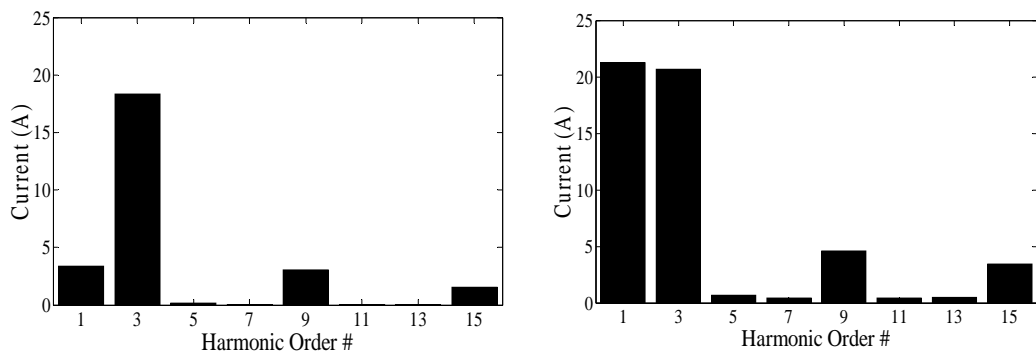
(a) Ideal Feeder   (b) Modified Actual Feeder
Figure 3.31 95% cdf value of the zero sequence harmonic current at the substation

Two important indices that can be used to compare different networks are the *TDD* and the *THD* since they are normalized to the loading of each network. Figure 3.32 and Figure 3.33 show the daily *TDD* and voltage *THD* at the substation of both feeders, respectively. One can observe a good correlation between the results associated to the ideal and actual feeders.
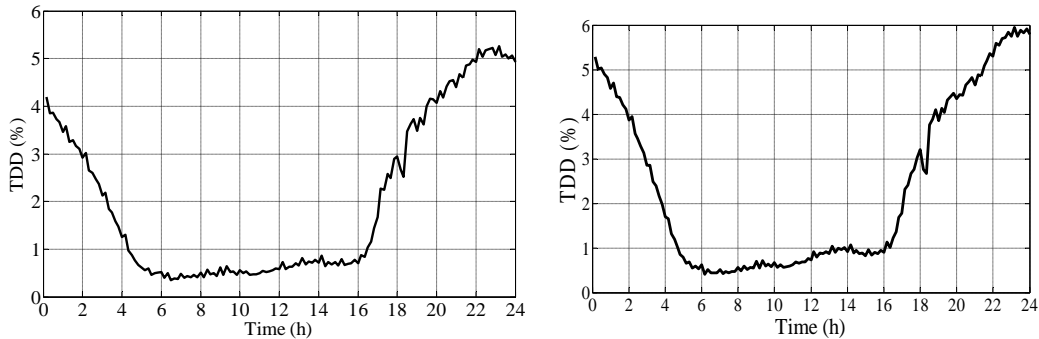
(a) Ideal Feeder   (b) Modified Actual Feeder
Figure 3.32 Daily Phase A TDD at the substation
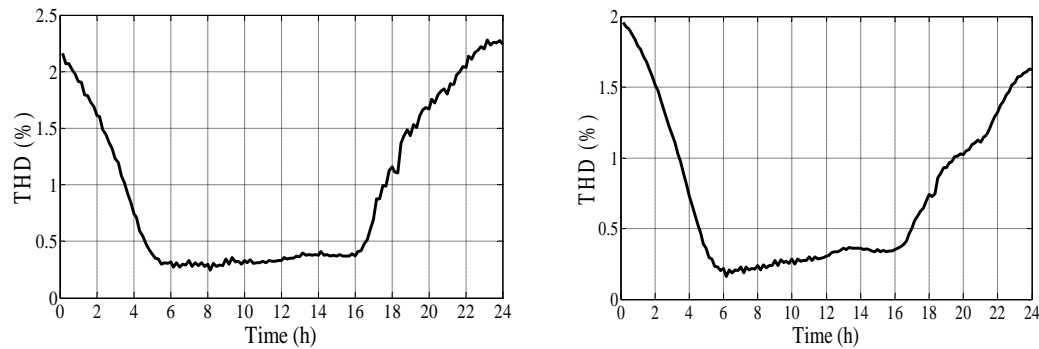
(a) Ideal Feeder   (b) Modified Actual Feeder
Figure 3.33 Daily voltage phase A THD at the substation

Figure 3.34 shows the average neutral to ground voltage calculated at the substation of both ideal and modified actual feeders. Again, one can observe a

good correlation between the results. The higher fundamental component associated to the modified actual feeder can be explained by the irregular distribution of the loads on that system. Again, the high fundamental component of the neutral to ground voltage shown in Figure 3.34(b) reveals the unbalance level of the actual feeder.
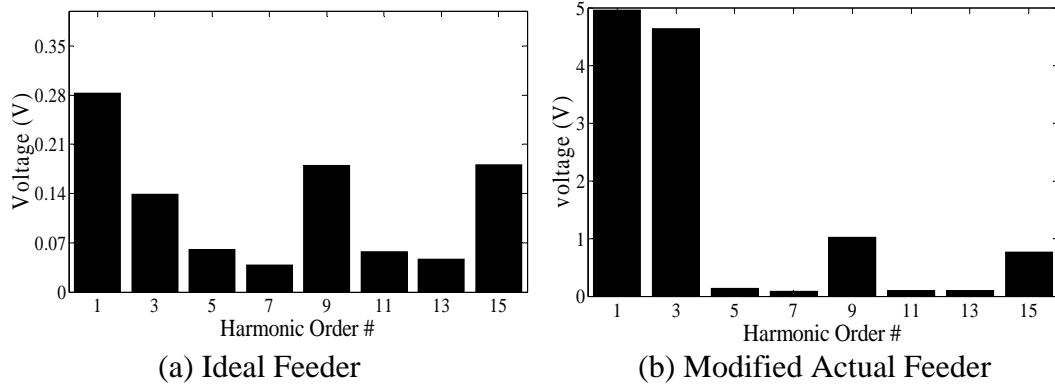
        (a) Ideal Feeder   (b) Modified Actual Feeder
Figure 3.34 95% cdf value of the neutral to ground voltage at the substation

Figure 3.35 and Figure 3.36 show the average individual IT and the daily total IT calculated at the substation of both feeders, respectively. Figure 3.36(b) illustrates that the results associated to the modified actual feeder confirm the conclusions obtained for the ideal feeder, which is that the individual 3rd, 9th and 15th harmonic orders are the components that most contribute for the IT level on the system.

(a) Ideal Feeder

(b) Modified Actual Feeder
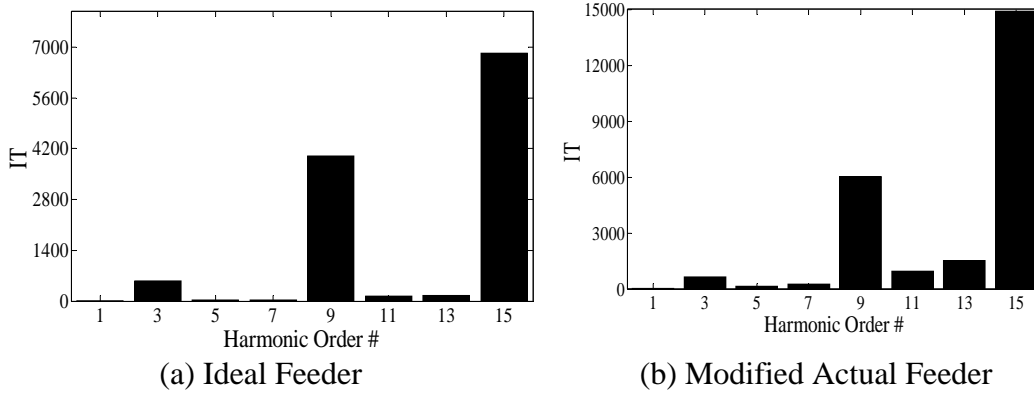
Figure 3.35 95% cdf value of the individual IT at the substation

(a) Ideal Feeder

(b) Modified Actual Feeder
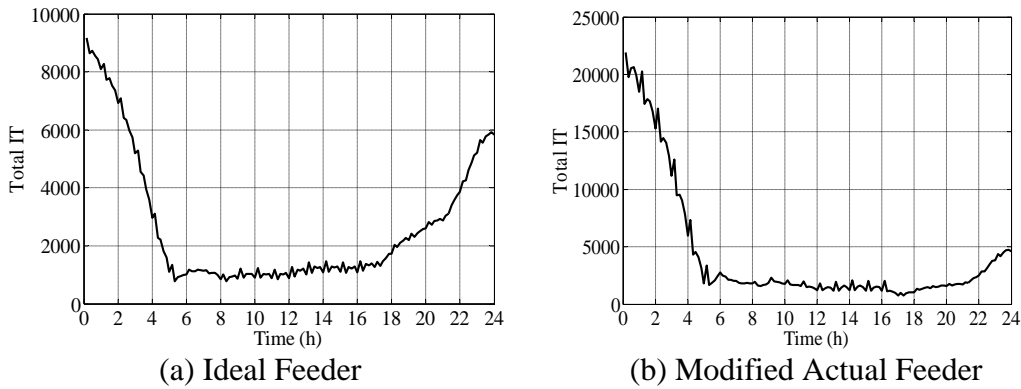
Figure 3.36 Daily Total IT at the substation

3.4.3. Impact of Underground Cables on the Distribution System

It is known that the underground cables have higher shunt capacitances if compared with overhead lines, which might impact significantly on the harmonic levels of the system. In this context, the objective of this section is to verify the impact of different types of conductors on the harmonic levels at the substation. In order to perform this comparison, two network scenarios are considered:

- **Original Actual Feeder**: as mentioned before, the original feeder contains a mix of underground cables and overhead lines composing the main trunk

- **Modified Actual Feeder**: this is the same network analyzed on previous section, which consists of the original actual feeder, but the underground cables of the main trunk are replaced by overhead lines.

Figure 3.37 shows the comparison between the original actual feeder and modified actual feeder (i.e., only overhead lines at the main trunk) for the 95% cdf value of the dominant and zero sequence harmonic current, daily phase *TDD* and voltage *THD* and average individual IT and total IT calculated at the substation.

(a) Dominant sequence current

(b) Average zero sequence current

(c) Daily Phase A TDD

(d) Daily Phase A voltage THD

(e) Average individual IT   (f) Daily Total IT
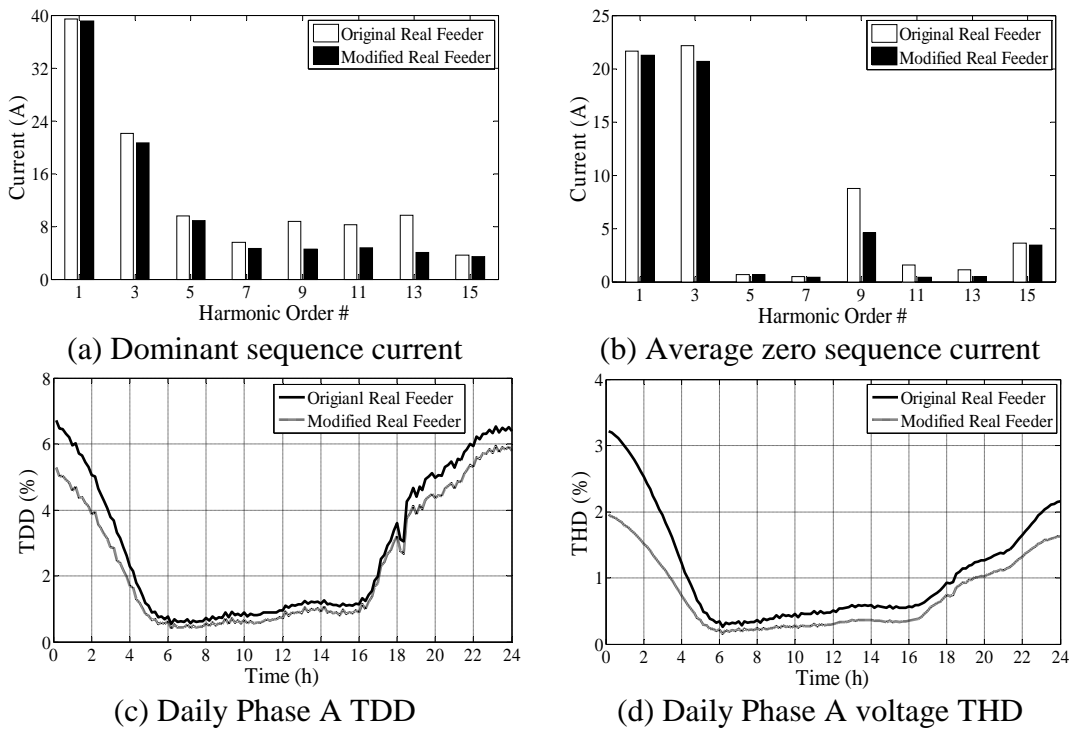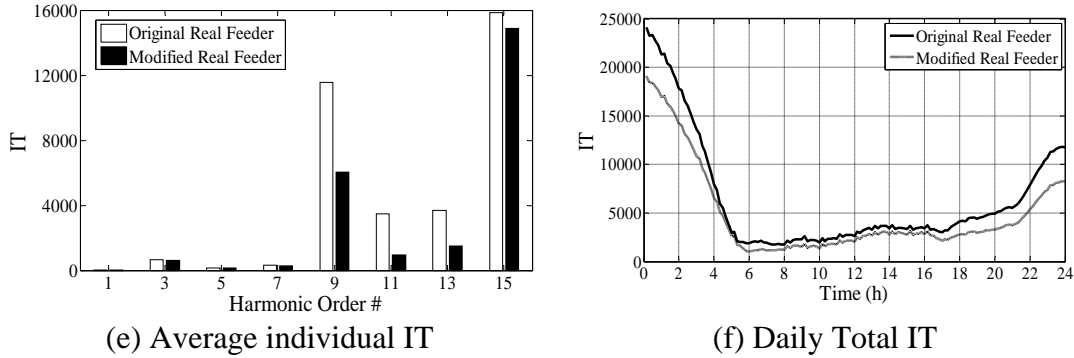
Figure 3.37 Impact of underground cables on the harmonic levels at the substation

The main findings are as follows:

- One can observe that the presence of underground cables lead to more distortion at the network since practically all harmonic components increased.

- The increasing distortion caused by the underground cables can also be seen by the *TDD* and voltage *THD* levels shown in Figure 3.37(c) and Figure 3.37(d).

- Figure 3.37 (e) shows that the presence of underground cables led to an increase of the 3rd and 9th and 15th individual IT levels. Eventually, most of the time, during the period of 24 hours, the total IT is higher when the underground cables are considered in the main trunk, as can be shown in Figure 3.37(f).

3.4.4. Ideal and Actual Feeder Comparison: Load Evolution

The objective of this section is similar to the previous subsection, which is to provide a validation of the results regarding the "Natural" Load Evolution case

study carried out for the ideal feeder in the Section 3.3.2. It must be noticed that the same actual distribution network from the base case of previous subsection is used and the number of customers remains the same as in the base case. Only the appliances penetration for each existing customer will change according to the load trend.

Just to remind, in the load evolution case study analyzed in Section 3.3.2, it was determined the average annual growth rate for each power quality (PQ) index. This chart provides an estimation of how much each PQ index will grow in the following years. This can be useful to see how long it will take to exceed some limit imposed by standards and utilities, like the voltage *THD* for example.

The same procedure is applied for the modified (only overhead lines on the main trunk) EPCOR actual feeder and for the original EPCOR actual feeder presented on the previous subsection in order to determine the annual growth rate for key PQ indices and these results are compared to those associated to the ideal feeder. The comparison results are shown in Figure 3.38. As it was done in the previous subsection, each PQ index was calculated at the substation of both the actual and ideal feeders.

One can observe from Figure 3.38 below that the annual growth rates for different PQ indices that were obtained for the ideal feeder in Section 3.3.2 are adequate because they are close to the annual growth rates obtained from both the modified

and the original actual feeder. For example, Figure 3.38(c) shows that the total IT

will grow at an average rate of 12.5% for the ideal feeder, 10.4% for the modified

actual feeder and 10.2% for the original actual feeder.

(a) Dominant sequence voltage

(b) Dominant sequence current

(c) Individual IT

(d) Neutral to ground voltage
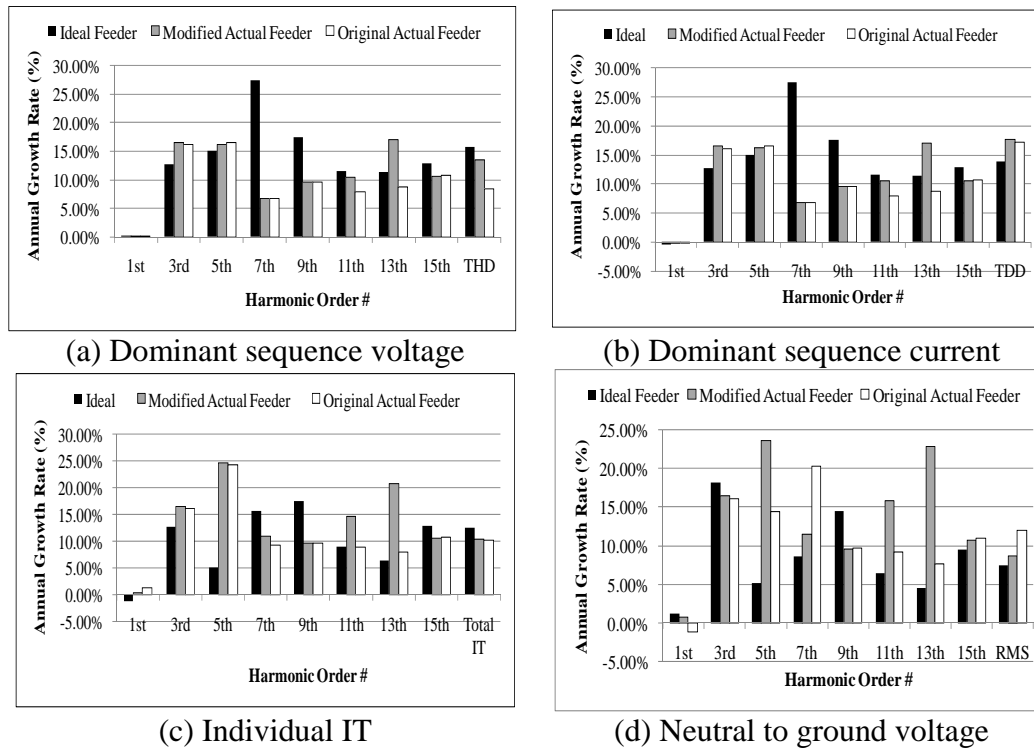
Figure 3.38 Comparison of the load evolution case study between the ideal feeder
and the actual feeder (all PQ indices were calculated at the respective substations).

3.5. Simulation Results Compared with Field Measurement

To further verify our model, our field measurements are compared with the one

from our ideal case and actual case simulation.

The field measurements conducted from 2008 to 2011 included 16 residential

feeders. The measurements were all taken in the substation so that the results

represent the total feeder currents. The comparison is done in the form of IT per

MW load (IT/MW) and harmonic currents per MW load (Ampere/MW)[4]. The

results are shown in Figure 3.39, Figure 3.40 and Figure 3.41 respectively.
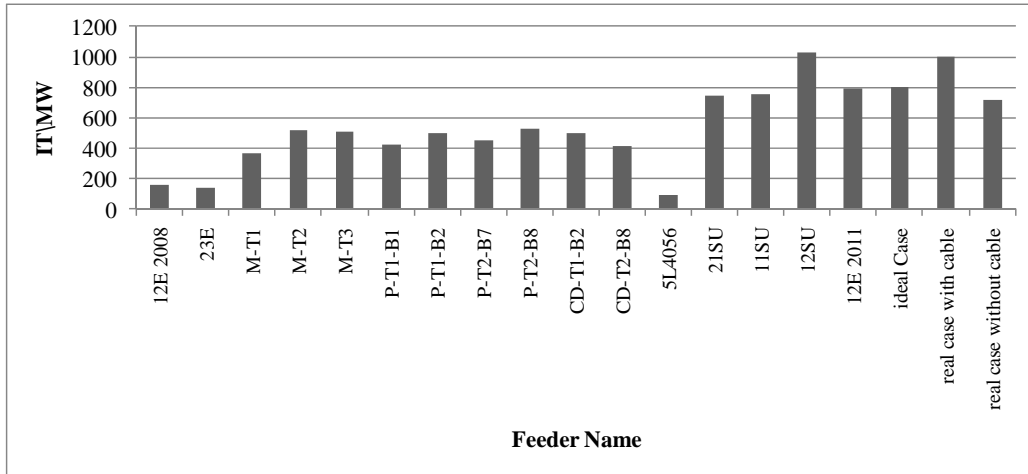
Figure 3.39 IT per MW for different feeders
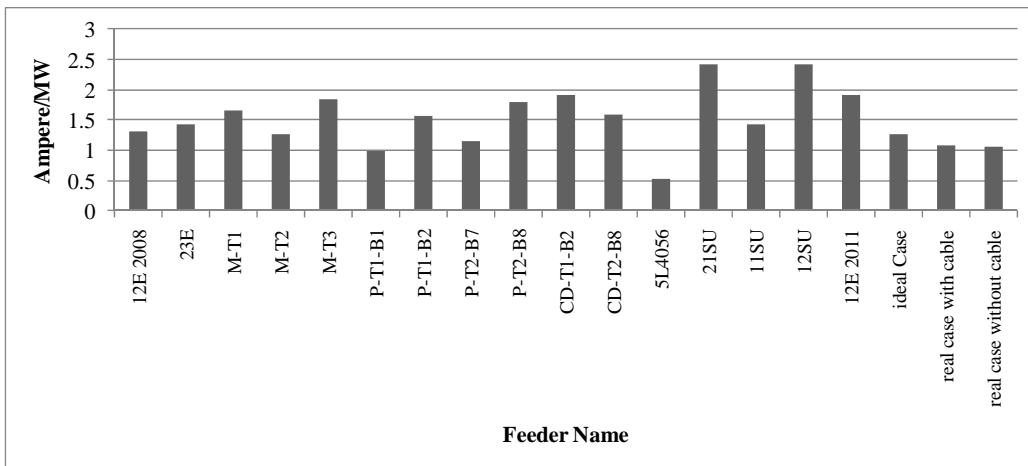
Figure 3.40 3rd harmonic per MW for different feeders

---

[4] Since feeders with different voltage ratings (V_{rated}) are present here, all the harmonic currents are converted to the same voltage level (V_{base}) based on the following equation

$$I_{new} = I_{real} \times V_{rated} / V_{base}$$

The harmonic current daily profile is divided by the substation power daily profile and the Ampere/MW is obtained from the average of this division. The IT daily profile is divided by the substation power daily profile and the IT/MW is obtained from the average of this division
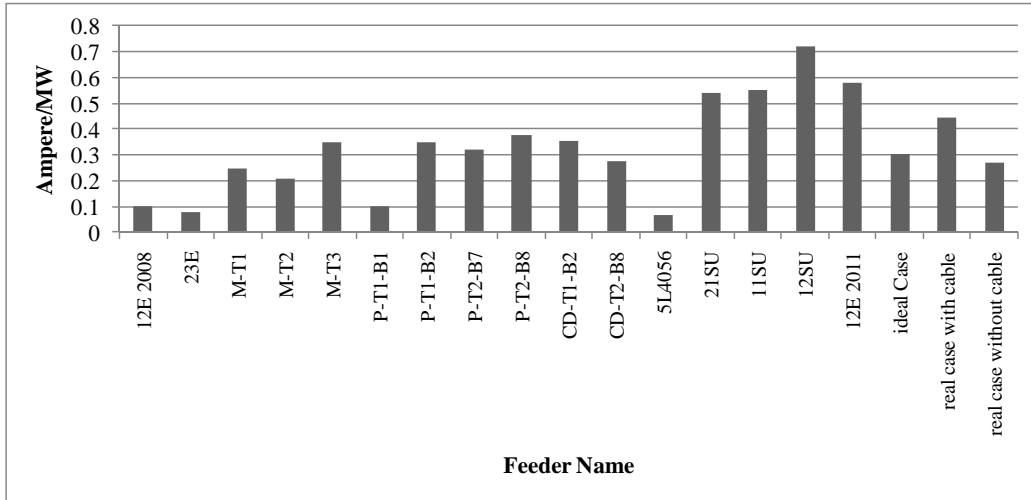
Figure 3.41 9th harmonic per MW for different feeders

Due to the differences in feeder configurations, seasonal and load composition[5], IT/MW level for different feeders are ranging from 180 to 1000. Simulation results from ideal feeder and actual feeder are around 800 and 900 respectively. Regardless of the differences, both measurement and simulation have shown the high IT levels have become a norm for residential feeders. Both utility and telephone companies need to face this new reality.

3.6. Summary

This chapter performed system-wide harmonic simulation in two cases: ideal case and actual case. Each case conducts two kinds of simulations: base case and load evolution.

---

[5] All the measurements are done before 2010, except feeder 21SU, 11SU, 12SU and 12E2011 done in 2010. The loads supplied by those four feeders are newly constructed residential houses. It is possible that these loads have more harmonic producing appliances.

The intention of ideal case study is to determine what the expected level of harmonics and IT is in an "ideal" residential feeder. Since the simulation case is "ideal", distributed residential loads are the only case of the resulting harmonics. Resonance, unbalance and other contributing factors are eliminated. The actual case study was then performed to further confirm the ideal case results.

Load evolution study provides a way to estimate the harmonic trend of near future, whose results are very useful for utility planners.

In addition, the results comparison with real measurement data, from another perspective, confirms our simulation results are rational.

The key findings of the simulation studies performed in this chapter are listed as follows:

- High harmonic and IT levels are expected for residential feeders. And the main contributor is the 9th and 15th harmonics. This is consistent with our field measurement.

- Neutral voltage rise and system power loss will not be a problem in a residential distribution system.

- The annual growth rate of voltage THD and current TDD are 15% and 14% respectively. The main contributing appliances are CFLs and PCs.

- The harmonic impact produced by multiple CFLs are comparable to those produced by individual home electronics such as desktop PCs. Switching to CFLs in a representative house is almost equivalent to adding a half desktop PC to the house.

- Residential loads have already caused excessive harmonic problems in a pure residential feeder. And in the near future, this problem will be getting worse and worse.

Chapter 4

Harmonic Mitigation Study

Harmonic distortions can have significant adverse effects on both power system components and customer devices. Various harmonic-mitigation techniques have been proposed and applied in recent years [43]~[46].

There are two major approaches to deal with excessive harmonic problems. One is system design modifications. Examples are, adding a neutral to mitigate the telephone interference problem, fixing the poor groundings to bring down the potential voltage rise in neutral, balancing loads among phases to decrease zero-sequence harmonic current, and so on. However, some of those methods are not clear to industry and utility, their effectiveness is doubtful. In the first section of this chapter, we carried out extensive sensitivity studies in our model, aiming to clarify those issues and guide utility in the future to better use those methods.

Another way for harmonic mitigation is quite intuitive and well developed, which is passive harmonic filters. However, few references ever talked about filters specially targeting at zero sequence harmonic current, which are promising for solving telephone interference problems. An ideal zero sequence filter will only affect the zero sequence harmonic currents in a feeder. It does not have an impact on positive and negative sequence currents. The second section of this chapter

will, therefore, focus on this kind of passive filters and their effectiveness will be verified using the modeling proposed in Chapter 2.

4.1 System Parameters Sensitivity Study

Several system sensitivity studies are conducted in both our ideal model and the actual case model in this section. The system parameters evaluated on the studies are outlined below (parameters values in bold refer to the base case). It must be noticed that the parameters values are based on several standards and technical guides [47][48]. The results are presented in the next subsections. Discussions and conclusions are given as well.

- Substation grounding (R_{gs}):

    o $R_{gs} = \{$**0.15 Ω**, 1 Ω, 3 Ω, 5 Ω$\}$

- Substation source impedance (data provided by different utilities including transformer impedance):

    o **Base Case**: MVA Level = 243 MVA; $Z_{positive} = 0.688 + j2.470$ ohms;

      $Z_{zero} = 0.065 + j2.814$ ohms

    o Case 1: MVA Level = 243 MVA; $Z_{positive} = 0.776 + j2.440$ ohms;

      $Z_{zero} = 0.419 + j3.279$ ohms

- o Case 2: MVA Level = 98 MVA; $Z_{positive} = 0.500 + j6.300$ ohms;

  $Z_{zero} = 2.400 + j11.400$ ohms

- Load distribution

- MGN primary system neutral grounding resistance (R_{gn}):

  - o $R_{gn} = \{5\ \Omega,\ 10\ \Omega,\ \mathbf{15\ \Omega},\ 20\ \Omega\}$

- MGN primary system neutral grounding span (s):

  - o s = $\{\mathbf{75\ m},\ 150\ m,\ 500\ m,\ 1000\ m\}$

- Neutral broken

- Load balancing

In the same manner as the base case and the load evolution study case, all the results are represented by the *time 95% cdf value* over the average of the index of interest if the ideal case has been used. For the actual case, since the loads are not evenly distributed, various locations need to be checked separately.

4.1.1. Substation grounding (R_{gs})

This sensitivity simulation has been done in both ideal case and actual case. The results from ideal case is presented in this section and discussed. The results for actual case can be found in Appendix B.1, which shows the same conclusion.

This case study considers the impact of different substation grounding (R_{gs}) on the harmonic levels of the primary system. The other system parameters remain the same as the base case. The results reveal that:

- Substation grounding resistance practically has no impact on the fundamental and harmonic components of phase and sequences current and voltages at the primary system.

- There is a slight change on the neutral current, on the IT levels and on telephone line induced voltage. Figure 4.1 illustrates the harmonic spectrum of the primary system neutral current and voltage induced at the telephone line.
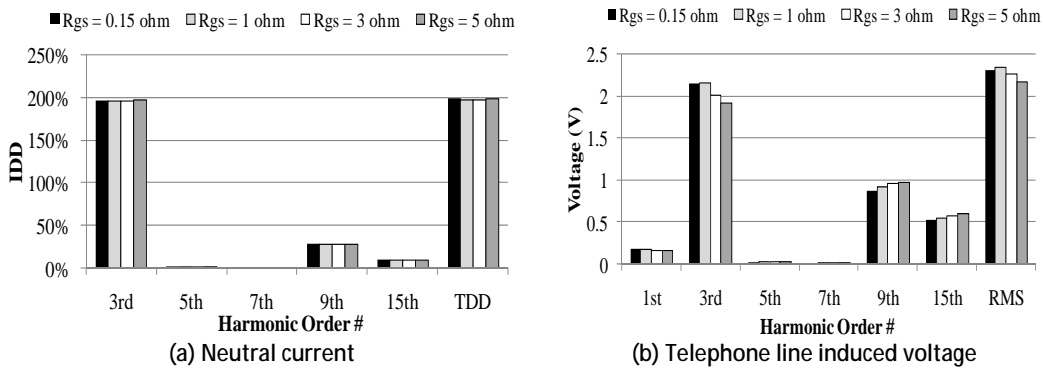
Figure 4.1 Impact of substation grounding resistance on the primary distribution system

- The larger the substation grounding resistance, less current circulates on the grounding, as a consequence the neutral current increases.

- It is observed that the neutral current and the telephone line have different behavior as *Rgs* increases, as shown by the 3rd harmonic component. This can be explained by the fact that the voltage induced is roughly

proportional to the difference between the phases current (or zero sequence) and the neutral current. As the latter remain constant and the former increases, the voltage induced decreases.

- The reason why the impact of the substation grounding is insignificant can be intuitively explained by the fact that the multi-grounded neutral circuit resistances dominate the substation grounding resistance.

Table 4.1 Impact of different substation grounding resistance

	R_{gs}				Diff. (%) 1 Ω	Diff. (%) 3 Ω	Diff. (%) 5 Ω	Impact
	0.15 Ω (base case)	1 Ω	3 Ω	5 Ω				
Dom. Sequence THD$_V$ (%)	4.15	4.15	4.18	4.20	0.00%	0.72%	1.20%	NO
Dom. Sequence TDD (%)	4.80	4.78	4.75	4.74	0.42%	1.04%	1.25%	NO
IT	2592	2586	2575	2570	0.25%	0.64%	0.85%	NO
RMS Neutral Voltage	0.26	0.26	0.26	0.26	0.00%	0.00%	0.04%	NO
RMS Telephone Line Voltage	2.30	2.33	2.25	2.17	1.39%	2.04%	5.69%	NO

- Phase and neutral losses remain at low levels for different substation grounding resistance so that it is not a concern.

4.1.2. Substation source impedance

Since the actual case has its own fixed source impedance provided by utility, this sensitivity study has been done on the ideal case.

This section analyzes the impact of different substation source impedances on the harmonic levels of the primary system. Three cases are analyzed and the

impedances are based on actual substation feeders data provided by Canadian distribution utility companies. Three cases are analyzed.

- **Base Case**: MVA Level = 243 MVA; $Z_{positive}$ = 0.688 + j2.470 ohms; Z_{zero} = 0.065 + j2.814 ohms

- Case 1: MVA Level = 243 MVA; $Z_{positive}$ = 0.776 + j2.440 ohms; Z_{zero} = 0.419 + j3.279 ohms

- Case 2: MVA Level = 98 MVA; $Z_{positive}$ = 0.500 + j6.300 ohms; Z_{zero} = 2.400 + j11.400 ohms
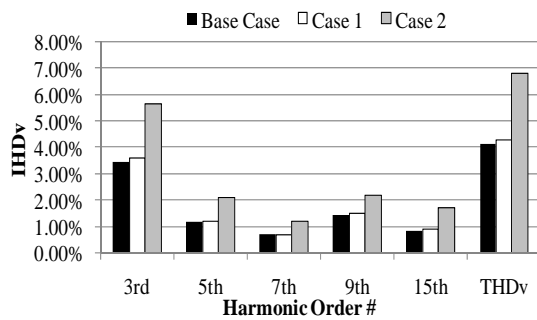
(a) Dominant sequence voltage (fundamental divided by 100)
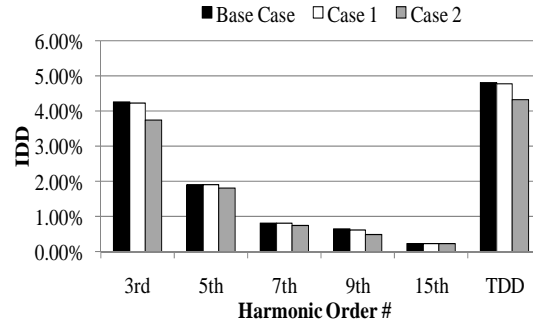
(b) Dominant sequence current (fundamental divided by 10)
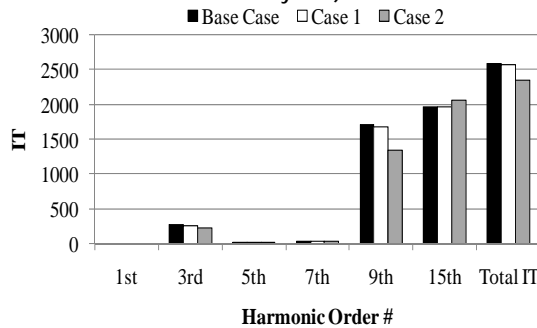
(c) Individual IT
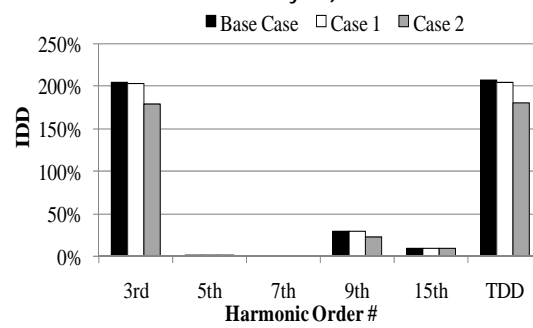
(d) Neutral current
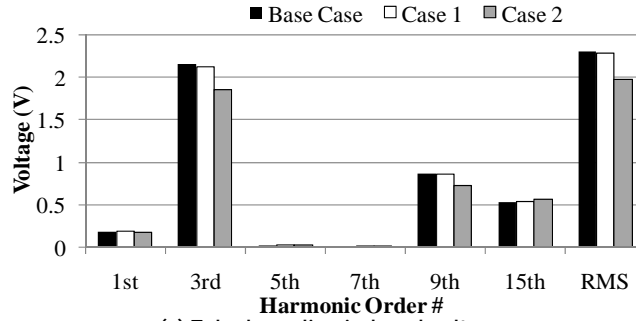
(e) Telephone line induced voltage

Figure 4.2 Impact of substation source impedance on primary distribution system

The main findings are as follows:

- Figure 4.2 shows that the substation source impedances considered have a significant impact on different parameters. The impact on the voltage distortion is the opposite if compared to the impact on the current distortion.

- For example, for Case 2, the harmonic components of the dominant sequence voltage increase significantly if compared to the Base case. On the other hand, the dominant sequence current, neutral current and IT levels decreased. The reason is because the Case 2 has much larger impedance if compared to the other cases.

Table 4.2 Impact of different substation source impedance

	Substation Impedance			Diff. (%)	Diff. (%)	Impact
	Base Case	Case 1	Case 2	Case 1	Case 2	
Dom. Sequence THD$_V$ (%)	4.15	4.28	6.79	3.20%	63.72%	YES
Dom. Sequence TDD (%)	4.780	4.77	4.33	0.21%	9.41%	YES
IT	2592	2566	2347	1.00%	9.46%	YES
RMS Neutral Voltage	0.26	0.26	0.26	0.00%	0.75%	NO
RMS Telephone Line Voltage	2.30	2.28	1.97	0.87%	14.24%	YES

- Phase and neutral losses remain at low levels for different substation source impedances so that it is not a concern.

4.1.3. Load distribution

The actual case has its fixed load distribution, so this sensitivity study has been done on the ideal case.

In this case study the distribution of the service transformers is changed in order to verify if there is any impact on the harmonic levels of the primary system. Three cases are analyzed:

- Base case: Service transformers are evenly distributed (12 per km and for each phase, which gives 540 installed service transformers)

- Case 1: 50% of the service transformers of the base case are at the middle of the line and 50% at the end of the line

- Case 2: 100% of the service transformers of the base case are at the end of the line
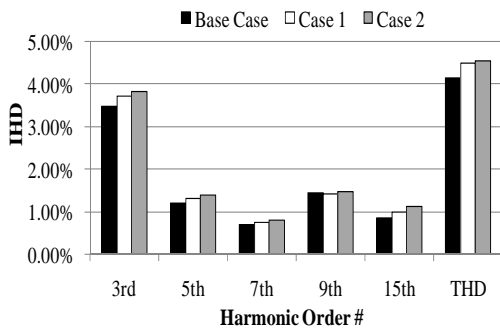
(a) Dominant sequence voltage (fundamental divided by 100)

(b) Dominant sequence current (fundamental divided by 10)

(c) Individual IT

(d) Neutral current

(e) Telephone line induced voltage
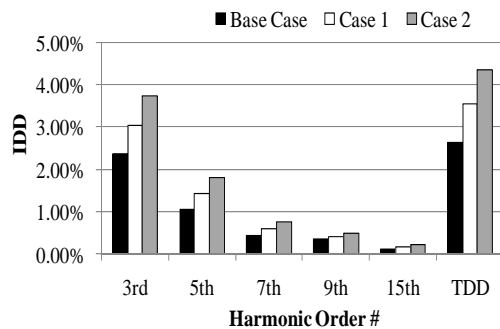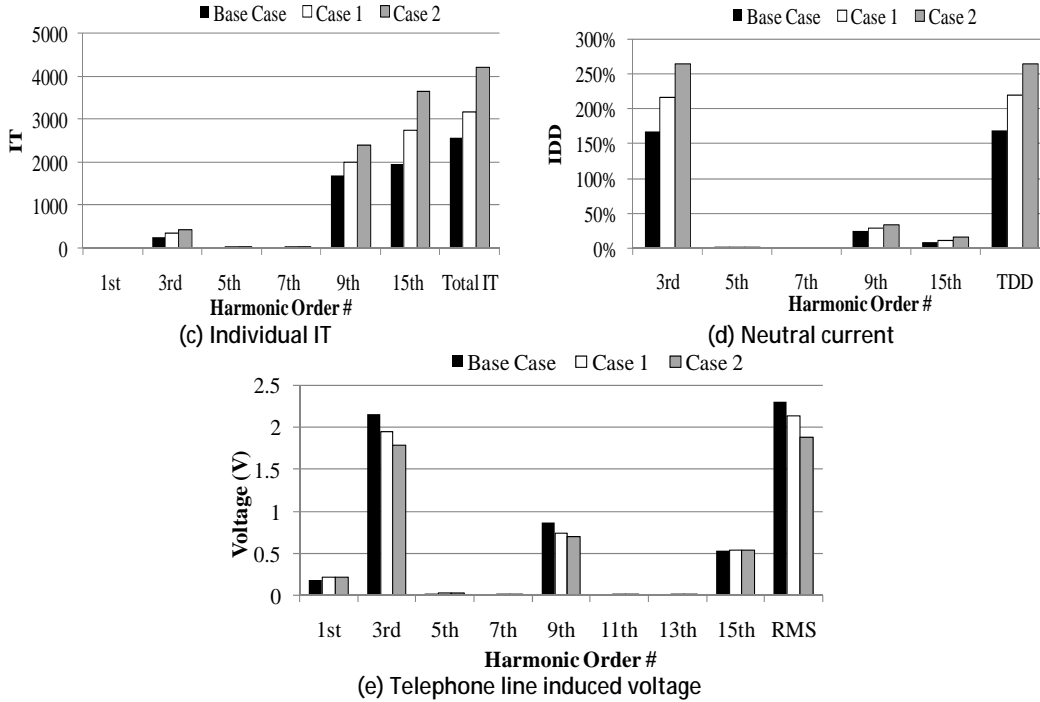
Figure 4.3 Impact of load distribution on primary distribution system

The main findings are as follows:

- Among all the parameter sensitivity studies, load distribution has the biggest impact on all the indices. Nonetheless, the phase and neutral losses remain at low levels so that it is not a concern.

- Figure 4.3 shows that current harmonic levels increase when the loads are more concentrated at one location, which is somewhat due to the fact the harmonic cancelation becomes smaller. That is why the case with 100% loads at the end has the largest zero sequence current for almost all the harmonics.

Table 4.3 Impact of different load distribution configurations

	Load Distribution			Diff. (%)	Diff. (%)	Impact
	Base Case	Case 1	Case 2	Case 1	Case 1	
Dom. Sequence THD$_V$ (%)	4.15	4.49	4.55	8.19%	9.64%	YES
Dom. Sequence TDD$_I$ (%)	2.64	3.55	4.35	34.47%	64.77%	YES
IT	2592	3166	4194	22.14%	61.80%	YES
RMS Neutral Voltage	0.26	0.21	0.27	19.55%	1.88%	NO
RMS Telephone Line Voltage	2.30	2.13	1.88	7.25%	18.10%	YES

- Figure 4.3(e) shows that the telephone line induced voltage has an opposite behavior if compared to the other parameters as the load configuration changes. It was observed that the increment on neutral current is larger if compared to the zero sequence when the loads are more concentrated. As a consequence, the induced voltage decreases.

- Phase and neutral losses remain at low levels for different load distribution configurations so that it is not a concern.

4.1.4. MGN system grounding resistance (R_{gn})

In this subsection, only the ideal case sensitivity results are given. The actual case counterpart can be found in Appendix B.2.

In this case study, the MGN system grounding resistance is varied in order to verify the impact on the distribution system harmonic levels. The findings are as follows:

- MGN grounding resistance practically has no impact on the fundamental and harmonic components of phase and sequence currents and voltages at the primary system.

- Similarly to the previous section results, there is a very slight change on the neutral current, which translates into a change on the telephone line induced voltage, as shown by Figure 4.4. There is almost no impact.
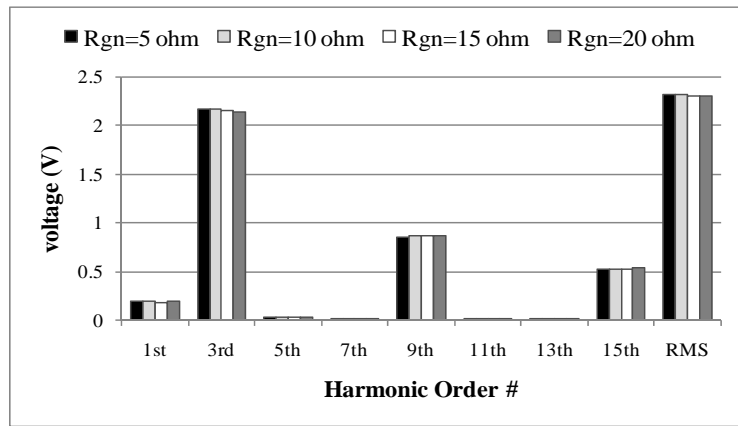
Figure 4.4 Impact of MGN system grounding resistance on the telephone line induced voltage

- Phase and neutral losses remain at low levels for MGN system grounding resistances so that it is not a concern.

As expected, the variation of MGN neutral grounding span (s) presented similar to results with the variation of the grounding resistance (R_{gn})

It is easy to understand that the grounding condition has little impact on the phase conductor harmonic currents, but intuitively it can still have some impacts on the

induced voltage on telephone line by affecting the neutral current. However, for a long enough feeder, the impact would be very small as explained below.

Table 4.4 Impact of different MGN system grounding resistances

	R_{gn}				Diff. (%) 5 Ω	Diff. (%) 10 Ω	Diff. (%) 20 Ω	Impact
	5 Ω	10 Ω	15 Ω (base case)	20 Ω				
Dom. Sequence THD$_V$ (%)	4.15	4.15	4.15	4.15	0.00%	0.00%	0.00%	NO
Dom. Sequence TDD$_I$ (%)	4.80	4.80	4.79	4.79	0.21%	0.21%	0.00%	NO
IT	2591	2591	2592	2592	0.02%	0.03%	0.01%	NO
RMS Neutral Voltage	0.26	0.266	0.266	0.26	0.00%	0.00%	0.38%	NO
RMS Telephone Line Voltage	2.31	2.32	2.30	2.298	0.48%	0.35%	0.26%	NO

Figure 4.5 shows the network topology for the ideal case used in Chapter 3. In order to see the current profiles in the neutral, loads are only connected to the last node (node # 195).
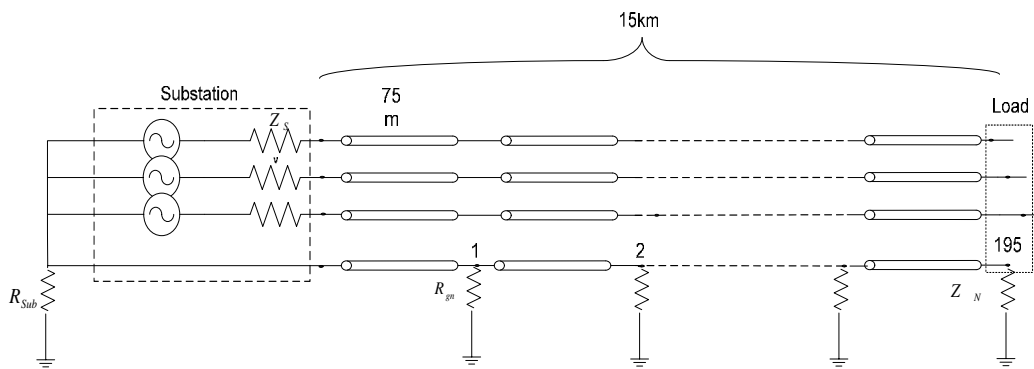
Figure 4.5 Network topology for neutral current case study

The neutral current consists of two components. The first one is the conducted zero sequence current flowing back to the substation. While the second

component is the induced current. Figure 4.6 show the simulation results from the simple case in Figure 4.5.
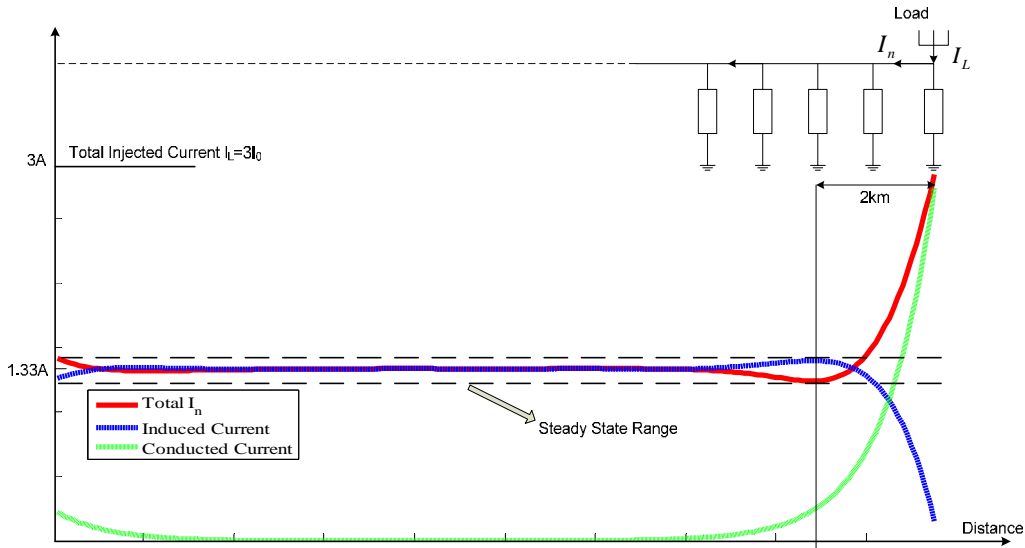
Figure 4.6 Two components of neutral current

It is difficult to differentiate induced current and conducted current, since the conducted current is always present in whatever case due to the multi-grounded network. In this simulation, a normal case was run in the network as shown in Figure 4.5. And then a second case was run after the coupling (mutual impedance) between phase and neutral were removed. The neutral current obtained from this case is pure conducted current, since there is no induced voltage in neutral at all.

According to circuit superposition theory,

$$I_{induced} = I_{n_{total}} - I_{conducted}$$

Equation 4.1

In this way, induced current and conducted current have been separated successfully, and shown in Figure 4.6. The conducted current is first diverted by the load grounding resistance. The remaining portion flows back to the substation. In this process, the neutral grounding resistances further divert the current to the ground. After around 2km, the conducted current decreases to around zero level.

Figure 4.6 shows the induced current increases from zero. After 2km, it also reaches a steady state value around 1.33A, which is mainly caused by the induced current.
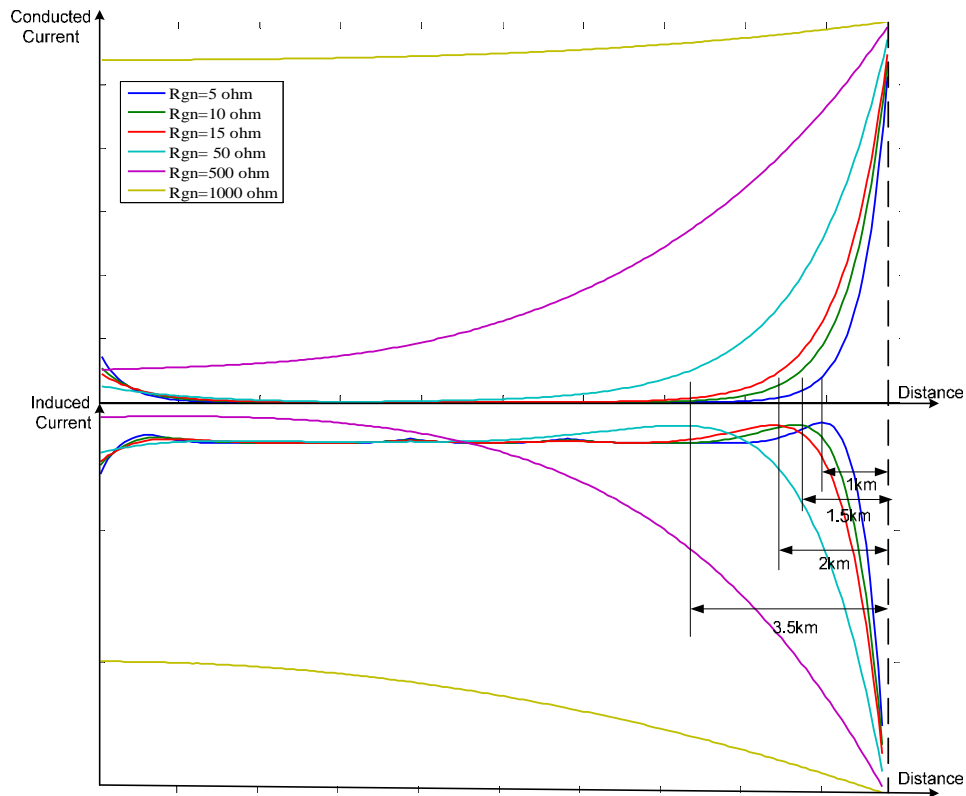
Figure 4.7 Conducted current and induced current profile for different R_{gn}

Figure 4.7 shows R_{gn} determines after how far away from load, both conducted and induced current will go to a steady state value. The bigger R_{gn} is, the longer the distance is that needed to get into steady state.

In the normal range of R_{gn} (5 ohm to 15 ohm), neutral current decreases to a steady state value after 2km away from the harmonic load. Out of this distance range, neutral current is not affected by R_{gn}.

To summarize:

- Both conducted current and induced current get into a steady state value when it is far away from the load.

- The distance they need to get into steady state is dependent on *Rgn*. The bigger *Rgn*, the longer distance needed.

- The steady state value for conducted current is zero, while a constant value for induced current. Therefore, the total steady state neutral current is determined by induced current.

Therefore, it is concluded that grounding resistance R_{gn} has little impact on neutral current (including both conducted current and induced current) in a big range of a typical distribution system, which also means no effect on induced voltage in the parallel telephone line. This can be simply explained as follows.

It is easy to understand that when R_{gn} increases, less conducted current at each section in the ladder network will go to ground, that is why the larger R_{gn} is, the longer distance it needs to get to zero.

Figure 4.8 shows induced current in the neutral. When the feeder is long enough, a big range of neutral sections in the middle can be considered same according to circuit symmetry (both sides are long enough), which implies:

$$I_{induced_n} = I_{induced_{n+1}}$$

Equation 4.2

According to KCL, therefore there is no current going through grounding resistor. That is why grounding resistance has little impact on the induced current as well.
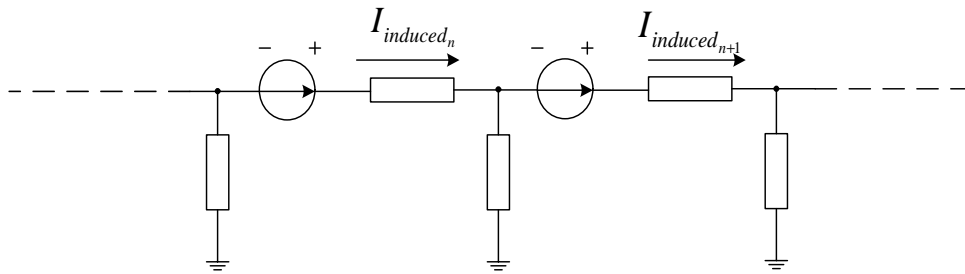
Figure 4.8 Induced current in neutral

4.1.5. Neutral Broken

Neutral broken happens very often due to conductor rot, physical damage, or even on purpose for saving conductor material [50]. However, its impact on harmonic behavior, especially for telephone interference is not quite clear. In [51], shielding effect was proposed to describe how a neutral line plays the role in telephone

interference. The neutral carries the current in the opposite way as the one in the parallel phase conductor. This cancels out the induced voltage in the parallel telephone line. So generally speaking, a neutral line could help shield part of the harmonic interference in parallel telephone line from power line. This effect is called shielding effect. And the bigger the neutral current is, the better the shielding effect is.

However, paper [51] only focuses on the induced current in neutral. When conduction current was taken into account, no more simple equations or theories are available to guide people when one deals with harmonic problem in a multi-grounding system.

Neutral broken is more dependent on the case, it is, therefore, hard to use our ideal case to draw a very generic conclusion. In this section we focus on the actual case with a actual telephone line, shown in Figure 4.9. It has a telephone line going from Location 1 to Location 2.
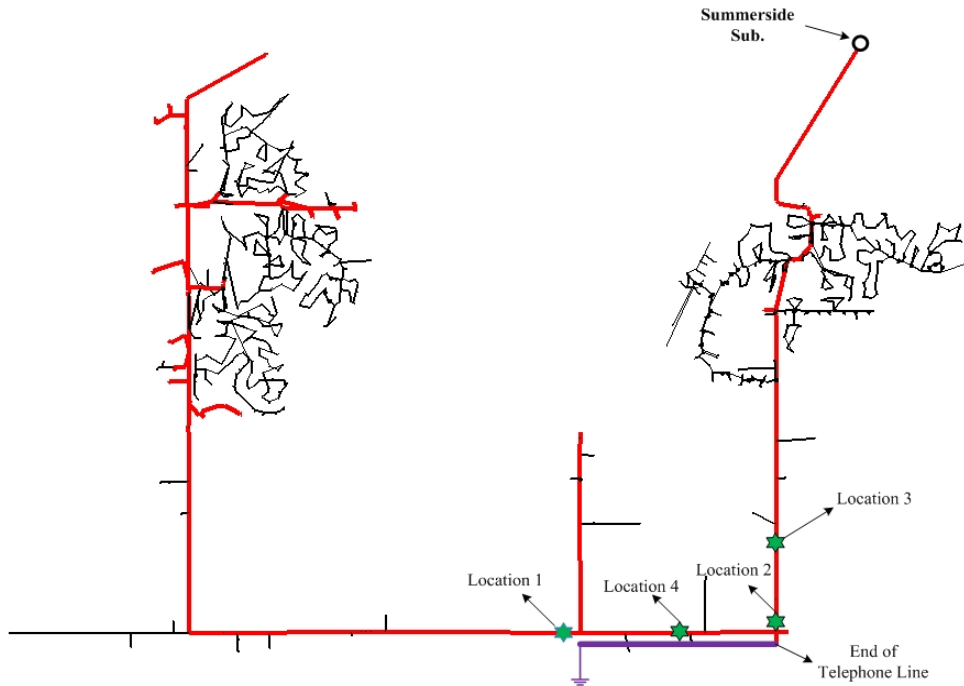
Figure 4.9 Actual telephone line in the actual case

Figure 4.10 shows the impact of the location of the broken neutral on the 9th harmonic voltage induced in the parallel telephone cable. It can be seen that if the broken neutral is located along the parallel telephone line (e.g., "Location 4"), the induced voltage increases significantly compared to base case. A break far away, like "Location 3", from the parallel telephone line does not cause noticeable increase on the induced voltage.
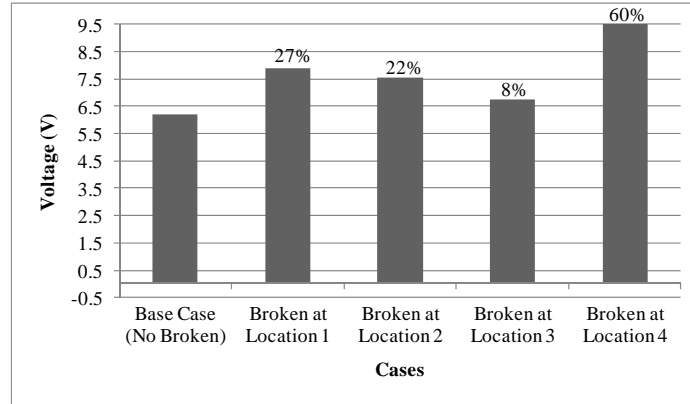
Figure 4.10 Impact of broken neutral on the 9th harmonic voltage induced in a parallel conductor (the percentage values above each bar shows the increase relative to the base case).

Basically, neutral broken decreases the neutral current at the adjacent location, which in turn, increases the induced voltage in telephone line. This phenomenon can be explained as follows.

In Figure 4.11, when part of neutral conductor is broken, harmonic currents conducted through the neutral will be blocked and diverted to ground. As a result, the neutral current around that point is lowered. Consequently, the aforementioned shielding effect of the neutral conductor will decrease in that area. After the broken point, harmonic current starts to return to neutral through the grounding points. Therefore, the neutral harmonic current profile has a funnel shape. As shown in Figure 4.11, neutral current will not decrease significantly for the segments far away from the broken point. That is why only the broken neutral points near the parallel telephone lines will affect the telephone interference level.

After understanding the mechanism of neutral broken, the next question which is useful to utility is, to what extent the neutral current will be affected when a neutral broken happens at a specific location.
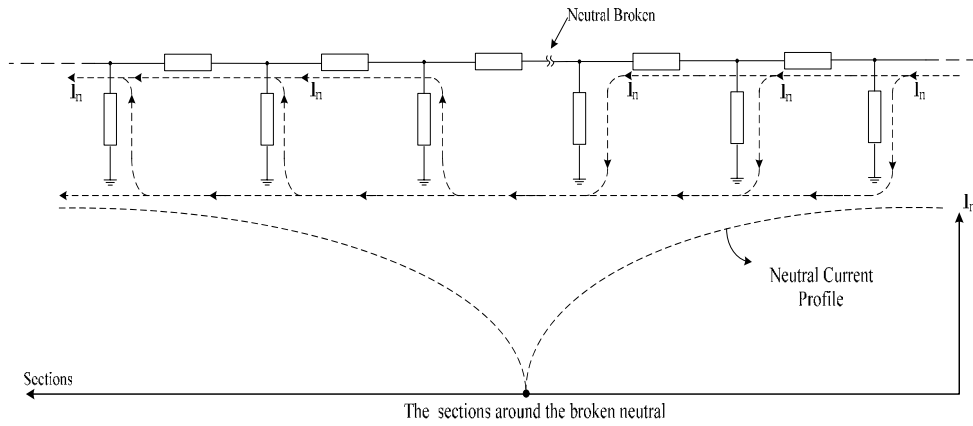
Figure 4.11 Circuit explanation when neutral broken happens
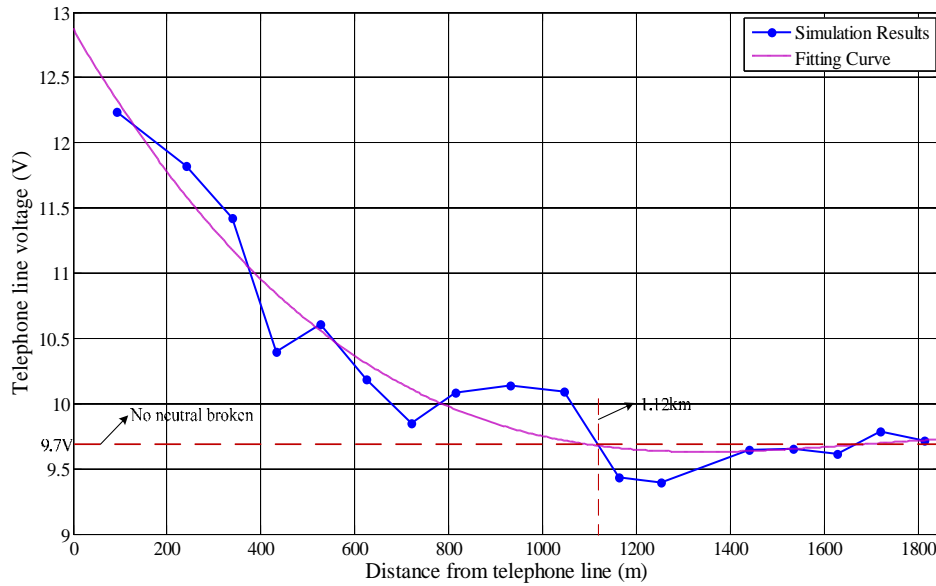
Figure 4.12 Telephone line voltage vs. broken distance from telephone line

Various locations have been applied neutral broken to check the impact on the actual telephone line as shown in Figure 4.9. The results are summarized in Figure 4.12. Telephone line RMS voltage is chosen as the indicator. The x-axis is the neutral broken distance from the telephone line. It is observed that when there is no neutral broken, the induced voltage in telephone line is around 9.7 volts. When neutral broken happens close to the telephone line, telephone line voltage increased 30%. While the neutral broken location gets far away, the telephone line voltage goes down, when it reaches around 1.1km, the telephone line voltage goes back to the range for no neutral broken case, and keeps constant after that. This also means, when neutral broken is 1.1km away from our telephone line in Figure 4.9, its impact on the telephone line would be insignificant.

4.1.6. Load Balancing

Practical distribution systems are never perfectly balanced due to the presence of numerous single-phase loads as shown in Figure 2.7. When the total loads of each phase are equal, the phase currents (Ia, Ig and Ic) will be equal. In this case, the neutral current would not have any non-triplen harmonic currents, since three-phase non-triplen harmonic currents have 120° phase displacement, and their vector sum will be zero [52][53].
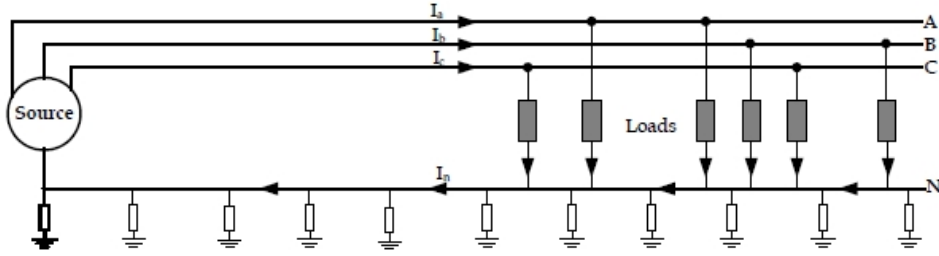
Figure 4.13 Many single-phase loads connected to the system

However, practical power systems always have unequal loads, and results in a much bigger zero sequence current (I_n) in the neutral wire due to the presence of non-triplen harmonic currents. This current returns to the source through the neutral conductor and the earth. Due to the nature of a multi-grounded system, part of the neutral current will be bypassed by the ground, which causes a residue current. As for a specific neutral system configuration, the bigger the neutral current is, the larger the residual current is. And the residual current is proportional to the induced voltage in the parallel telephone line due to coupling effects. Therefore, an unbalanced system was always considered a potential incentive that caused telephone interference problem.

In this subsection, we ran two simple cases (ideal case and actual case) study to investigate the load balancing impact on telephone interference problem.

1.   For ideal Case

Three cases have been investigated[6] .

- Case 1. Loads assigned evenly between three phases.

- Case 2. Loads assigned to phase A, B & C is 100% : 85% : 92%.

- Case 3. Loads assigned to phase A, B & C is 100% : 60% : 80%.

2. For Actual Case (the same case in Section 3.4)

There are also three cases that have been investigated.

- Case 1. Loads assigned evenly between three phases.

- Case 2. Loads are assigned between phases just like what is like in reality.

- Case 3. Loads assigned to phase A, B & C is 100% : 60% : 80%.

Four indices at the substation side are adopted here to indicate the impact of different system parameters, they are dominant sequence current, power individual IT, neutral harmonic current and induced voltage in a virtual 100m long parallel telephone line. The first two show the impact in phases, while the second last in neutral line, the last one investigates the residue current.

---

[6] All the three cases are made to have the same power. Only the loads distribution between phases is different.
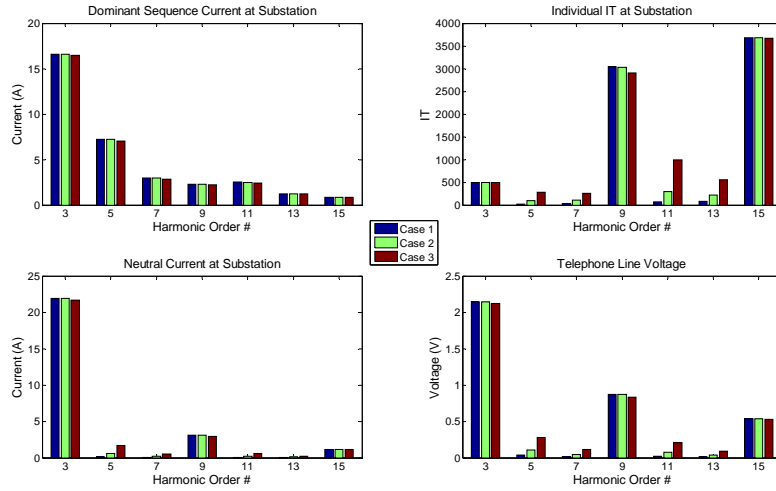
Figure 4.14 Load balancing sensitivity results for hypothetical case

Table 4.5 Load balancing sensitivity results for hypothetical case

Case.	Case 1	Case 2	Case 3
N.S. Imbalance Ratio (%)	3.83	5.88	15.81
Z.S. Imbalance Ratio (%)	4.05	5.89	15.33
IT	4714	4724	4810
Telephone Line Voltage (V)	2.30	2.35	2.90
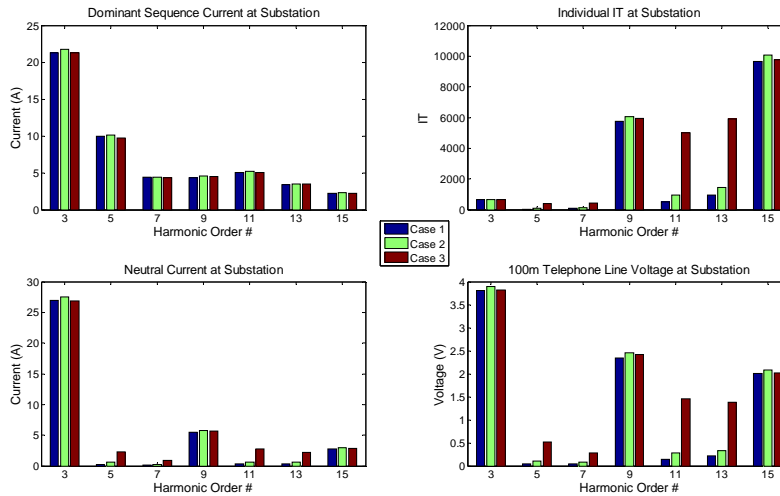
Figure 4.15 Load balancing sensitivity results for actual case

Table 4.6 Load balancing sensitivity results for actual case

Case.	Case 1	Case 2	Case 3
N.S. Imbalance Ratio (%)	4.17	6.64	18.62
Z.S. Imbalance Ratio (%)	2.44	2.78	13.73
IT	11290	11897	13841
Telephone Line Voltage (V)	4.22	4.33	4.89

Figure 4.14, Figure 4.15 and Table 4.5, Table 4.6 all show the load imbalance has almost no impact on the dominant sequence current, while it does have a great impact on the non-triplen zero sequence harmonic current. The bigger the imbalance is, the bigger the impact is.

However, as discussed in above sections, triplen zero sequence harmonic current is the main cause of telephone interference problem. The unexpected behavior for triplen zero sequence harmonic current (load imbalance has no impact) was explained as follows.

	A triplen harmonic (such as 9th)		A non-triplen harmonic (such as 7th as a pos-sequence harmonic)	
	Balanced situation	Imbalanced situation	Imbalanced situation	Balanced situation
Harmonic currents in phase domain	I_h^A I_h^B I_h^C	I_h^A I_h^B I_h^C	I_h^C I_h^A I_h^B	I_h^C I_h^A I_h^B
Harmonic currents in the dominant sequence domain	I_h^A I_h^B I_h^C $3I_{zero-seq}^{bal}$	I_h^A I_h^B I_h^C $3I_{zero-seq}^{imbal}$	I_h^A I_h^C $120°$ $120°$ I_h^B $3I_{pos-seq}^{imbal}$	I_h^A I_h^C $120°$ $120°$ I_h^B $3I_{pos-seq}^{bal}$
	$3I_{zero-seq} = I_h^A + I_h^B + I_h^C$ $I_{zero-seq}^{bal} = I_{zero-seq}^{imbal}$		$3I_{pos-seq} = I_A^{bal} + I_B^{bal}\mathbf{R}120° + I_C^{bal}\mathbf{R}-120°$ $I_{pos-seq}^{bal} = I_{pos-seq}^{imbal}$	

Figure 4.16 Sequence transformation for different harmonics

For each harmonic current, the dominant sequence is proportional to summation of absolute magnitude of harmonic current associated with each phase. Therefore, no matter how the load is distributed between the phases, as long as the total load on the three phases is constant, the dominant sequence component of current remains constant. Figure 4.16 illustrates this explanation for a triplen and non-triplen harmonic showing that the dominant sequence of harmonics remains constant even when the load is made unbalanced.

It must be noted that the above explanation is based on the assumption that for each harmonic, the current is merely consisting of the dominant sequence current. In reality, there are always also some amounts of other sequence components. However, most of the harmonic current is usually in its dominant sequence.

4.1.7. Conclusion

Table 4.7 The impact of each system parameter on the harmonic levels of the distribution system

	Factor	Effect
1	Substation grounding	Different substation grounding resistances do not impact on the harmonic levels.
2	Substation source impedance	Different substation source impedances impact on the harmonic levels. The larger the impedance, the lower the harmonic current level along the primary feeder.
3	Load distribution	Load distribution impact on the harmonic levels. The higher the concentration of loads at the same location, the lower the chance of cancelation.
4	MGN neutral grounding resistance	Different MGN neutral grounding resistances do not impact on the harmonic levels.
5	MGN neutral grounding span	Different grounding spans do not impact on the harmonic levels.
6	Neutral broken	Neutral broken has impact on the adjacent area. When it goes far away (around 1km), the impact fades away.
7	Load balancing	Imbalance loads has on impact on telephone interference. It only has impact on the non-triplen zero sequence harmonics.

Table 4.7 shows a summary of the impact of each system parameter analyzed in this section.

4.2 Harmonic Passive Filters

Apart from system modifications, passive filter is another special interest in this thesis for telephone interference mitigation.

All practical passive filters are used as shunt branches to bypass harmonic currents. Passive filter is a series combination of an inductance and a capacitance. In reality, in the absence of a physically designed resistor, there will always be a series resistance, which is the intrinsic resistance of the series reactor. The single tuned filter type is widely used in today's utility system, due to its reliability and low price. A typical single tuned filter consists of a capacitor in series with an inductor, as shown in Figure 4.17(a). The inductor is sized in such a way that the branch resonates at a particular harmonic frequency called tuning (resonance) frequency, h_t on Figure 4.17(b). So the branch impedance approaches zero at the tuning frequency, enabling the branch to bypass harmonic current at that frequency. This is the most common filter [54].
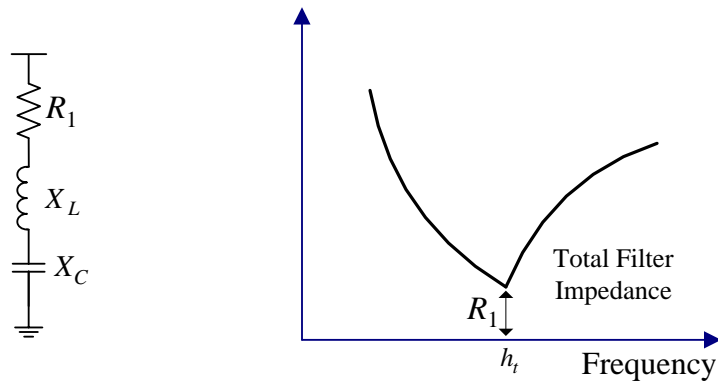
(a) Single tuned filter topogy   (b) Frequency scan
Figure 4.17 Single tuned filter and associated frequency scan

The total impedance of the single tuned filter is given by:

$$Z = R_1 + j \times (X_L - X_C)$$

Equation 4.3

The branch impedance approaches to zero, at the resonance frequency (h_t), if $X_L \approx X_C$. Therefore, the tuned inductor reactance can be calculated as:

$$X_L = \frac{X_C}{h_t^2}$$

Equation 4.4

For example, shunt capacitors or power factor correction requires installing a capacitor of X_C = *100 ohms*. If we want to make the capacitor as a 5th harmonic filter too, we can choose X_L = *100/4.92*, where h_t is selected as 4.9. The three phase single tuned filter can be obtained by connecting three branches like the one shown in Figure 4.17(a) in wye connection.

One main disadvantage related to the single tuned filters is that they affect the other harmonic orders apart from the resonance frequency. This can be explained by the fact that all the filters are capacitive below their tuning frequencies. So they can be treated as a capacitor branch below that frequency. This branch will interact with the system impedance creating a parallel resonance, as can be shown in Figure 4.18.

For example, if a 7th filter is installed like the one in Figure 4.18(a), it may create a parallel resonance close to the 5th harmonic. To address this problem, a 5th filter must be added. This is why when filters are applied at a location, they typically as a group consisting of 5th, 7th and other higher frequency filters.

(a) Single tuned filter connected to the system   (b) Adverse effect of the filter (parallel resonance)

Figure 4.18 Filter and system interaction
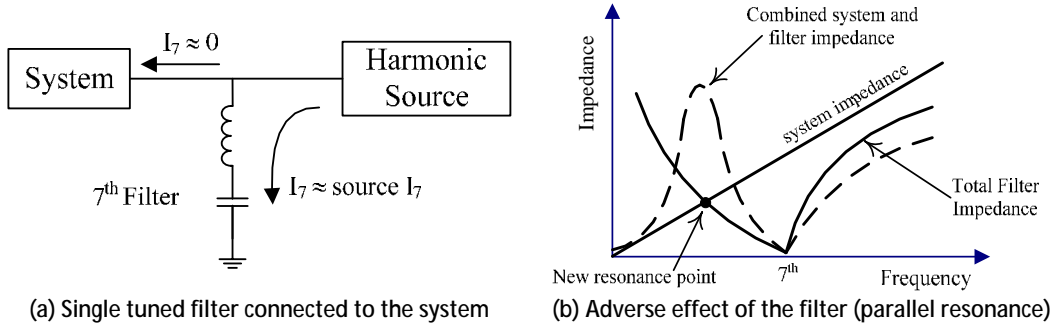
As mentioned before, the 3rd harmonic has become a main contributor to the feeder voltage distortion and the 9th harmonic has caused telephone interference in a number of cases. Since most industrial loads don't produce such harmonics, the sources of 3rd and 9th harmonics must be the distributed residential and commercial loads. As it was shown before, the dominant sequence associated to triplen harmonic (3rd, 9th, 15th, etc) is the zero sequence so that this phenomenon was used to design another filter type, generally called zero-sequence filters.

One type of zero sequence filter is proposed in reference [55], which is a combination of a Y/Δ transformer and one capacitor in the secondary winding, as shown in Figure 4.19. By tuning the capacitor with the zero sequence impedance of the transformer, it is possible to further decrease the zero sequence impedance for sinking triplen harmonics.
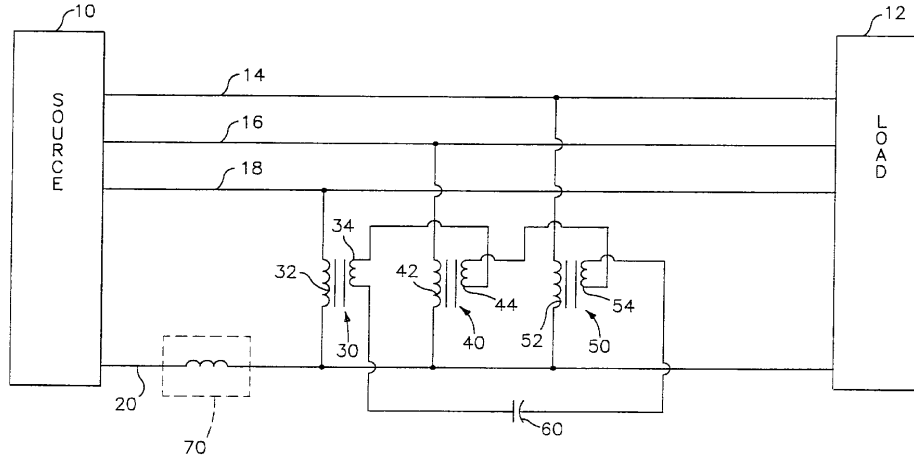
Figure 4.19 Schematic diagram of a zero-sequence trap proposed by [40]

Compared to the single tuned filter, this filter affects only the zero sequence harmonics. For example, if a zero-sequence filter is tuned to mitigate the 9th harmonic, it might cause a zero sequence parallel resonance (due to interaction with the system) for a frequency lower than 9th, but the impact will be very low because the zero sequence component associated to this lower frequency is very small.

The procedure to tune a zero sequence filter is explained as follows. The zero sequence network of a Y/Δ transformer with a capacitor (with an impedance of X_C) connected at the Δ (as illustrated in Figure 4.19) side is shown in Figure 4.20.
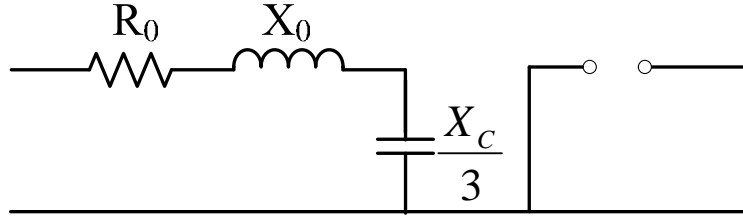
Figure 4.20 Zero sequence network of Y/Δ transformer with a capacitor

From the circuit above, the zero sequence impedance becomes close to zero, at the resonance frequency (h_t), if $X_C/3 \approx X_0$. Therefore, the tuned capacitor reactance can be calculated as:

$$X_C = h_t^2 \times 3 \times X_0$$

Equation 4.5

The objective of this section is to show how the presence of the previously discussed filters will affect the harmonic levels of the primary distribution system. Issues like the proper location and size of the filters will be taken into account. In the next subsection, it is shown how to tune the single tuned and zero sequence filter and the associated frequency scan in order to check the interaction of filters and the supply system. Following, it is investigated the impact of the combination of a single tuned filter and a zero sequence filter on the harmonic levels of the primary system.

4.2.1. Filter Data and Frequency Scan

This section presents the procedure necessary to tune single tuned and zero sequence filters. The single tuned filter is built from a 1 Mvar capacitor (a small

inherent resistance of 5 ohms is assumed in series with the capacitor). A typical

Y/Δ three-phase transformer is employed to build the zero sequence filters. The

transformer's data are provided by EPCOR Utilities and consists of a 1 MVA,

25/0.480 kV three-phase transformer with a reactance of 5% and an X/R ratio of

6.68.

As mentioned in the previous subsection, an inductor can be placed in series with

the 1 Mvar capacitor to build a single tuned filter and a capacitor can be

connected at the Δ side of the 1 MVA transformer to build a zero sequence filter.

Following, the harmonic orders that are of concern for filtering need to be defined.

It was shown in Chapter 3, that the 3rd and 5th harmonic components are the ones

that have the highest levels on the primary system and the 9th and 15th are the

components that have the most significant impact on the telephone interference

problem. Therefore, three zero sequence filters are built to mitigate the 3rd, 9th and

15th harmonic component and one single tuned filter to mitigate the 5th harmonic

component.

The 5th single tuned filter can be obtained by tuning the inductor in series with the

1 Mvar three-phase capacitor as shown by Equation 4.4. As mentioned before, the

primary system line-to-line voltage is 25 kV, which is the voltage level the filter

is connected to. The calculation is shown below.

$$X_C = \frac{V^2}{\text{Mvar}} = \frac{\left(25 \times 10^3\right)^2}{1 \times 10^6} = 625\,\Omega$$

$$X_L = \frac{X_C}{h_t^2} = \frac{625}{5^2} = 25\,\Omega$$

$$L = \frac{X_L}{2 \times \Pi \times 60} = 66\,\text{mH}$$

The tuning procedure for the zero sequence filter is done according to Equation 4.5. The calculation is shown below considering that the 3rd harmonic component is of concern ($h_t=3$). Similar calculation can be done for the 9th and 15th components. As mentioned before, the objective is to tune the capacitor located at the Δ side of a 1 MVA, 25/0.480 kV Y/Δ transformer with a reactance of 5% and an X/R ratio of 6.68.

$$X_0 = 5\,\%$$

$$X_C(\%) = h_t^2 \times 3 \times X_0 = 135\,\%$$

$$X_C(\Omega) = \frac{135}{100} \times \frac{\left(480\right)^2}{10^6} = 0.31\,\Omega$$

$$Q_C = \frac{480^2}{0.31} = 740\,\text{Kvar}$$

Table 4.8 summarizes the tuned parameters for the zero sequence filters applied to mitigate the 3rd, 9th and 15th filter.

After tuning the filters, the next step is to evaluate their performance through a frequency scan for each individual filter in order to verify if the impedance at the

resonance frequency is close to zero. Figure 4.21 shows the frequency scans for

the 5th single tuned filter and the 3rd, 9th and 15th zero sequence filters.

Table 4.8 tuned capacitor installed for different zero sequence harmonic filters

Zero Sequence Filter	Tuned capacitor
3rd	740 Kvar
9th	82 Kvar
15th	30 Kvar
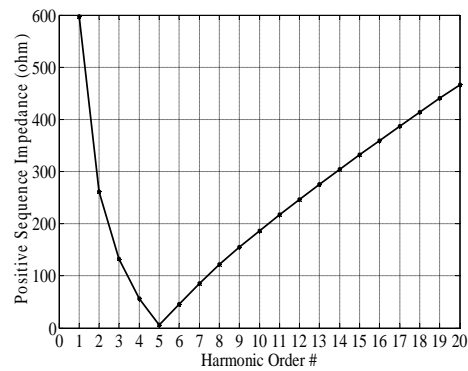
(a) 5th harmonic single tuned filter
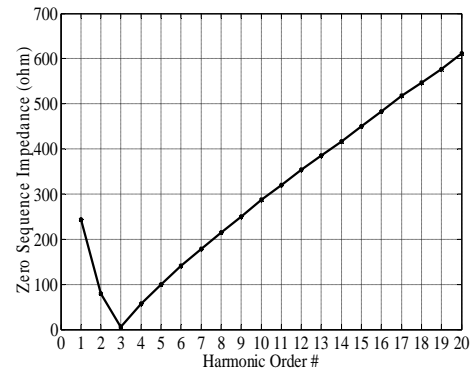
(b) 3rd harmonic zero sequence filter
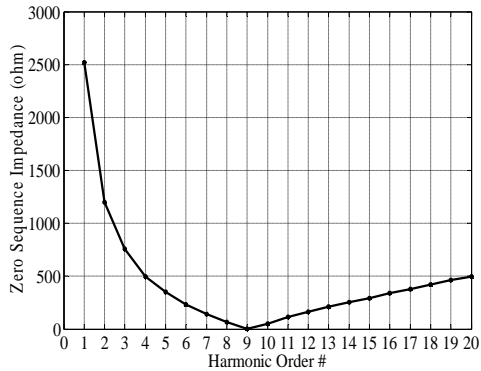
(c) 9th harmonic zero sequence filter
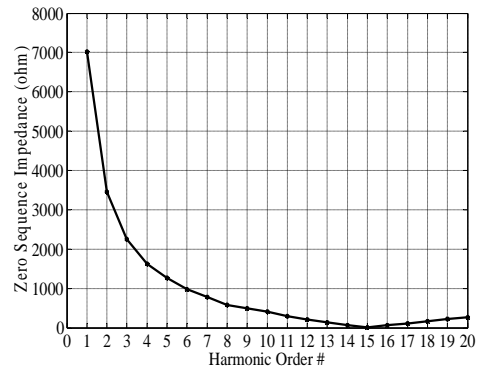
(d) 15th harmonic zero sequence filter

Figure 4.21Frequency scan for each individual tuned harmonic fitler

One can observe that each filter was tuned correctly because the impedance at the

respective resonance frequency is very close to zero.

In the following subsection, it is discussed how the distribution system is affected due to presence of the filters previously discussed. Issues like the location of the filters along the primary distribution system are also discussed.

4.2.2. Impact of Location of the Filters on the Primary Distribution System

Normally, a combination of filters tuned at different harmonic frequencies is employed to mitigate the harmonic distortion on the distribution systems. Previous results, presented on Chapter 3, showed that the highest harmonic levels on the primary distribution system are the 3rd and the 5th components. The idea of the following section is to perform multiphase harmonic load flow simulations to determine how the power quality indices are affected if filters are presented and compare with the case studied in Chapter 3 that does not consider any mitigation solution. Therefore, it is proposed to use a combination of a 3rd zero sequence filter and a 5th filter single tuned filters for the simulations.

In the previous subsection, it was studied the individual performance of each filter. The next step is to connect the 3rd and 5th combination filter on the same ideal feeder used to perform the case studies in Chapter 3. This network is shown again in Figure 4.22.

One can observe that the filters can be connected at different locations along the primary system. In order to find out the best location to install the filters, the following case studies have been conducted.

In order to determine the best location to install the filters, harmonic power flows are conducted over the system shown in Figure 4.22 considering the filters at five different locations along the primary system. The locations are 1, 5, 8, 11 and 15 kilometers from the substation. The simulations are conducted for a period of 24 hours to consider the appliance usage. After running the simulations, the dominant sequence of the harmonic currents at every 1 km of the primary feeder are determined and the average is determined. Finally, the 95% cdf (cumulative distributive function) value is obtained from this 24 hours average, in the same way it was done for the base case in Chapter 3. This procedure is repeated for 5 different locations for the filters (3rd and 5th filters) placement. The tuned parameters for the 3rd and 5th filter were provided in the previous Section. The results are shown in Figure 4.23.
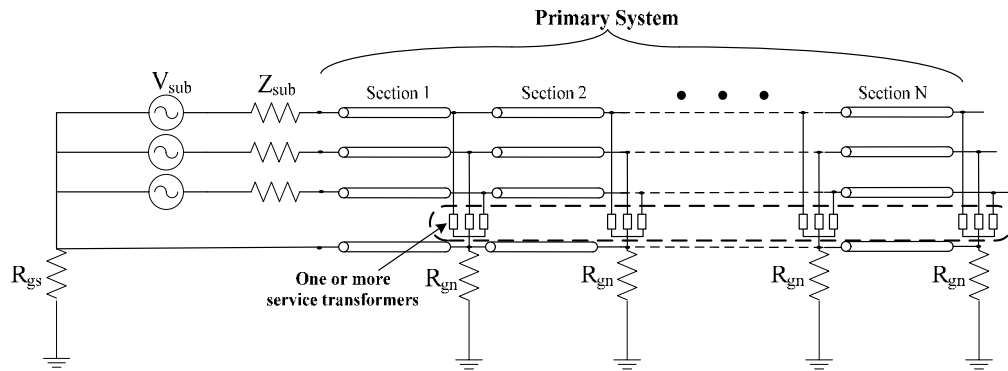
Figure 4.22 Ideal distribution network model for primary system analysis
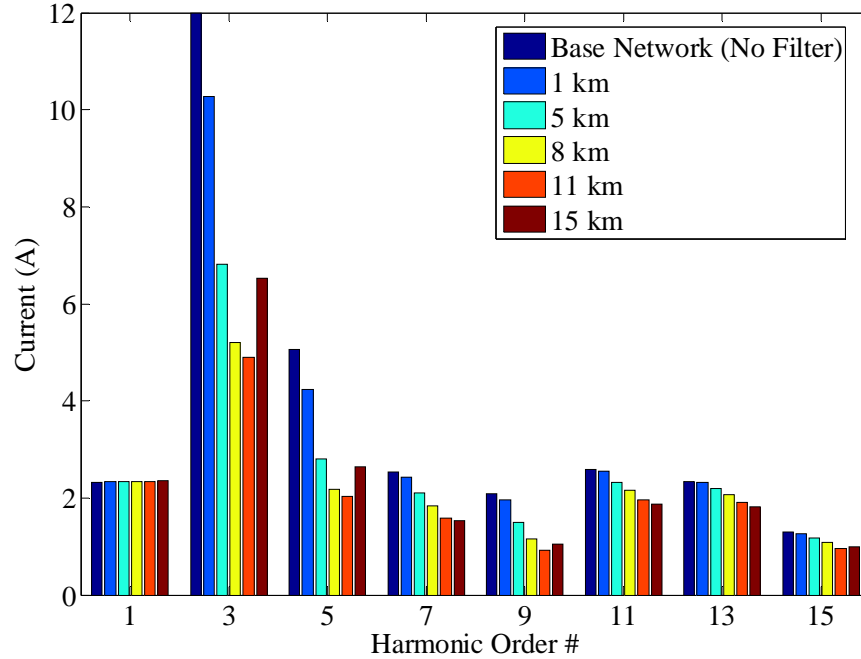
Figure 4.23 Average dominant sequence current at the primary system for different filters location

One can observe from Figure 4.23 that the best location to install the filters is at 11 kilometers from the substation since this is the configuration that reduced the most the average current at the primary system if compared to other the locations.

It is still necessary to verify if the size of the 3rd and 5th filters employed are lower than the system impedance at the respective resonance frequencies. For that, a system frequency scan is performed with the filters located at 11 kilometers from the substation since this was chosen to be the best location. The frequency scan is shown in Figure 4.24. The solid line represents the system impedance and the dashed line represents the 3rd and the 5th filters combined impedance. One can observe that the system impedance is higher than the filters impedance at the 3rd and 5th harmonic. It can also be observed that the filters impedance is very close

to zero at the resonance frequencies, which helps to sink more 3rd and 5th harmonic currents.
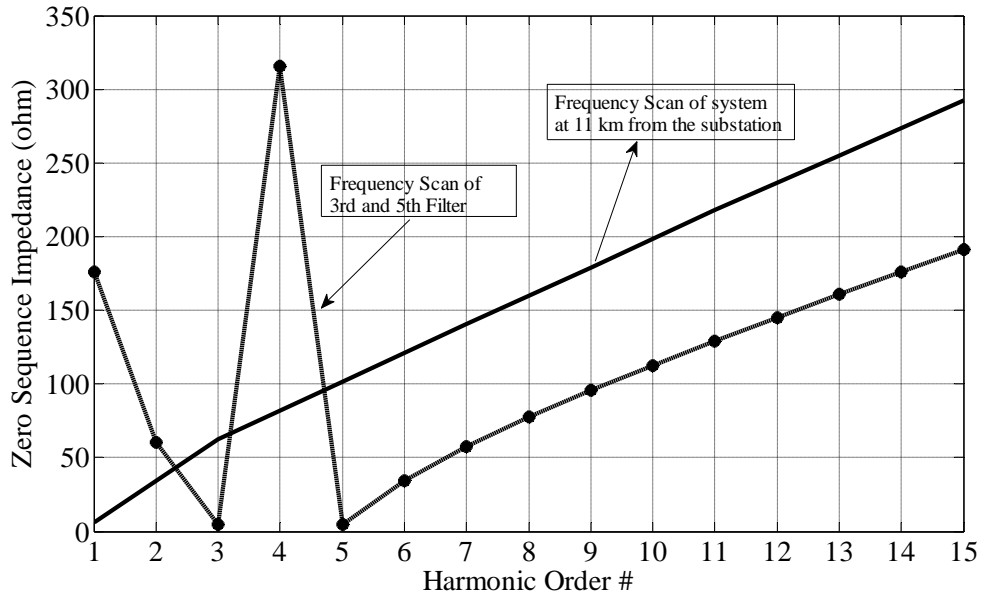
Figure 4.24 System and 3rd and 5th filters frequency scan

4.2.3. Harmonic Filtering Analysis on a Actual Distribution System

The objective of this section is to evaluate the impact of the 3rd harmonic zero sequence and 5th single tuned filters (analyzed on Section 4.2.2) on the harmonic levels of the EPCOR real distribution system presented on Chapter 3 and shown again in Figure 4.25. In this system, each neighborhood has been represented by an aggregated harmonic load model as described in Section 3.4.1. The main issue on this system is the different locations that the combination filters can be installed along the system main trunk.
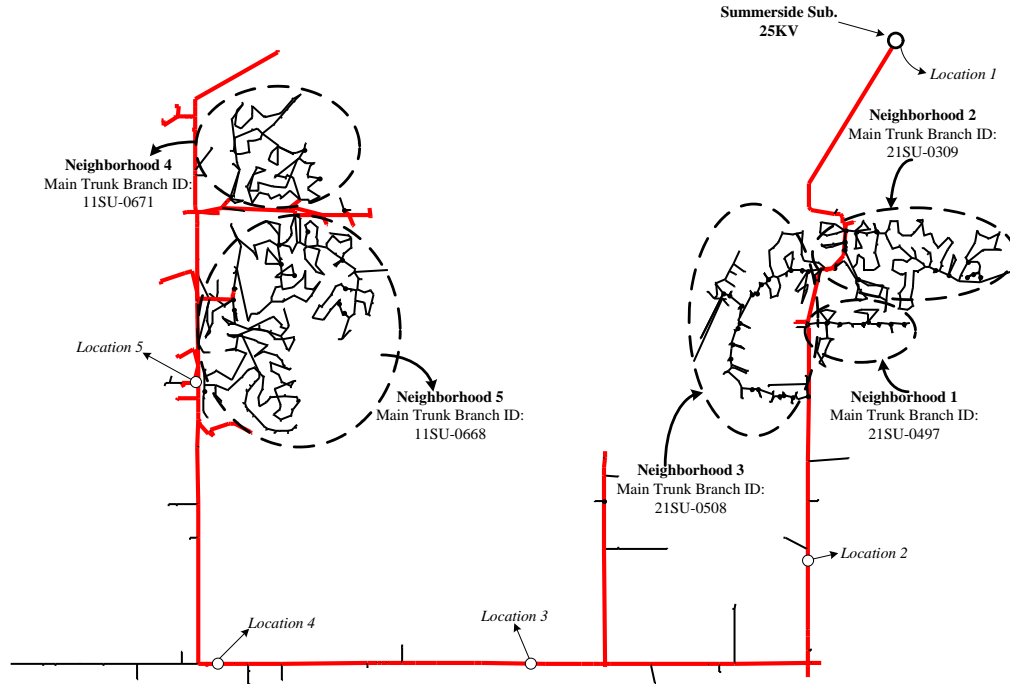
Figure 4.25 EPCOR actual distribution system

Therefore, six case studies referring to different filters location are analyzed in order to investigate how the harmonic levels on the primary system are affected. At each location a combination of the 3rd and the 5th filters are installed. The six case studies are as follows:

- Case 1: The filters are installed at the substation (marked as "Location 1" on Figure 4.25);

- Case 2: The 3rd and the 5th filters are installed at the middle of the feeder (marked as "Location 3" on Figure 4.25);

- Case 3: The 3rd and the 5th filters are installed at the end of the feeder (marked as "Location 5" on Figure 4.25);

- Case 4: The 3rd and the 5th filters are installed at two locations:

  o At the connection between the main trunk and Neighborhood 1

  o At the connection between the main trunk and Neighborhood 5

- Case 5: The 3rd and the 5th filters are installed at three locations:

  o At the connection between the main trunk and Neighborhood 1

  o At the connection between the main trunk and Neighborhood 4

  o At the connection between the main trunk and Neighborhood 5

- Case 6: The 3rd and the 5th filters are installed at five locations, which are the connection points between the main trunk and the five neighborhoods shown in Figure 4.25.

The next step was to define the locations along the main trunk to observe the different power quality indices. Three locations of observation were chosen and are marked as "Location 1", "Location 3" and "Location 4" and the results are shown in Figure 4.26, Figure 4.27, Figure 4.28, respectively, for four different power quality indices (dominant sequence voltage, dominant sequence current, individual IT and neutral current). For example, Figure 4.26 shows these power quality indices (all of them are represented by the respective 95% cdf value over a 24 hours period) observed at "Location 1" for the base case (no filtering) and the six cases outlined above.
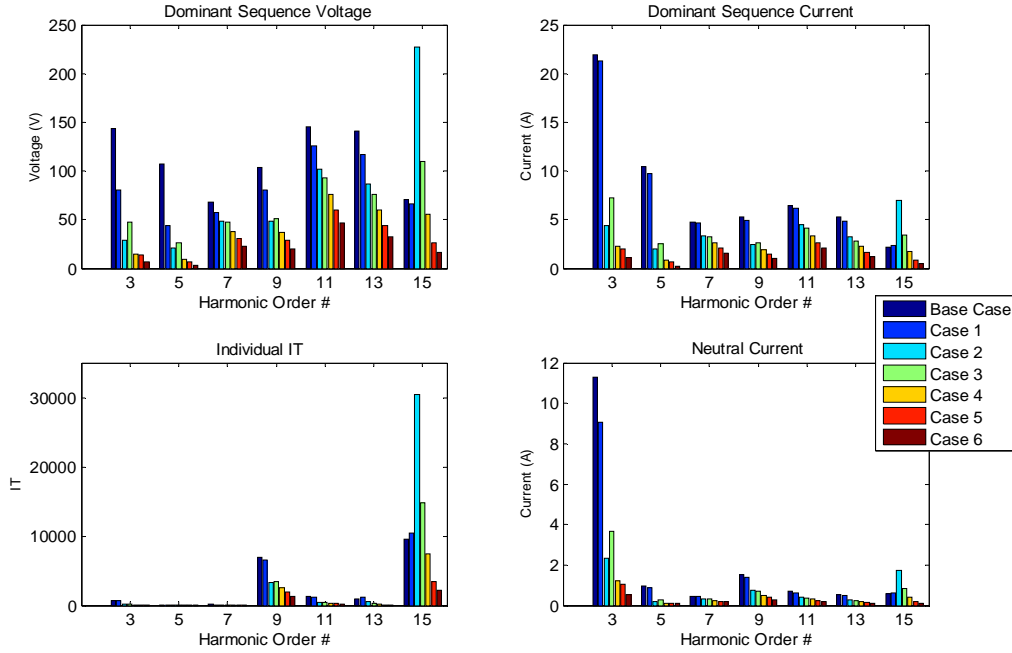
Figure 4.26 Impact of filters at different places observed at "Location 1"
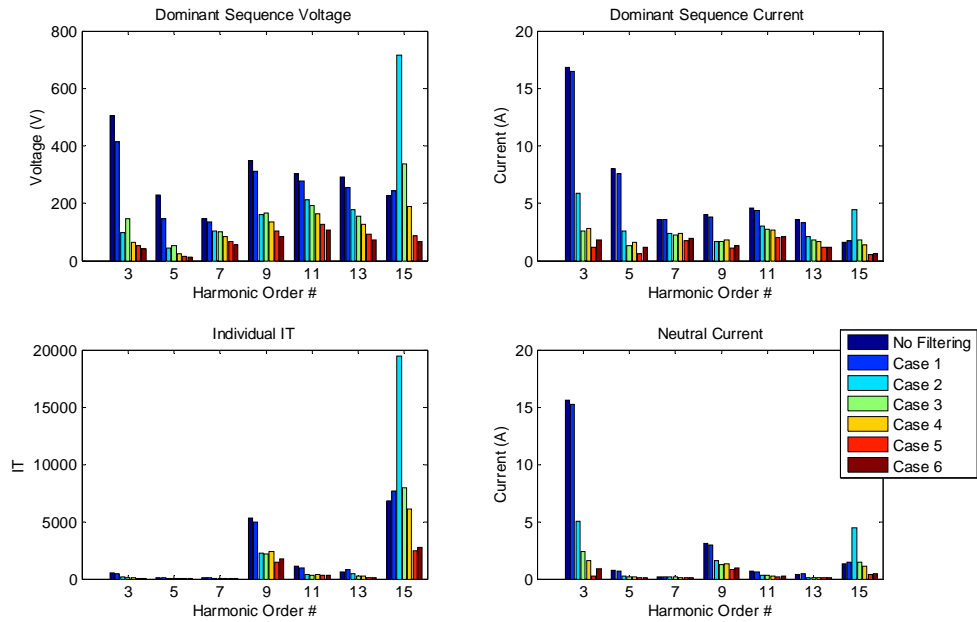
Figure 4.27 Impact of filters at different places observed at "Location 3"
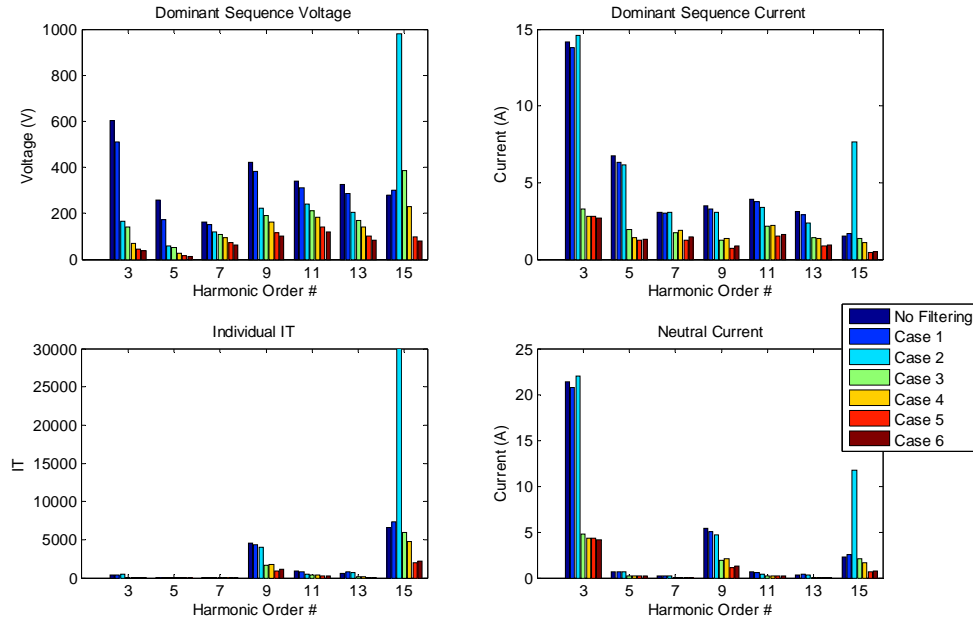
Figure 4.28 Impact of filters at different places observed at "Location 4"

The filter installed at all the five neighborhoods (Case 6) has the best filtering performance, it can bring down the IT at least 60%. In practice, filter installed at Neighborhoods 1, 4 and 5 (Case 5) is a good option. Its performance is comparable with Case 6.

Figure 4.29 shows the zero sequence frequency scan observed at "Location 3" while the filter installed at the end of the feeder ("Location 5"). It shows when the filter exists, the resonance point will be shifted. In this case, it happens to be shifted to 15th harmonic frequency, which is the reason why we see the 15th harmonic is increased when the filter is installed. This feeder has a long cable, whose shunt capacitance will very likely resonant with the inductance of the filter at frequencies higher than 3rd and 5th.

Figure 4.29 Zero sequence frequency scan observed at "Location 3" with filter at end of the feeder

4.2.4. Conclusion

The zero sequence filter has been carefully investigated in this chapter. By inserting a specific capacitance, the reactance of the filter could be reduced to zero at the tuned frequency. Therefore, the impedance at tuned frequency is equal to the resistance of the Y/Δ transformer. By frequency scan study of our two cases, we found the 1 MVA, 25/0.480 kV three-phase transformer with a reactance of 5% and an X/R ratio of 6.68 (which is commonly seen as service transformer is North America's distribution system) is durable. The impedance at tuned frequency is around 4.6 ohm, which is much smaller than the system impedance.

Since zero sequence filter only has impact on zero sequence harmonics, its impact on the other triplen harmonics (other than the harmonic at tuned frequency) need to be studied before implementation.

On the other hand, the location to install the zero sequence filter to get the best performance is also case dependent. The case study on the Epcor feeder shows a 3rd zero sequence filter plus a 5th filter could have a good enough performance to mitigate the telephone interference along the feeder.

Chapter 5

Conclusion and Future Work

5.1 Harmonic Impact of Residential Loads

This thesis has been trying to estimate what the impact of residential loads is on today's distribution system. This requires an accurate load harmonic model and system model.

A service transformer harmonic model has been developed based on the bottom-up house harmonic model. The simplified load model has a simple equivalent circuit, which only consists of five parameters. This model can be applied in a system-wide simulation easily without causing a dramatic increase of computation time and complexity.

Two kinds of case studies have been conducted on the ideal system and actual system. They are base case study and load evolution study.

The base case adopts the practical system configuration and parameters, with today's home appliance usage profile. The simulation result gives a solid evidence that the collective effect of today's home appliances on distribution system is much bigger than what we expected, but consistent with our field measurement. This fully confirms why more and more distribution systems in Alberta are

experiencing telephone interference problems. Therefore, this work is essential and valuable to utility for an advanced estimation.

The load evolution study uses the penetration level of major home appliances to predict how the harmonic voltage/current levels in the network will change in the next 5 years. This study shows the voltage THD has an annual growth rate of 15% and the current TDD of 14%, and they are mainly caused by CFLs and PCs. This growth rate is tremendous and worth an increasing attention. Take the voltage THD as an example, our numerous field measurements shows the voltage THD level in today's residential distribution system is around 2.5%. With the growth rate of 15%, in the next fifth year, the voltage THD will be 5.02%, which exceeds the voltage distortion limit defined in IEEE Std. 519-1992.

5.2 Harmonic Mitigation Solutions

This thesis focuses on two kinds of mitigation methods aiming at the excessive harmonic problem caused by today's increasingly used electronic based home appliances. One is system modification. The other one is the zero sequence filter.

The system configuration and parameters sensitivity studies in terms of harmonic mitigation have been conducted with simulation and detailed analysis. No similar work has been done before. However, due to the increasing numbers of excessive harmonic related problems in distribution system, such as telephone interference, voltage rise in the parallel denergized conductors and so on, utilities are paying

more and more attentions to their system configuration and parameters. While debugging the harmonic problems, there is no guideline for utility to follow. The work in this thesis gives clear idea of the impact of various system configurations and parameters on harmonic level. Their effect has also been fully explained theoretically.

So far, the most commonly seen harmonic problem in today's distribution system is telephone interference problem. This problem is mainly caused by the zero sequence harmonic current in power line. This thesis, therefore, developed a zero sequence filter using Y/Δ transformer. A carefully selected capacitor has been inserted in series at the secondary side to get rid of the reactance, to minimize the total impedance at the tuned frequency. The design procedure has been given and its effectiveness has been carefully discussed and testified in our ideal and actual case network. The simulation results show this kind of filter has a good performance of zero sequence harmonic mitigation. Its little interaction with non-triplen harmonics decreases the opportunity of the potential resonance at other harmonic frequencies. The simulation shows that by carefully selecting the location to install zero sequence filter, the IT level could be brought down by 60%.

5.3 Recommendations and Future Research

The excessive harmonic level problem caused by increasingly used electronic based home appliances is getting worse and worse. Its system-wide distribution instead of major harmonic source location in old days makes it difficult to

understand how the total harmonic level builds up in today's distribution system. The mitigation method is also very different from the one in old days.

In this thesis, detailed harmonic simulation has been adopted to help understand the harmonic characteristics in today's distribution system. This is not easy and simple to apply, and simple theory on this cannot be easily obtained. The future work should be focusing on developing more analytical theory for collective harmonic effect of distributed harmonic sources.

Due to the over complicated model in this thesis, different simplified model should be developed in the future for different purpose. For example, to investigate the telephone interference problem in distribution system, only the zero sequence harmonic is under concern, therefore, it is important and necessary to develop a zero sequence harmonic load model and system model to conduct the simulation study.

In this thesis, various simulations have been conducted to decide where to install the filter to get the best performance of the whole system. To avoid repeating this work for different cases in the future, a theory or a guideline is needed to help decide the best location. This theory and guideline have to be practical and simple. It should not require a detailed harmonic loads and system model, like the one in this thesis.

Reference

[1]   Alexander Kusko, Marc T. Thompson, Power quality in electrical systems, McGraw-Hill, 2007.

[2]   Roger C. Dugan, Surya Santoso, Mark F. McGranaghan, H. Wayne Beaty, Electrical power systems quality, McGraw-Hill, 2003.

[3]   W. E. Reid, "Power Quality Issues-Standards and Guidelines", IEEE Transactions on Industry Applications, vol. 32, no. 3, May/June 1996

[4]   IEEE Recommended Practices and Requirements for Harmonic Control in Electrical Power Systems, IEEE Standard 519-1992.

[5]   Task Force on Harmonics Modeling and Simulation, "Modeling and Simulation of the Propagation of Harmonics in Electric Power Networks, Part I: Concepts, Models, and Simulation Techniques", IEEE Transactions on Power Delivery, vol. 11, no. 1,January 1996.

[6]   Wakileh, G. J., Power Systems Harmonics, Fundamentals, Analysis and Filter Design, 2001, Springer.

[7]   Kimbark, E. W., Direct Current Transmission, vol. 1, 1971, John Wiley & Sons.

[8]   IEEE Working Group on Nonsinusoidal Situations: Effects on Meter Performance and Definitions of Power, "Practical Definitions for Powers in Systems with Nonsinusoidal Waveforms and Unbalanced Loads: a Discussion", IEEE Transactions on Power Delivery, vol. 11, no. 1, January 1996, pp. 79-101.

[9]   E. F. Fuchs, D. J. Roesler, F. S. Alashhab, "Sensitivity of Electrical Appliances to Harmonics and Fractional Harmonics of the Power System Voltage. Part I: Transformers and Induction Machines", IEEE Transactions on Power Delivery, vol. 2, no. 2, April 1987, pp. 437-444.

[10] Das, J. C., Power System Analysis, Short Circuit Load Flow and Harmonics, 2001, Marcel Dekker.

[11] E. F. Fuchs, D. J. Roesler, F. S. Alashhab, "Sensitivity of Electrical Appliances to Harmonics and Fractional Harmonics of the Power System Voltage. Part I: Transformers and Induction Machines", IEEE Transactions on Power Delivery, vol.2, no. 2, April 1987, pp. 437-444.

[12] E. F. Fuchs, D. J. Roesler, K. P. Kovacs, "Sensitivity of Electrical Appliances to Harmonics and Fractional Harmonics of the Power System Voltage. Part II: Television Sets, Induction Watthour Meters and Universal Machines", IEEE Transactions on Power Delivery, vol 2, no. 2, April 1987. pp. 445-453.

[13] Wilsun Xu; Drakos, J.E.; Mansour, Y.; Chang, A.; , "A three-phase converter model for harmonic analysis of HVDC systems ," Power Delivery, IEEE Transactions on , vol.9, no.3, pp.1724-1731, Jul 1994

[14] Yuanyuan Sun; Guibin Zhang; Wilsun Xu; Mayordomo, J.G.; , "A Harmonically Coupled Admittance Matrix Model for AC/DC Converters," Power Systems, IEEE Transactions on , vol.22, no.4, pp.1574-1582, Nov. 2007

[15] Yuanyuan Sun; Weijie Zheng; Xu, W.; , "A New Method to Model the Harmonic Generation Characteristics of the Thyristor Controlled Reactors," Power Tech, 2007 IEEE Lausanne , vol., no., pp.1785-1790, 1-5 July 2007

[16] Jalali, S.G.; Lasseter, R.H.; , "A study of nonlinear harmonic interaction between a single phase line-commutated converter and a power system," Power Delivery, IEEE Transactions on , vol.9, no.3, pp.1616-1624, Jul 1994

[17] Christi, N.; Hedin, R.; Johnson, R.; Krause, P.; Montoya, A.; , "Power system studies and modelling for the Kayenta 230 kV substation advanced series compensation," AC and DC Power Transmission, 1991., International Conference on , vol., no., pp.33-37, 17-20 Sep 1991

[18] Baghzouz, Y.; Burch, R.F.; Capasso, A.; Cavallini, A.; Emanuel, A.E.; Halpin, M.; Imece, A.; Ludbrook, A.; Montanari, G.; Olejniczak, K.J.; Ribeiro, P.; Rios-Marcuello, S.; Tang, L.; Thaliam, R.; Verde, P.; , "Time-varying harmonics. I. Characterizing measured data," Power Delivery, IEEE Transactions on , vol.13, no.3, pp.938-944, Jul 1998

[19] Baghzouz, Y.; Burch, R.F.; Capasso, A.; Cavallini, A.; Emanuel, A.E.; Halpin, M.; Langella, R.; Montanari, G.; Olejniczak, K.J.; Ribeiro, P.; Rios-Marcuello, S.; Ruggiero, F.; Thallam, R.; Testa, A.; Verde, P.; , "Time-varying harmonics. II. Harmonic summation and propagation," Power Delivery, IEEE Transactions on , vol.17, no.1, pp.279-285, Jan 2002

[20] Cavallini, A.; Montanari, G.C.; Cacciari, M.; , "Stochastic evaluation of harmonics at network buses," Power Delivery, IEEE Transactions on , vol.10, no.3, pp.1606-1613, Jul 1995

[21] Cavallini, A.; Montanari, G.C.; , "A deterministic/stochastic framework for power system harmonics modeling," Power Systems, IEEE Transactions on , vol.12, no.1, pp.407-415, Feb 1997

[22] Mau Teng Au; Jovica V. Milanovic; , "Development of Stochastic Aggregate Harmonic Load Model Based on Field Measurements," Power Delivery, IEEE Transactions on , vol.22, no.1, pp.323-330, Jan. 2007

[23] ANSI/IEEE C2 – 2002, The National Electrical Safety Code®, Section 09, IEEE Inc, 1995

[24] R. Rudenberg, Transient Performance of Electric Power Systems, New York: McGraw-Hill, 1950.

[25] A. P. Meliopoulos, "Impact of Grounding System Design on Power Quality", IEEE Power Engineering Review, Nov 2001, p. 3-7.

[26] A. P. Meliopoulos, G. J. Cokkinides, K. R. Chakravarthi, "Effects of Grounding on Distribution System Harmonic Resonance Conditions", IEEE Transactions on Power Delivery, Vol. 4, No. 1, January 1989, p. 475-682.

[27] Francisco C. De La Rosa, Harmonics and Power Systems, CRC/Taylor & Francis, 2006.

[28] Kimbark, E. W., Direct Current Transmission, John Wiley & Sons, 1971.

[29] Electromagnetic compatibility (EMC) – Part 3-2: Limits – Limits for harmonic current emissions (equipment input current ≤16 A per phase), IEC 61000-3-2, International Standard, 2005

[30] NEMA, CFL Share of Household Lamps Reaches New High, Nov. 10, 2008, available online on January 23, 2009 at: http://www.nema.org/media/pr/20081110a.cfm

[31] D. J. Pileggi, E. M. Gulachenski, C. E. Root, T. J. Gentile, A. E. Emanuel, "The Effect of Modern Compact Fluorescent Lights on Voltage Distortion", IEEE Transactions on Power Delivery, vol. 8, no. 3, July 1993, pp. 1451-1459.

[32] R. Dwyer, A. K. Khan, M. McGranaghan, L. Tang, R. K. McCluskey, R. Sung, T. Houy, "Evaluation of Harmonic Impacts from Compact Fluorescent Lights on Distribution Systems", IEEE Transactions on Power Systems, vol. 10, no. 4, Nov. 1995, pp. 1772-1779.

[33] IEEE Recommended Practice for Voice-Frequency Electrical-Noise Tests of Distribution Transformers, 1994

[34] C. B. Cooper, "IEEE recommended practice for electric power distribution for industrial plants," Electron. Power, vol. 33, no. 10, p. 658, Oct. 1987.

[35] Nino, E.E.; Wilsun Xu; , "Measurement of Harmonic Sources in Three-Wire Single-Phase Supply Systems," Power Delivery, IEEE Transactions on , vol.22, no.4, pp.2527-2533, Oct. 2007

[36] Gorman, M.J.; Grainger, J.J.; , "Transformer modelling for distribution system studies. I. Linear modelling basics," Power Delivery, IEEE Transactions on , vol.7, no.2, pp.567-574, Apr 1992

[37] T. A. Short, Electric Power Distribution Handbook, CRC Press, 2004

[38] Neves, W.L.A.; Dommel, H.W.; Wilsun Xu; , "Practical distribution transformer models for harmonic studies," Power Delivery, IEEE Transactions on , vol.10, no.2, pp.906-912, Apr 1995

[39] H.E. Mazin and W. Xu, "Harmonic Cancellation Characteristics of Specially Connected Transformers," Electric Power System Research, Vol. 79, No. 12, 2009, pp. 1689-1697

[40] Xu, W.; Marti, J.R.; Dommel, H.W.; , "A multiphase harmonic load flow solution technique," Power Systems, IEEE Transactions on , vol.6, no.1, pp.174-182, Feb 1991

[41] William H. Kersting, Distribution System Modeling and Analysis, CRC Press, 2006

[42] Engineering Reports of the Joint Subcommittee on Development and Research of the Edisson Electric Institute and the Bell Telephone System, New York, 5 volumes, July 1926 to January 1943

[43] Contreras, M.; Cardenas, V.; Calleja, H., "A Review of Solutions for Harmonic Propagation Damping in Power Distribution Networks," International Power Electronics Congress, 10th IEEE , vol., no., pp.1-6, 16-18 Oct. 2006

[44] Nassif, A.B.; Wilsun Xu; Freitas, W., "An Investigation on the Selection of Filter Topologies for Passive Filter Applications," Power Delivery, IEEE Transactions on , vol.24, no.3, pp.1710-1718, July 2009

[45] Jain, Taruna; Jain, Shailendra; Agnihotri, Ganga, "Comparison of topologies of hybrid active power filter," Information and Communication Technology in

Electrical Sciences (ICTES 2007), 2007. ICTES. IET-UK International Conference on , vol., no., pp.503-509, 20-22 Dec. 2007

[46] Abdel-Galil, T.K.; El-Saadany, E.F.; Salama, M.M.A., "Implementation of different mitigation techniques for reducing harmonic distortion in medium voltage industrial distribution system," Transmission and Distribution Conference and Exposition, 2001 IEEE/PES , vol.1, no., pp.561-566 vol.1, 2001

[47] IEEE C62.92.4-1991, Guide for the Application of Neutral Grounding in Electrical Utility Systems, Part IV-Distribution, 1992

[48] IEEE Std. 80, Guide for Safety in AC Substation Grounding, 2000

[49] Janak R. Acharya, Power Quality Characteristics of MGN Distribution Systems, PHD thesis, Fall 2010

[50] Burke, J.; Marshall, M.; , "Distribution system neutral grounding," Transmission and Distribution Conference and Exposition, 2001 IEEE/PES , vol.1, no., pp.166-170 vol.1, 2001

[51] Yunfei Wang, Janak Acharya and Wilsun Xu, "Shielding effect of multi-grounded neutral wire in the distribution system", Euro. Trans. Electr. Power 2011.

[52] IEEE Working Group on Nonsinusoidal Situations: Effects on Meter Performance and Definitions of Power, "Practical Definitions for Powers in Systems with Nonsinusoidal Waveforms and Unbalanced Loads: a Discussion", IEEE Transactions on Power Delivery, vol. 11, no. 1, January 1996, pp. 79-101.

[53] IEEE Trial-Use Standard Definitions for the Measurement of Electric Power Quantities under Sinusoidal, Nonsinusoidal, Balanced or Unbalanced Conditions, IEEE Standard 1459-2000.

[54] Arrillaga, J., Neville, R. W., Power System Harmonics, 2nd Edition, 2003, John Wiley & Sons

[55] US patent 5914540 "Filter for removing harmonic current from a neutral conductor", published June 22, 1999

[56] A. Capasso, W. Grattieri, R. Lamedica, and A. Prudenzi, A bottom-up approach to residential load modeling, IEEE Trans. Power Syst., vol. 9, pp. 957-964, May 1994

Appendix A Bottom-up Single-house Model and Load Evolution

Bottom-up single-house model is based on the accurate harmonic model of various home appliances. It was built up by PDS-LAB of University of Alberta.

In this model, residential consumers' usage habits are formulated and used to bind up multi-appliances to obtain the house harmonic model. Consumers' usage habits are represented in the time series way, so the final house harmonic model is in time series.

Furthermore, the penetration level of the main home appliances has also been integrated in this model for harmonic level and trend forecast.

A.1 Modeling of Home Appliances and Load Evolution

The aim of this section is to present the characteristics of common appliances through actual measurement carried out in some houses in Canada. Table A.1 shows the list of measured home appliances, which basically includes all the typical home appliances commonly seen in North America [1].

Table A.1 Measured home appliances

Group	Code	Appliance Type	Number Tested
	CFL	Compact Fluorescent Lamp	12
Lighting	EBL	Electric-Ballast Fluorescent Lamp	3
	MBL	Magnetic-Ballast Fluorescent	1

		Lamp	
	INC	Incandescent Lamp	1
Entertainment	PC	Desktop PC	3
	LCD	LCD Computer Monitor	3
	LAP	Laptop	3
	LCD TV	LCD Television	3
	CRT TV	CRT Television	2
Major Appliances	R FR	Regular Fridge	2
	ASD FR	ASD-based Fridge	3
	FRE	Freezer	1
	WSH	ASD-based Washer	1
	DRY	Regular Dryer	1
	ASD DRY	ASD-based Dryer	1
	RAN	Electric Range	3
	OVE	Electric Oven	1
Kitchen	MW	Microwave Oven	3
	TOA	Toaster	1
	COF	Coffee Maker	1
	GRI	Griddle	1
	WAF	Waffle Iron	1
	BRE	Bread Maker	1
	BLE	Blender	2
	FOO	Food Processor	1
Office	PRIN	Printer	1
	COP	Copier	1
Others	KET	Electric Kettle	2
	FUR	Furnace	1
	GAR	Garage Door	1
	VAC	Vacuum Cleaner	2

The appliances listed in Table A.1 are like the bottom "bricks" in the pyramid like bottom-up harmonic model (as shown in Figure 2.1). This list defined the bottom targets needed to be modeled. The next two subsections in this appendix will show the harmonic model of each appliances and their load evolution respectively.

A.1.1 Harmonic Modeling of Home Appliance

Based on the correlation between the input current and the applied voltage, appliances can be divided into two classes. One is linear, while the other is nonlinear loads. Table A.2 shows the linear and nonlinear classification for appliances.

Table A.2 Linear and nonlinear appliances

Appliance Name	Characteristic of Appliance
Compact Fluorescent Lamp	Non-linear
Electric-Ballast Fluorescent Lamp	Non-linear
Magnetic-Ballast Fluorescent Lamp	Linear
Incandescent Lamp	Linear
Desktop PC	Non-linear
LCD Computer Monitor	Non-linear
Laptop	Non-linear
LCD Television	Non-linear
CRT Television	Non-linear
Fridge	Non-linear
Freezer	Non-linear
Washer	Non-linear
Dryer	Linear
Electric Range	Linear
Electric Oven	Linear
Microwave Oven	Non-linear
Toaster	Linear
Coffee Maker	Linear
Griddle	Linear
Waffle Iron	Linear
Bread Maker	Non-linear
Blender	Non-linear
Food Processor	Non-linear

Printer	Non-linear
Copier	Non-linear
Electric Kettle	Linear
Furnace	Non-linear
Garage Door	Non-linear
Vacuum Cleaner	Non-linear

This classification is necessary and essential, which decides how the load will be modeled in the harmonic study [2].

Injected harmonic current form each appliance consists of two essential parts, the harmonic current magnitude and angle. Both of them can be obtained from the real measurement.

The appliances under study were categorized as linear and nonlinear load types. Therefore, the next step is to determine the modeling for each type so they can be incorporated in a study of harmonic impact analysis.

How to model linear loads is still under research. However, it is acceptable to model linear loads as constant power loads at fundamental frequency (60 Hz) and as impedance for harmonic frequencies, as shown in Figure A.1[3].

The parameters for the model of each linear appliance can be obtained from the measurements according to the following equations:

$$P + jQ = V_1 \times conj(I_1)$$

<div align="right">Equation A.1</div>

$$R = \frac{V_1^2}{P} \quad X_h = h\frac{V_1^2}{Q}$$

<div align="right">Equation A.2</div>
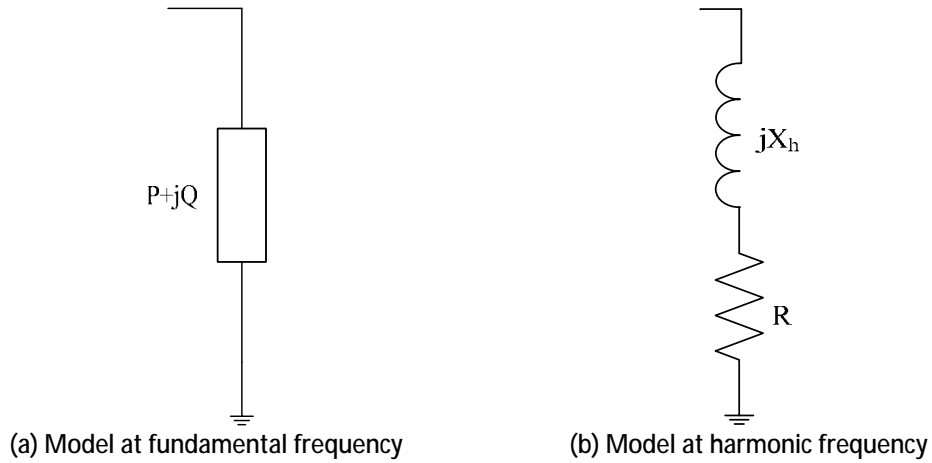
(a) Model at fundamental frequency   (b) Model at harmonic frequency
Figure A.1 Model for linear appliances

A harmonic source causes harmonic distortion by injecting harmonic currents into the power system. So it is natural to consider harmonic sources as harmonic current sources. In fact, harmonic current source has become the most commonly used model for harmonic source representation [3]. Therefore, nonlinear appliances are modeled by a constant $P + jQ$ for the fundamental frequency and as current source for the harmonic frequencies, as shown in Figure A.2.

(a) Model at fundamental frequency   (b) Model at harmonic frequency

Figure A.2 Model for nonlinear appliances
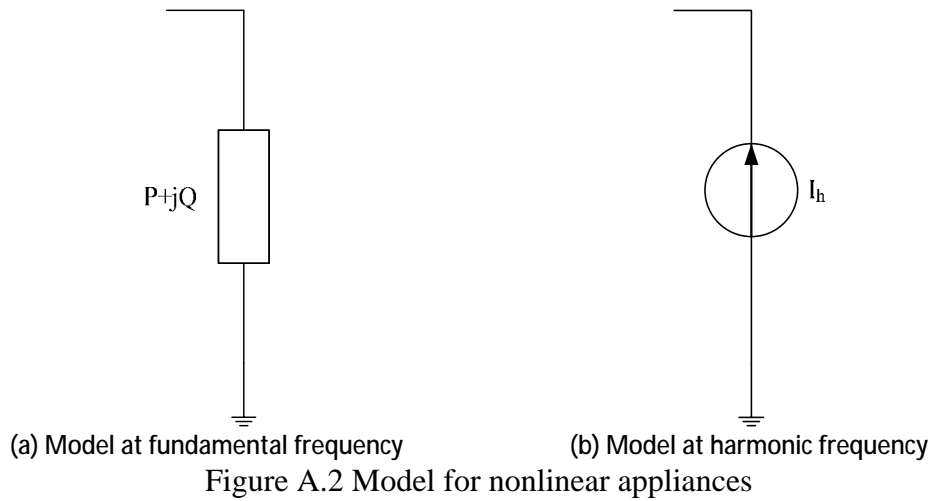
A commonly used procedure to establish the current source model is as follows:

1) The harmonic-producing load is treated as a constant power load at the fundamental frequency, and the fundamental frequency power flow of the system is solved

2) The current injected from the load to the system is then calculated and is denoted as $I_1 \angle q_1$

3) The magnitude and phase angle of the harmonic current source representing the load are determined as follows:

$$I_h = I_1 \frac{I_{h-spectrum}}{I_{1-spectrum}}$$

Equation A.3

$$q_h = q_{h-spectrum} + h(q_1 - q_{h-spectrum})$$

Equation A.4

where subscript "spectrum" stands for the typical harmonic current spectrum of the load. The meaning of the magnitude formula is to scale up the typical harmonic current spectrum to match the fundamental frequency power flow result (I_1). The phase formula shifts the spectrum waveform to match the phase angle of q_1. Since the *h*-th harmonic has h-times higher frequency, its phase angle is shifted by *h* times of the fundamental frequency shift. This spectrum-based current source model is the most common one used in commercial power system harmonic analysis programs. The input data requirement is minimal.

A.1.2 Load Evolution

As stated above, the load evolution can help predict how the harmonic situation looks like in the near future, which is helpful to utility to make decision earlier before it is too late.

According to a reports [4]~[14] published by various marketing research institutions, trend of lighting appliances, televisions, PC & printers, laptops & desktops, fridges and washers are listed in Table A.3.

Table A.3 Appliance number trend per household

Year	2010	2011	2012	2013	2014	2015
CFLs	4.55	6.73	8.33	9.92	11.52	13.7
Incandescent Bulbs	32.45	30.68	29.5	28.32	27.14	25.37
LCD TV	1.11	1.41	1.68	1.88	2.03	2.11
CRT TV	1.13	0.83	0.55	0.36	0.21	0.13

Laptops	1.48	1.61	1.75	1.91	2.08	2.27
Desktops	1.19	1.22	1.24	1.26	1.28	1.29
Printers	0.3	0.31	0.33	0.35	0.37	0.4
Energy Cons. Fridges	0.66	0.74	0.82	0.9	0.98	1.06
Regular Fridges	0.61	0.53	0.45	0.37	0.29	0.21
Front Washers	0.4	0.45	0.5	0.55	0.6	0.63
Top Washers	0.6	0.55	0.5	0.45	0.4	0.37

A.2 Harmonic Modeling of Residential House Load Profile

In a general way, the bottom-up approach is based on the determination of individual models for each component of the actual system. In the load modeling problem, this approach permits the determination of individual models that represent the behavior of different equipment: lamps, showers, heating devices, air conditioners, among others [15]. This approach is like building up the second level of the pyramid based on the bottom "bricks"/appliances shown in Figure 2.1, which can be characterized as determining the type and number of appliances in operation at a given time. This would be done by using a probability model to model switch-on event of appliances based on several aspects.
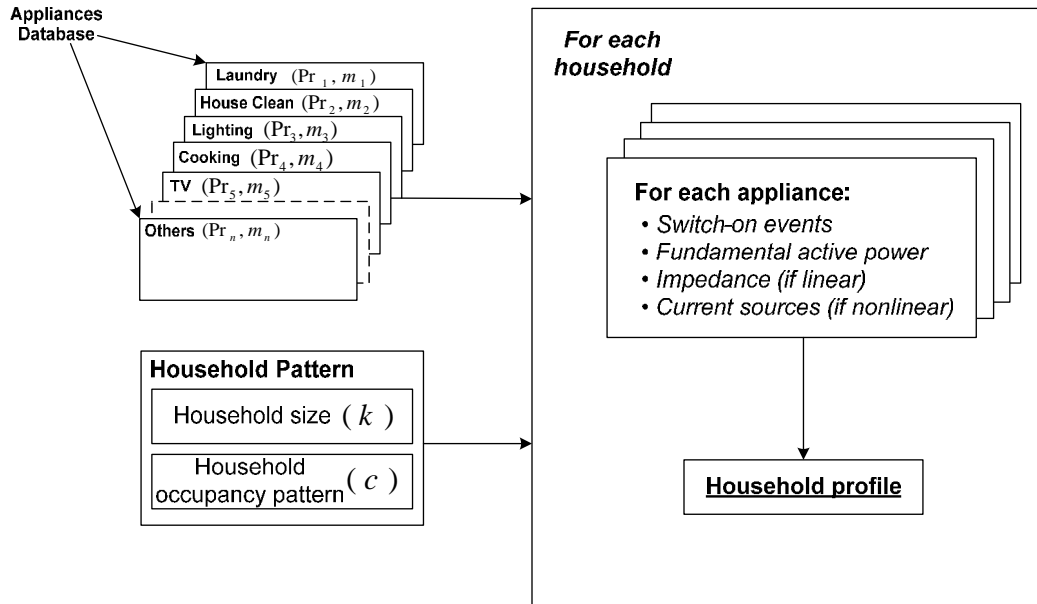
Figure A.3 Structure of the bottom-up approach model for a residential household

Four parameters have been used to determine which time certain appliance is in operation, as shown in Figure A.3:

1) Usage times of certain appliance m

2) Daily Time of Use Probability Profiles Pr

3) Household calibration factor k in terms household size

4) Household occupancy pattern factor c

A.2.1 Usage times of certain appliance m

Usage times of certain appliance m have been obtained from Canadian Center for Housing Technology (CCHT) twin house research facility [16], Canadian Standards Association (CAN/CSA-C373-92, CAN/CSA-C361-92 and CAN/CSA-C360-98)([16]~[19]).

A.2.2 Daily time of use probability profiles *Pr*

Daily time of use probability profiles *Pr* was first proposed by Walker and Pokoski [20] in 1985, by introducing the concept of using 'proclivity' functions to predict the tendency of the occupants to switch on an appliance at any given time. From then on, many have researched on how to quantify the probability of the specified activity being undertaken as a function of time-of-day (Time of Use Probability Profiles). In our simulation, we mainly use the data profiles from the Building America research Benchmark Definition [21] and UK 2000 Time Use Survey (TUS) [22], also provided from reference [23].

Figure A.4 shows a typical daily time of use probability profile for cooking activity. The curves are applied to predict the occupants' cooking related actions. At each specific time during a day, one can read the corresponding probability of event from the y-axis.

A.2.3 Household calibration factor *k*

The size of household has a significant impact on daily electricity demand. The appliance usage characteristics described above are obtained based on average household size, different number of occupants will more or less change the characteristics. In view of this, a household calibration factor *k* is introduced, which is equal to the ratio of specified number of n occupants and the average

household size[7]. Therefore, the real usage times of certain appliance will be multiplied by *k*.
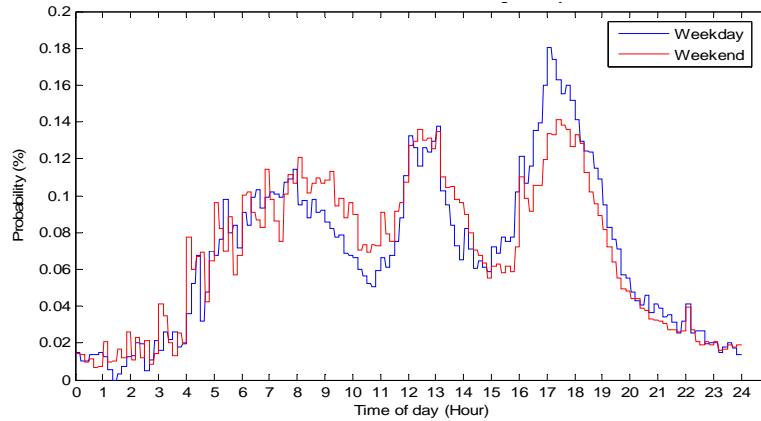
Figure A.4 Time of use probability profile for cooking activity

A.2.4 Household occupancy pattern factor *c*

Appliance usage within a residential house is also naturally related to the number of occupants who are at home and awake, or called occupied period. For example, most of the appliances will not be used when people are not at home. This occupancy pattern is of course associated with personal life style. The calibration scalar *c* is introduced to reflect the influence of household occupancy pattern. *c* can be calculated from the rule that summation of probabilities over a day is equal to '1'.

When the above four parameters have been obtained, the switch-on probability of a specific appliance at a specific time can be calculated by Equation A.5.

---

[7] According to the 2006 census data of statistics Canada [24], the average number of people per household is 2.5.

$$P = P_r \times m \times k \times c$$

<div align="right">Equation A.5</div>

With the obtained *P*, the statistical random number generator would be used to finally decide if the selected appliance was in operation at that specific time or not.
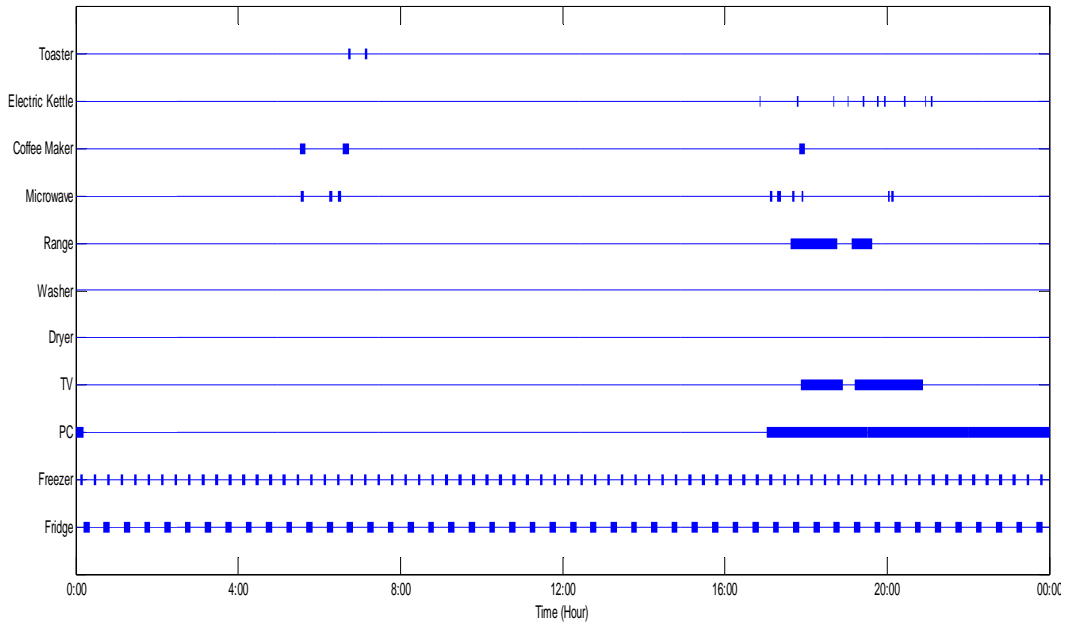
Figure A.5 The simulated multiple-appliances usage time

Figure A.5 shows an example simulation results. One can observe that the PC is used between 17:00 and 24:00 and washer and dryer are not used throughout the day. In the bottom of Figure A.5, the fridge and freezer are activated periodically throughout the whole day and not associated with household occupancy pattern.

Appendix B System Parameters Sensitivity Results

This section gives the supplemental simulation results for Section 4.1.

B.1 Substation Grounding Sensitivity for Actual Case

The actual case map is re-drawn here, in Figure B.1.
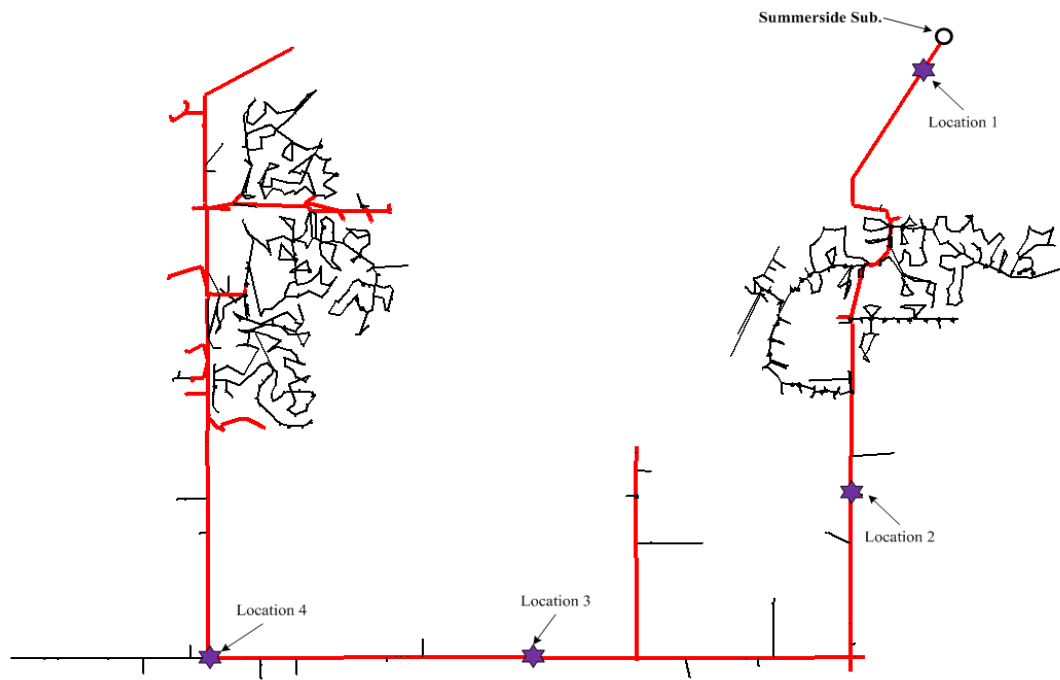
Figure B.1 Circuit map for actual case

In the same way as the substation grounding sensitivity for ideal case, R_{gs} will be varied from 0.15 ohm to 5ohm.

Dominant Sequence Voltage at Location of Location 1

Voltage (V)

Harmonic Order #

Rgs=0.15(ohm)
Rgs=1(ohm)
Rgs=3(ohm)
Rgs=5(ohm)

Dominant Sequence Current at Location of Location 1

Current (A)

Harmonic Order #

Individual IT at Location of Location 1

IT

Harmonic Order #

Neutral Current at Location of Location 1

Current (A)

Harmonic Order #

100m Telephone Line Voltage at Location of Location 1

Voltage (V)

Harmonic Order #

Rgs=0.15(ohm)
Rgs=1(ohm)
Rgs=3(ohm)
Rgs=5(ohm)

Rgn (ohm)	5	10	15	20
IT	11897	11887	11778	11642
Telephone Line Voltage (V)	4.3	4.2	3.7	3.3

Figure B.2 Substation grounding sensitivity results for Location 1

Dominant Sequence Voltage at Location of Location 2

Voltage (V)

Harmonic Order #

Dominant Sequence Current at Location of Location 2

Current (A)

Harmonic Order #

Rgs=0.15(ohm)
Rgs=1(ohm)
Rgs=3(ohm)
Rgs=5(ohm)

Individual IT at Location of Location 2

IT

Harmonic Order #

Neutral Current at Location of Location 2

Current (A)

Harmonic Order #

Figure B.3 Substation grounding sensitivity results for Location 2

Rgn (ohm)	5	10	15	20
IT	10530	10520	10425	10294
Telephone Line Voltage (V)	2.6	2.6	2.6	2.5
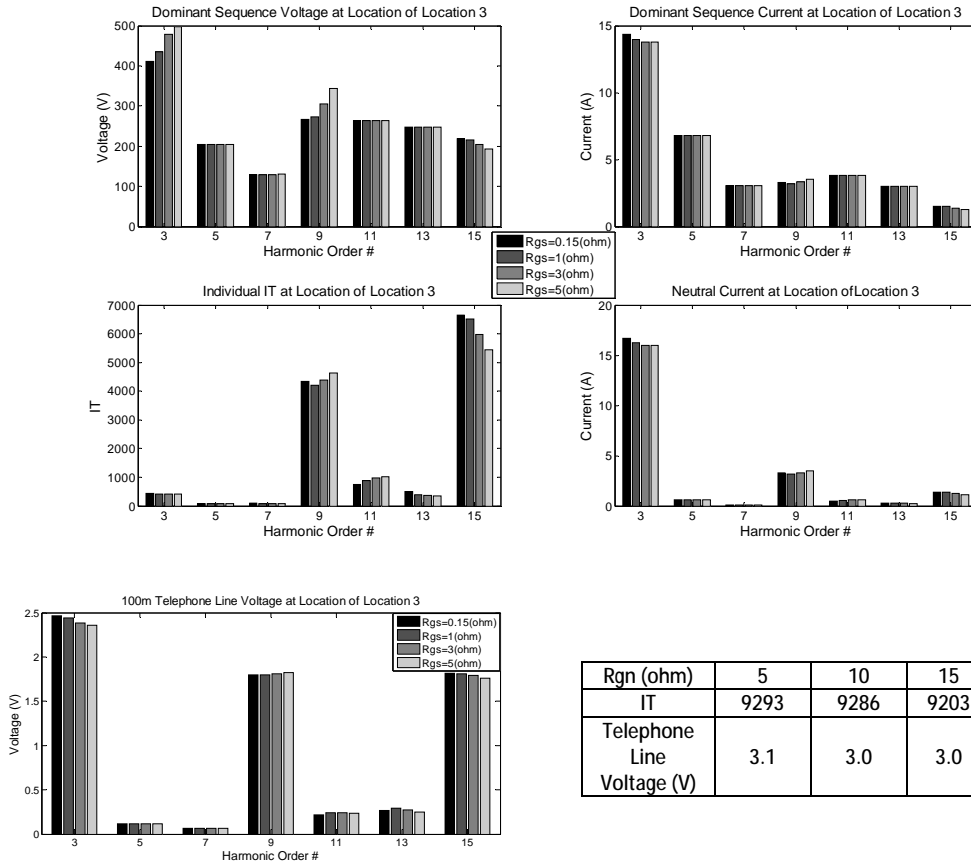
Rgn (ohm)	5	10	15	20
IT	9293	9286	9203	9090
Telephone Line Voltage (V)	3.1	3.0	3.0	3.0

Figure B.4 Substation grounding sensitivity results for Location 3
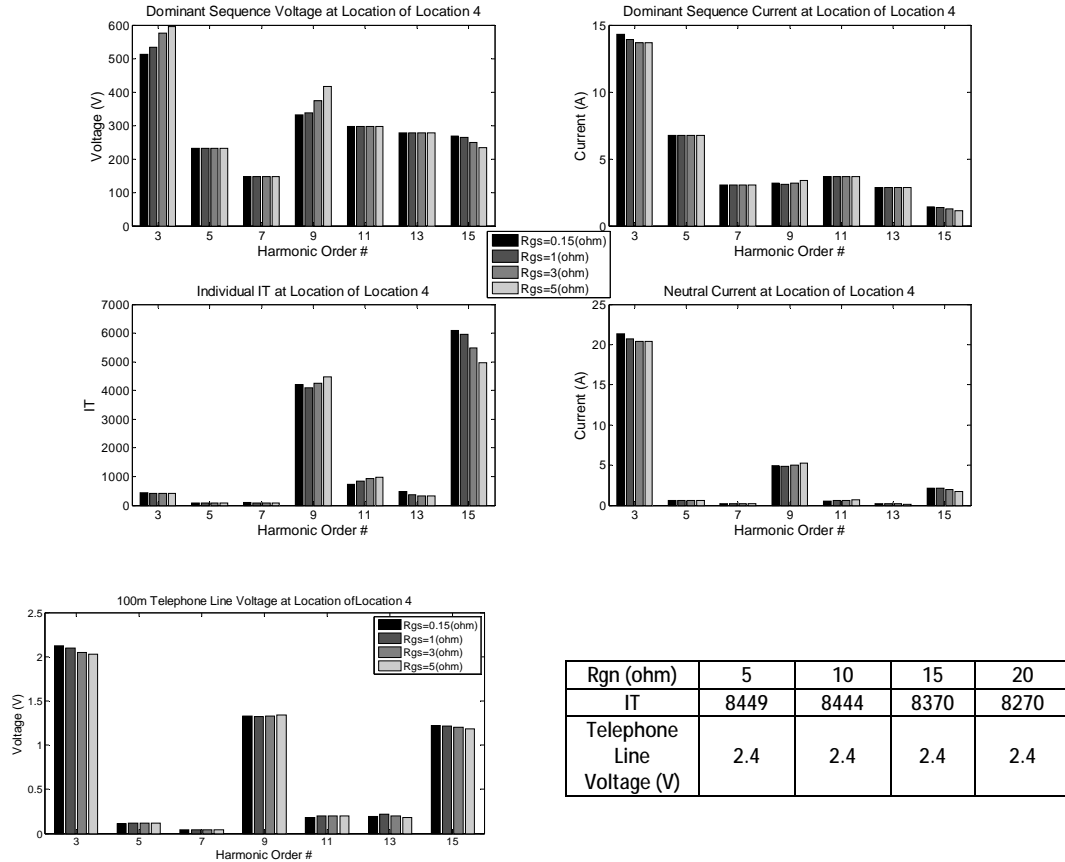
Figure B.5 Substation grounding sensitivity results for Location 4

The finding is: For most locations, R_{gs} has little impact on phase current, neutral current and induced voltage of parallel telephone line. However, at substation side, it has a big impact (as big as 50%) on the neutral current and parallel telephone line. This finding is consistent with the results from ideal case in Section 4.1.1

B.2 Multi-grounding Resistance Sensitivity for Actual Case

In the same way as we did for ideal case in Section 4.1.4, multi-grounding resistance Rgn varies from 5 ohm to 20 ohm.
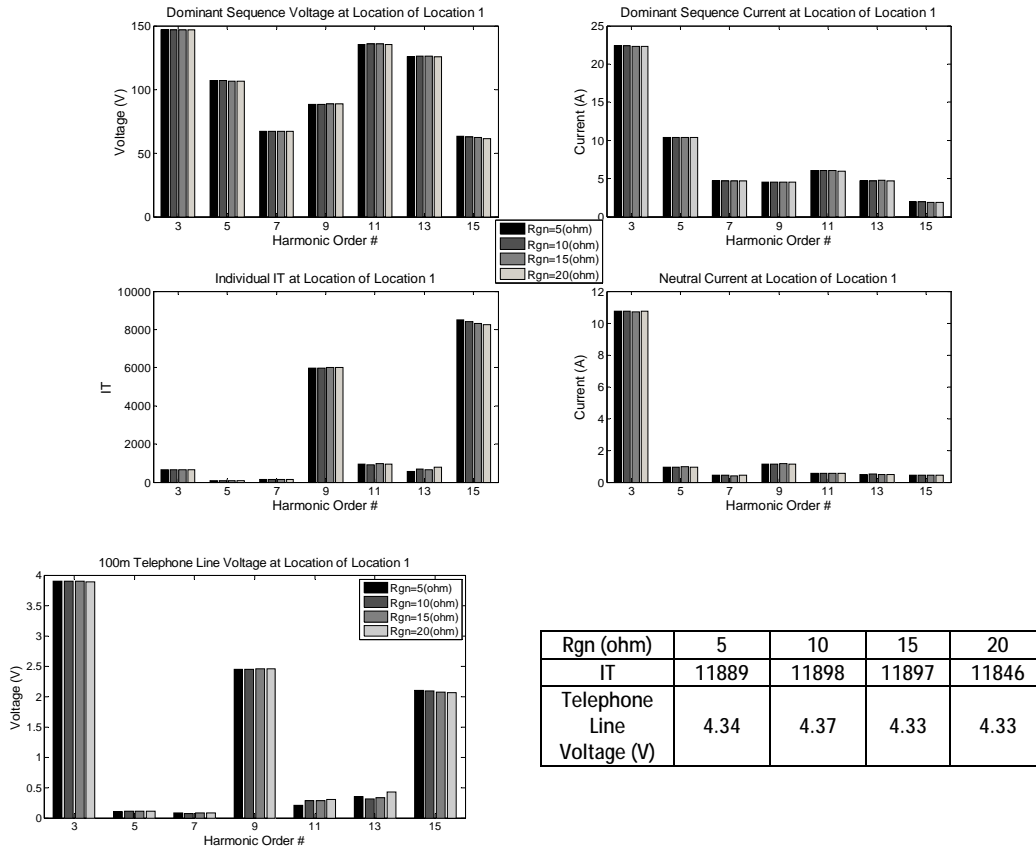
Figure B.6 Multi-grounding resistance sensitivity for Location 1

Rgn (ohm)	5	10	15	20
IT	11889	11898	11897	11846
Telephone Line Voltage (V)	4.34	4.37	4.33	4.33

Figure B.7 Multi-grounding resistance sensitivity for Location 2
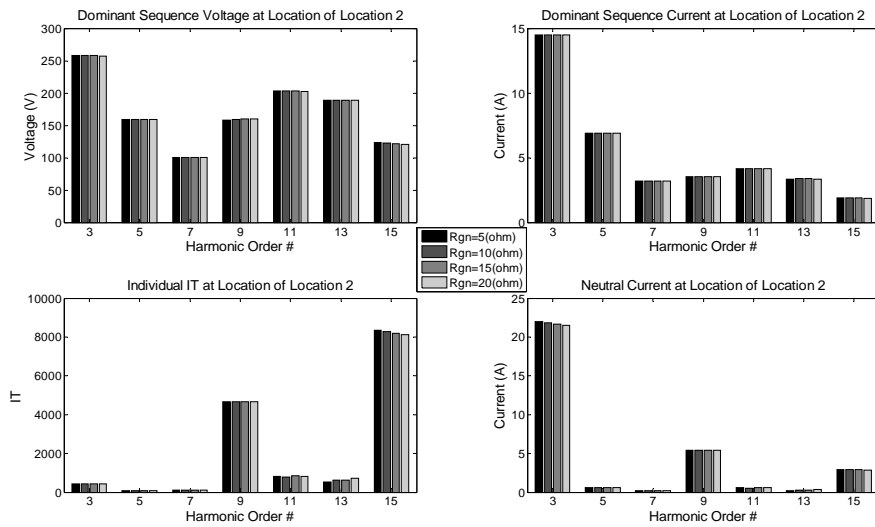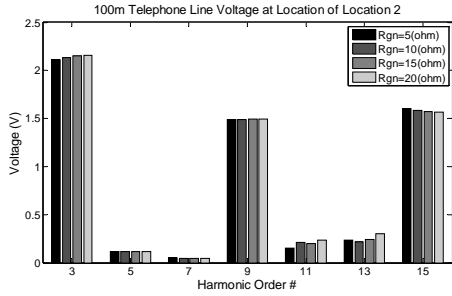
Rgn (ohm)	5	10	15	20
IT	10519	10538	10530	10482
Telephone Line Voltage (V)	2.59	2.60	2.62	2.63
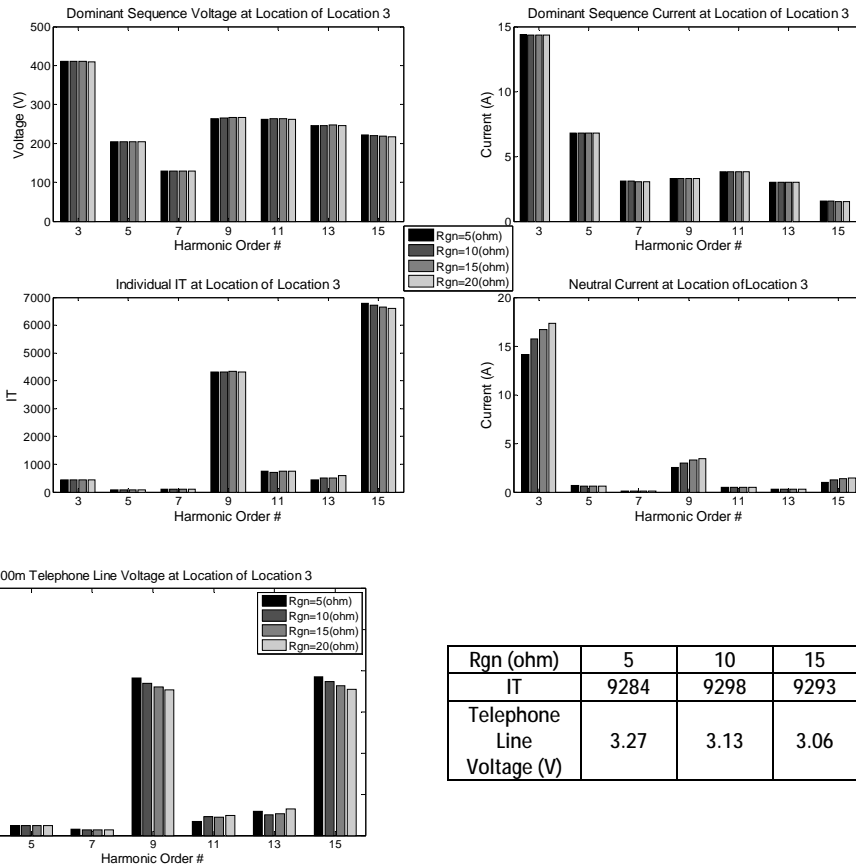
Rgn (ohm)	5	10	15	20
IT	9284	9298	9293	9247
Telephone Line Voltage (V)	3.27	3.13	3.06	2.30

Figure B.8 Multi-grounding resistance sensitivity for Location 3

Rgn (ohm)	5	10	15	20
IT	8428	8448	8449	8418
Telephone Line Voltage (V)	2.41	2.41	2.44	2.50
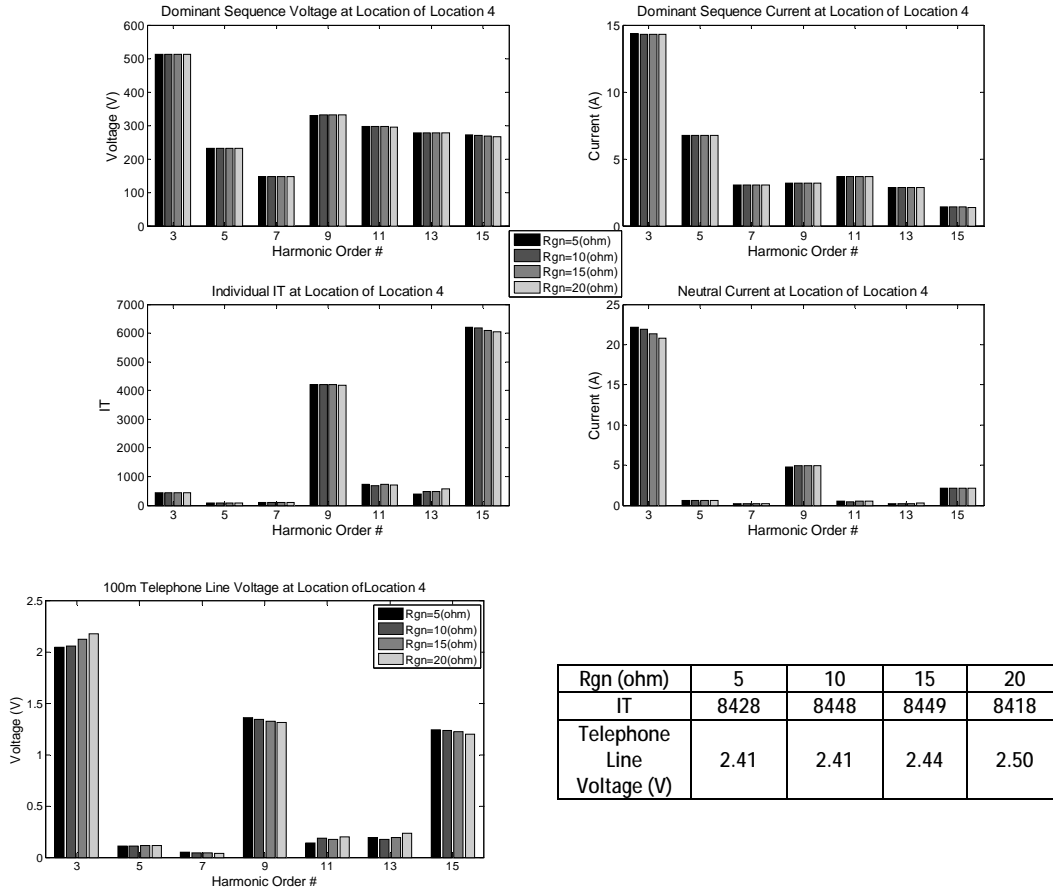
Figure B.9 Multi-grounding resistance sensitivity for Location 4

The finding is: *Rgn* has little impact on phase current (less than 1%), neutral current (less than 10%) and induced voltage of telephone line (less than 20%), which is consistent with what we found in the ideal case.

Appendix C Reference

[1] Alexandre B. Nassif, Modeling, measurement and mitigation of power system harmonics, PhD Thesis. University of Alberta, Fall 2009.

[2] HW Dommel, Electromagnetic transients program (EMTP) theory book, 1986

[3] Task Force on Harmonics Modeling and Simulation, Modeling and Simulation of the Propagation of Harmonics in Electric Power Networks, Part I: Concepts, Models, and Simulation Techniques, IEEE Transactions on Power Delivery, vol. 11, no. 1, January 1996.

[4] IEA, Light's Labour's Lost, International Energy Agency, OECD, Paris, 2006.

[5] ESource, Who's Buying CFLs? Who's Not Buying Them? Findings from a Large-Scale, Nationwide Survey, 2008 ACEEE Summer Study.

[6] V. Letschert, Potential Impact of Adopting Maximum Technologies as Minimum Efficiency Performance Standards in the U.S. Residential Sector, eScholarship, 2010.

[7] LCD TV Market Growing Despite Weakness in North America; LED-Backlit Set to Take Lead in 2011, available online at: http://www.displaysearch.com/

[8] The Economist, Pocket World in Figures 2006 and 2010.

[9] World Development Indicators, World Bank Group, 2010.

[10] Canadian laptop ownership, IPSOS, 2009, available online at http://www.ipsos-na.com/news-polls/.

[11] 2008 could be the year laptop sales eclipse desktops in US, January 2008, available online at: http://arstechnica.com

[12] Gartner Says Worldwide PC Market Grew 13 Percent in 2007, January 2008, available online at: http://www.gartner.com/it/page.jsp?id=584210

[13] Natural Resources Canada, Energy Consumption of Major Household Appliances Shipped in Canada-Trends for 1990-2006, December 2008.

[14] A. M. Jungreis, A. W. Kelley, Adjustable Speed Drive for Residential Applications, IEEE Transactions on Industry Applications, vol. 31, no. 6, Nov./Dec. 1995, pp. 1315-1322.

[15] Clément C. Lefebvre, Electric Power: Generation, Transmission And Efficiency, Nova Science Publishers, Inc, 2008

[16] Bell, M. Swinton, M.C. Entchev, E. Gusdorf, J. Kalbfleisch, W. Marchand, R.G. Szadkowski, F., Development of Micro Combined Heat and Power Technology Assessment Capability at the Canadian Centre for Housing Technology, pp. 48. 2003-12-08.

[17] CSA, Energy Consumption Test Methods for Household Dishwashers, CSA Standard CAN/CSA-C373-92, 1992.

[18] CSA, Test Method for Measuring Energy Consumption and Drum Volume of Electrically Heated Household Tumble-Type Clothes Dryers, CSA Standard CAN/CSA-C361-92, 1992.

[19] CSA, Energy Performance, Water Consumption and Capacity of Automatic Household Clothes Washers, CSA Standard CAN/CSA-C360-98, 1998.

[20] Walker, C. and J. Pokoski, Residential load shape modelling based on customer behavior, Power Apparatus and Systems, IEEE Transactions on, 1703-1711, 1985.

[21] R. Hendron, Building America Research Benchmark Definition, Technical Report NREL/TP-550-40968, January 2007.

[22] Ipsos-RSL and Office for National Statistics, United Kingdom Time Use Survey, 3rd ed., UK Data Archive, Colchester, Essex, September 2003.

[23] Richardson, I., M. Thomson, et al, Domestic electricity use: A high-resolution energy demand model, Energy and Buildings 42(10): 1878-1887, 2010.

[24] Statistics Canada, Selected dwelling characteristics and household equipment, available online at: *http://www40.statcan.gc.ca/l01/cst01/famil09b-eng.htm*